Universidade de Aveiro
Departamento de
Electrónica, Telecomunicações e Informática
2014

António Jorge Dinis
da Silva de Carvalho

Wireless Power Transmission para Drones

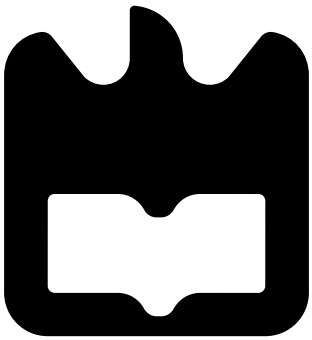

António Jorge Dinis da Silva de Carvalho

Wireless Power Transmission para Drones

Wireless Power Transmission for Drones

Dissertação apresentada à Universidade de Aveiro para cumprimento dos requisitos necessários à obtenção do grau de Mestre em Engenharia Electrónica e Telecomunicações, realizada sob a orientação científica do Doutor Nuno Miguel Gonçalves Borges de Carvalho, Professor Catedrático do Departamento Electrónica, Telecomunicações e Informática da Universidade de Aveiro e sob co-orientação científica do Doutor Pedro Renato Tavares de Pinho, Professor Adjunto da Área Departamental de Engenharia Electrónica e Telecomunicações e de Computadores do Instituto Superior de Engenharia de Lisboa.

O júri

presidente

Professor Doutor José Carlos Esteves Duarte Pedro
Professor Catedrático do Departamento Electrónica, Telecomunicações e Informática da Universidade de Aveiro

vogais

Professor Doutor Rafael Ferreira da Silva Caldeirinha
Professor Coordenador do Departamento de Engenharia Electrotécnica da Esc. Sup. de Tecnologia e Gestão do Inst. Politécnico de Leiria do Instituto Politécnico de Leiria

Professor Doutor Nuno Miguel Gonçalves Borges de Carvalho
Professor Catedrático do Departamento Electrónica, Telecomunicações e Informática da Universidade de Aveiro

Agradecimentos

Seria ingrato da minha parte tomar todos os louros pelo trabalho aqui presente dado que sem o incentivo, ajuda e análise crítica de um grupo fantástico de pessoas não teria sido possível chegar a este ponto.

Aos meus orientadores, pela orientação técnica prestada nesta minha primeira abordagem à investigação académica e pelo seu gosto em inovar e descobrir novos desafios no mundo da Rádio Frequência.

Ao Ricardo Gonçalves, aluno de Doutoramento, por todos os seus conselhos, sempre concretos e elucidativos.

Aos meus pais, que toda a minha vida me apoiaram com carinhoso empenho, e irmãos, que me incetivam a sonhar mais alto.

À minha namorada, Marta Veiga, que me apoiou sempre nas decisões mais difíceis ao longo do meu percurso em Aveiro, se esforçou, e esforça, por me manter focado e com as ideias organizadas, nunca me deixando desistir.

Aos meus colegas do laboratório de Rádio Frequência, que ajudaram a tornar os momentos de maior frustração em recordações divertidas.

Aos amigos que fiz em Aveiro e com quem partilhei objectivos, expectativas e aventuras.

À equipa técnica do Instituto de Telecomunicações que se mostrou sempre disponível para ajudar.

Obrigado.

Palavras-chave

Agregados de antenas, Antenas, Antenas microstrip, $Rectennas$, Transmissão de potência sem fios, Veículos aéreos não tripulados

Resumo

Drone é a designação normalmente atribuída a veículos aéreos não tripulados que se têm proliferado no mercado devido ao seu baixo custo e inúmeras aplicações. Além do seu uso em actividades lúdicas, como o já comum registo aéreo de eventos, demonstram um enorme potencial noutras aplicações, tanto militares, missões de busca e salvamento e reconhecimento de terreno, como comerciais, sendo exemplo a vigilância e inspecção de campos de colheita. No entanto, maioria dos dispositivos comerciais actualmente disponíveis padecem de uma grande limitação no que toca à sua dependência de baterias que, de modo a alimentar os motores do drone, rapidamente se descarregam. Além disso, o peso que estas baterias implicam levam a que seja necessária uma maior potência para que o drone se mantenha a voar. Estes problemas podem ser contornados, ou atenuados, recorrendo a sistemas de transmissão dedicada de energia electromagnética que possibilitem aos dispositivos manter vôo sem recurso a baterias ou carregando-as quando em uso. Ao longo desta dissertação será descrito em detalhe um sistema de transferência de energia sem fios projectado para trabalhar à frequência de 5.8 GHz, dando ênfase ao desenho de um agregado de antenas microstrip, desenvolvido para possibilitar uma transmissão directiva, e a *rectenna* proposta para recepção da energia electromagnética e sua conversão em corrente contínua. O sistema proposto possibilita ao quadricóptero ter energia suficiente para se conseguir ligar e estabelecer comunicação com o seu controlo remoto sendo que a arquitectura proposta demonstra potencial para ser adaptada em futuras abordagens.

Keywords Antennas, Microwave antenna array, Microstrip antennas, $Rectennas$, Unmanned Aerial Vehicles, Wireless power transfer

Abstract Drones are unmanned aerial vehicles that have proliferated the market due to their low cost and the many applications that can already be associated to them. Besides the common use of these devices for playful activities, as aerial event recording, they demonstrate an enormous potential in other applications, such as military, as search and rescue or reconnaissance missions, or commercial, for example: surveillance and inspection of crops. However, most commercial devices currently available suffer from a major drawback in terms of their dependence of batteries which, in consequence of the large energy demand supplied to the drone's engines, quickly discharge. In addition, the weight of these batteries typically implies that more power is needed to keep the drone flying. This drawback can be overcome, or attenuated, using dedicated wireless power transmission systems that enable the devices to maintain flight without the need of batteries or simply charging them while in use. Throughout this dissertation a microwave wireless power transmission system working at 5.8 GHz will be described in detail, with emphasis on the design of the microstrip antenna array developed to allow directive transmission and the *rectenna* proposed for reception and power conversion. The proposed system allows the used quadcopter to boot and link with its remote control and demonstrates the potential to be adapted for other purposes.

Contents

List of Figures

List of Tables

List of Acronyms

AC	Alternating Current
ADS	Advanced Design Systems
A4WP	Alliance for Wireless Power
CAD	Computer Aided Design
CST	Computer Simulation Technology
COST	European Cooperation in Science and Technology
DC	Direct Current
DTT	Digital Terrestrial Television
EAGLE	Easily Applicable Graphical Layout Editor
FIA	Federation Internationale de l'Automobile
IC	Integrated Circuits
IDT	Integrated Device Technology
ISM	Industrial, Scientific and Medical
LSSP	Large-Signal S-Parameter
MIT	Massachusetts Institute of Technology
MWS	Microwave Studio
NASA	National Aeronautics and Space Administration
NIMBUS	Nebraska Intelligent MoBile Unmanned Systems
PA	Power Amplifier
PCE	Power Conversion Efficiency
PDL	Power Delivered to Load
PLF	Polarization Loss Factor
PMA	Power Matters Alliance
PTE	Power Transfer Efficiency

POE	Power Overall Efficiency
RAMP	Raytheon Airborne Microwave Platform
RCA	Radio Corporation of America
RHCP	Right Hand Circularly Polarized
RF	Radio Frequency
SMA	SubMiniature version A
SPICE	Simulated Program with Integrated Circuits Emphasis
SPS	Solar-Power Satellite
TED	Technology, Entertainment, Design
UAV	Unmanned Aerial Vehicles
VSWR	Voltage Standing Wave Ratio
URSI	International Union for Radio Science
WCT	Wireless Charging Technology
WIPE	Wireless Power Transmission for Sustainable Electronics
WPC	Wireless Power Consortium
WPT	Wireless Power Transmission

Chapter 1

Introduction

Unmanned Aerial Vehicles (UAV) are non-crewed aircrafts that can either be autonomous or remotely controlled. These UAV, or drones, as they are commonly referred to, have become massively used, from the remote controlled models that can be bought online or at any common R/C shop to the models developed and studied at renowned academic laboratories, as the Massachusetts Institute of Technology (MIT)'s Human and Automation Lab or Georgia Tech's UAV Research Facility. These small aircrafts can already be considered a consumer trend and therefore further growth in sales and R&D is expected.

Creative ideas based on these fairly low-cost systems proliferate the internet and have already lead to the appearance of several entertaining capabilities. Control algorithms that enable UAV to show perfect balance whilst balancing a glass full of wine and swarms of nano-drones that can be coordinated in order to play short musical compositions using different instruments are some of the currently functioning examples. Many other ideas are still being developed, as MIT's Skycall that will lead campus tours or Nebraska Intelligent MoBile Unmanned Systems (NIMBUS) Labs' use of drone to wirelessly charge sensors.

Drones are being commercialized with video cameras that enable them to film while in-flight and some are even prepared to perform the most various stunts. Still, these robots show a major fault that has delayed the development of more advanced functionalities: their reduced autonomy. Commonly marketed drones typically present running times of around 15 minutes and an even longer charging time is implied so that the device can be used again. But given we live in a society that shows an hunger for technology and a constant need for innovative solutions this problem might be solved in a short period of time.

A reply to this shortcoming can be derived from a couple of concepts that have become quite popular in the past 10 years: energy harvesting and Wireless Power Transmission (WPT), used so that these drones can be continuously charged, while in flight, without any physical restriction to where the charging happens.

WPT is an old concept, over 100 years old, that was advocated and investigated intensely by notorious scientists such as Nikola Tesla or William C. Brown, and can be defined as the

wireless transfer of energy throughout a given distance without resorting to wires or cables. From this concept a truly wireless world can be imagined, where anyone can access energy at any point and electronic devices can function anywhere without sudden power losses that could make them shut-down.

Recently, there have been many developments in the area of low power energy transfer using inductive or resonant inductive coupling so that power can be transmitted over small distances in order to charge multiple devices, from mobile phones to common household appliances. However, low power energy transfer will not suffice to guarantee the power needed for an improved running time regarding UAV. This notion pushes us to another level, medium power energy transfer.

This chapter is organized in order to contextualize this document with regards to the importance that UAV pose for future academic, commercial and military applications and to underline the motivation and main objectives that guided this work. It also enumerates and presents a brief description of the various chapters in which this dissertation is organized and the original contributions it has resulted in.

1.1 Motivation

The use of electronic devices has almost become a basic need given that the majority of jobs today depend on electronic computers to be executed. Even common social interaction is being shifted more and more to an online environment. The great investment in research regarding the *Internet of Things* is even pushing us to a greater dependency on self-sufficient electronic systems. With needs come problems and with those problems come solutions that promise to bring more comfort to a given target audience.

A major fault of current electronic devices comes from their dependence of external power connections or batteries in order to function. These connections can lead to a rapid degradation of the hardware given that the pins needed to connect the devices to the power source tend to get lax and can prevent proper battery charging after some use, not to mention that batteries have limited lifespans. It is thus necessary to make these devices able to be powered in a more effective and versatile way.

The development of WPT systems gets us closer to a truly wireless world, as it was imagined by several brilliant minds before us. This will enable society a more comfortable use of electronics, be it from the integration of these mechanisms in implantable medical devices, the use of backscattering on sensors in crop fields, easier charge of UAVs for search and rescue missions in locations of difficult access, or even just by enabling the common user to be home without ever tripping on a charging cable again.

1.2 Objectives

In this dissertation, a wireless power transmission system is to be developed in order to enable a drone to be charged while in flight so that it can present a superior running time. In order to reach this goal an iterative methodology will be used.

Firstly, the available drone will be studied in order to gather information about the power consumption it requires to successfully take flight. Then the various methods of wireless power transmission will be reviewed, with regard to the currently available systems, so that the one that better fits the drone's characteristics might be implemented.

After this initial literature review and observations, a wireless charging system will be proposed detailing the transmission, reception and power conversion architectures. Once all three of these elements are considered to be rightfully simulated, with satisfactory results, they will be implemented, independently tested and adapted so that their behaviour can be considered to meet the requirements. When all parts are validated, a series of tests will be applied to the system as a whole, so the initial assumptions might be confirmed, aiming ultimately at a practical proof of concept.

1.3 Organization of the Dissertation

Including this introductory chapter, this dissertation is divided into a total of 7 chapters. Chapters 1 through 4, serve as a contextualization of wireless power transmission and the basic theoretical concepts required for the design of the proposed system, while chapters 5 and 6 present the design and implementation of such system.

More specifically, chapter 2 presents a contextualization and state of the art regarding wireless power transmission.

Chapter 3 serves as a theoretical introduction to the most relevant characteristics of antennas and how they can be applied for microwave power transmission. While in chapter 4 the behaviour of semiconductor diodes is introduced, as well as the benefits they bring to high frequency rectification. Also, some circuit topologies are presented.

Chapter 5 introduces the overall characteristics of the proposed system and describes the various components that were designed for it. The simulated values of each individual section of the system are presented. Then, in chapter 6, the measured results, experimental considerations and the behaviour of each component is analyzed.

The remaining chapter summarizes the work done and main conclusions drawn, presenting suggestions to further deepen and improve this topic.

1.4 Original Contributions

This dissertation has lead to the writing of scientific papers that were submitted to two separate conferences.

The first, António Carvalho, Nuno Carvalho, Pedro Pinho and Ricardo Gonçalves, "*Wireless power transmission and its applications for powering Drones*", was accepted to compete for the *Best Student Paper Award* at the 8$^{\text{th}}$ Congress of the Portuguese Committee of the International Union for Radio Science (URSI) - "Drones e veículos autónomos: desafios do presente e do futuro". This article is presented in **Appendix A**.

The remaining article, António Carvalho, Nuno Carvalho, Pedro Pinho, Apostolos Georgiadis, Alessandra Costanzo and Ricardo Gonçalves, "*5.8 GHz Microstrip Antennas and Array for Microwave Power Transfer*" (see **Appendix B**), was submitted for the 2015 European Conference on Antennas and Propagation. This article is currently awaiting acceptance.

Chapter 2

State of the Art

In this chapter, the current level of development with regards to the field of wireless power transmission will be discussed.

The first section is divided into two parts and shows a summary of the history of wireless power transmission, underlining a few relevant facts and developments of the past couple of centuries and then presenting a brief introduction to the life and work of William C. Brown.

Regarding the second section, some of the most commonly used methods for wireless power transmission will be presented and briefly examined.

Companies that currently invest in the upcoming concepts and development of wireless power solutions are presented, in the third section, while in the fourth, and final, section some of the most notable achievements in the research on UAV are described.

2.1 A Timeline in Wireless Power Transmission

The concept of transferring energy through a given distance without the need of physical connections has been around for quite a long time, be it through the laws of physics or magical properties of prana. However, the idea of using electromagnetic waves for this end can be said to have only been born in 1826, when André Marie-Ampére demonstrated that a magnetic field can be produced around a closed loop by the flow of electrical current through that same loop [1].

Some years later, James Clerk Maxwell united various apparently separate laws of physics in order to devise a set of partial differential equations that model the behaviour of electromagnetic radiation. The four Maxwell's equations and the concept of displacement current were introduced in 1861 throughout a paper entitled "On Physical Lines of Force" and then, in 1864, Maxwell showed light to be a magnetic field phenomenon in "A Dynamical Theory of the Electromagnetic Field", these groundbreaking concepts made it possible so that electrical engineering could become what we know today. Around 24 years later, in 1888, Heinrich Hertz empirically proved these concepts thus confirming the existence of electromagnetic waves [2].

Then came Nikola Tesla, seen in Figure 2.1, probably the first and most frequently mentioned supporter of the concept of wireless power transmission, to help this field take its first steps. This Serbian American inventor and physicist first went to the United States of America in 1884 to work under Thomas Edison. However, given some differences in their view towards the paradigm of current distribution, Tesla took the lead on his own, under the financial support of the Western Union, setting up laboratories and companies that dedicated themselves to implement his patents. This divergence in opinion and further altercations between Tesla and Edison would be remembered as the "war of currents".

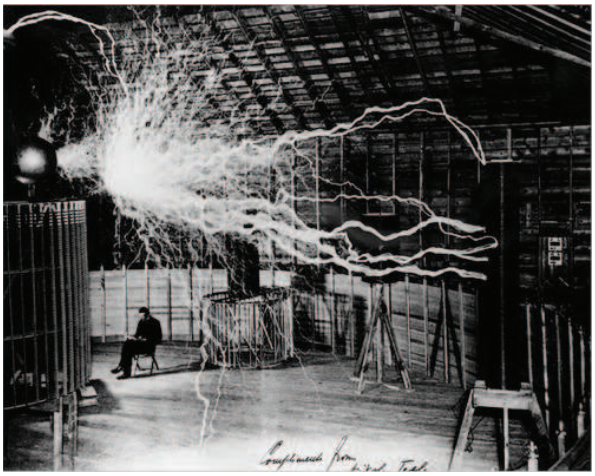

Figure 2.1: A photograph of Nikola Tesla sitting inside a circular framework demonstrating the largest Tesla coils ever built [3].

Tesla envisioned wireless communications and power transfer through radio waves and therefore dedicated a considerable amount of time and money to the development of these fields [4]. In 1893, Tesla was able to demonstrate the wireless illumination of phosphorescent lamps at the World's Columbian Exposition, Chicago. Between 1900 and 1917, he focused his efforts to the development of the Wardenclyffe tower, a tower that would work as an antenna for wireless transatlantic telephony and demonstrate the transmission of power through long distances without cables. Given the difficulty to find enough financial support for this project, and other political reasons, the tower was demolished in the 1st World War [5].

Many advances were made during the two World Wars in the fields of radio frequency electronics and antenna design. From these advances, an electrical engineer from the Raytheon Company, William C. Brown, devised a somewhat entertaining experiment as proof of concept for his developments in rectifying antennas (*rectennas*). He planned, and succeeded in 1964, to fly a wirelessly powered helicopter 15 meters in the air and, even though to maintain flight the helicopter required that kilowatts of power were transmitted to it, this experiment proved the feasibility of microwave power transmission [6].

By 1968, Peter Glaser of the Arthur D. Little Company had presented the concept of

harvesting solar energy in geosynchronous orbit, thus taking advantage of longer collection periods and energy that would otherwise be reflected or absorbed in the atmosphere, converting it into microwave power and transmitting it to earth [7]. The feasibility of this Solar-Power Satellite (SPS) caught the support of Arthur D. Little, Raytheon, Grumman Aerospace, and Textron, who concluded through a six-month long technical study, in 1971, that the concept was favourable to collect the support of National Aeronautics and Space Administration (NASA) [7].

Between 1977 and 1980 both NASA and the United States Department of Energy had been authorized by the United States Congress to study in detail the concept of the SPS. The *"Satellite Power System Concept Development and Evaluation Program"* resulted in a 670-page long study on the feasibility of this technology. By 1980 the program was ended, concluding that "no "show stoppers" of any nature that would preclude a program of research and development to protect this future energy option had been found." [7].

Both studies on the SPS still lead to several developments such as increased efficiency of rectennas at lower power levels and the design of simple control loops that could hold the amplitude of the magnetron directional amplifier to a reference value[7].

In the 21st century, various companies that are focusing their efforts in the development of high frequency operating devices for wireless power transmission have emerged. Of these, probably the most popular would be WiTricity, a company that spun off from an MIT project with the same name lead by Prof. Marin Soljačić.

WiTricity, from the junction of the words *wireless* and *electricity*, is a company that manufactures devices for wireless energy transfer using resonant inductive coupling and has already demonstrated at the Technology, Entertainment, Design (TED) Global Conference in Oxford, 2009, a unit powering simultaneously a television set and three cellphones [8]. This, and other companies, will be more thoroughly analysed further along this chapter.

In order to standardize the wireless charging mechanism of products at a global level, a consortium was established in 2008 and baptized as the Wireless Power Consortium. They have established the *Qi* norm which defines the interface for low power devices (working with up to 5 W) and their member roster already includes over 180 companies, industry leaders in the most various of fields, e.g. mobile phones, batteries and infrastructure [9]. The Wireless Power Consortium is currently working on the *Qi* standard for medium power devices, up to 120 W.

Even though the Wireless Power Consortium (WPC) was the first consortium to appear with this goal, other major industry associations have appeared in the past 6 years with the same goal, but for slightly different architectures.

Besides corporate associations, members from academia have joined efforts to have their slice of the developments in WPT. As an example of this, one can refer to the Wireless Power Transmission for Sustainable Electronics (WIPE) European Cooperation in Science

and Technology (COST). It began its activity in May 2013 and counts with the backup of 25 COST member states and 1 Non-COST country. This COST aims at defining and discussing the future of the development on wireless power transmission circuits and systems by creating a wide network of experts both in academia and industry. It is divided into 5 working groups, each focusing in different fields, from the developments of novel techniques to regulation and society impact.

2.1.1 William C. Brown and Microwave Power Transmission

William Cyrus Brown, seen in Figure 2.2, was an American electrical engineer that pioneered advancements in the field of wireless power transmission.

Born and raised in a simple farm in Iowa, May 22nd 1916, Brown showed talent and skill from a very ripe age, growing up to win the prestigious Fisher Body Competition during his high school career. Soon after, he went on to study at Iowa State University in Ames where he earned his Bachelor of Science Degree in Electrical Engineering in 1937.

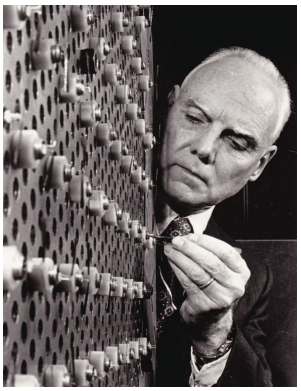

Figure 2.2: Photograph of William C. Brown observing a panel of dipole antennas [10].

After finishing his Bachelor's he began to work as a trainee for the Radio Corporation of America (RCA) where he became interested in high-power vacuum tubes, but he was lured back to school with a scholarship offer from MIT. This experience was also shortened and he ended up signing a contract with the Raytheon Company, currently one of the world's largest defence contractors.

At Raytheon, he became part and even led the department responsible for the development of magnetron tubes, which are vacuum tubes capable of producing microwaves based on the interaction of electrons with a magnetic field while passing a series of cavity resonators. Nowadays these tubes can be found in any ordinary microwave oven.

In this department he invented the Amplitron, latter called a Cross-Field Amplifier. This device works as a microwave oscillator and enables the amplification of a wide band of microwave frequencies with high output power and efficiency.

Around the late 1950's, besides the design of the Amplitron, another important development led to the study and proposal of the Raytheon Airborne Microwave Platform (RAMP). It was the theoretical and experimental demonstrations by Goubau, et al, that microwave power could be transmitted with efficiencies close to 100 % using a waveguide consisting of lenses or reflecting mirrors [11].

Given these developments, and the need of line of sight, the concept of placing a platform at high altitudes was considered a reasonable implementation to efficiently enable long distance communications. This idea led to the practical use of satellites as we know them today, however, at that time, the Raytheon Company proposed that a platform ought to be placed in the atmosphere (see Figure 2.3) to preform this function , hence the RAMP concept was devised.

Figure 2.3: Proposed RAMP[12].

Despise these concepts, efficient conversion of microwaves directly to Direct Current (DC) was still not fully guaranteed. At this time the semiconductor diode was being investigated at the University of Purdue as a feasible and efficient way of rectification, but unaware of these developments Raytheon invested in the investigation on close-spaced thermionic diodes, also known as vacuum tubes, and was able to produce a working demonstration of transferring power wirelessly.

The Raytheon Company demonstrated this concept of wireless microwave power transfer to a board consisting of Air Force and other Department of Defence officials and soon after gained further funding in order to build a proof of concept with a smaller device, the microwave-powered helicopter [7].

Brown was then aware of the developments of the University of Purdue regarding solid-state diode rectifiers, which presented reliability for a smaller size, and was able to propose a solution that took individual full-wave rectifiers and attached them to half-wave dipoles in

order to build the receiving part of the system. In this way, the device commonly known as "rectenna" was conceived.

By October 1964, Brown demonstrated to the media a helicopter with a 1.8 meter diameter blade in flight, about 15 meters above a transmitting antenna [7].

He passed away at the 3rd of February, 1999, leaving behind him a great deal of contributions to electrical and microwave engineering, and has been undoubtedly a reference for many of the developments on wireless power transmission.

The Microwave-Powered Helicopter

One of the experiments that is clearly pointed out after a brief investigation regarding Brown's curriculum is his demonstrations on wirelessly powering a helicopter with the use of microwaves. This helicopter typically took off from a support mechanism located 7 m from the ground and flew up to 15 m. The prototype can be seen in Figure 2.4.

The system that was used to undertake these experiments can basically be divided into two parts: a microwave beam system responsible for providing the helicopter with the needed power and the power receiving mechanism. These parts will be briefly described in this section.

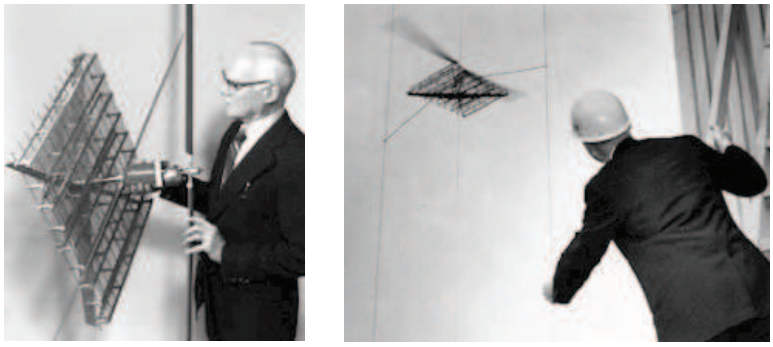

Figure 2.4: On the left, a photograph of William C. Brown hold the helicopter prototype and, on the right, of the helicopter in-flight [13].

Combining Antennas and Rectifiers

When discussing power applications for DC conversion and efficiency, any student or engineer is immediately confronted with the need to decide on the more adequate matter for rectification and, in the particular case of microwave power, radio wave interception.

Antennas are the obvious choice regarding the second part. Still, the receiver antenna should present non-directional characteristics in order for it not to suffer too much from the lack of line-of-sight resultant from oscillations of the given target [6].

Regarding the rectifying circuitry, the initially proposed solution implied breaking up the receiving aperture into a number of smaller horns or parabolic reflectors, each terminated

with an efficient rectifier. This would imply that the receiver array should present significant directivity but it would be troublesome to dispose of the power dissipated by the individual rectifiers. At that time the initial steps in the development of the now common semiconductor diode were still being made and, despite that initially their power handling characteristics still fell short of what was needed, they were eventually placed in the design of the architecture of the power receiver. An efficiency of around 50 % was first obtained by combining 4 rectifying diodes to each antenna element of the receiving array, in this case: half-wave dipoles, distanced half a wavelength from each other.

In total, a 0.2 m^2 half-wave dipole antenna array, composed of about 4480 diodes, was built, weighing slightly over 0.90 kg and presenting an operating level of 250 watts, whereas the helicopter needed a minimum of 180 watts to fly [6].

The Transmitter Beam

The microwave beam system consisted essentially of a 3 m diameter ellipsoidal reflector with a focal length of 1.3 m, illuminated by means of a diagonal horn and a power source, a magnetron oscillator, capable of generating from 3 to 5 kilowatts of power at a frequency of 2.45GHz.

The RF spot size obtained at a distance of 15 m presented a size of approximately 1.2 m [6].

2.2 Methods for Wireless Power Transmission

There are several methods that enable wireless power transmission, being that most of them rely on electromagnetic waves and can be divided into two major groups: near field and far field energy transfer.

Besides the distance between power receivers and transmitter, the biggest difference that distinguishes these methods is the frequency at which the systems are designed to work and the power transfer efficiencies that are possible to be obtain [14].

2.2.1 Near Field Methods

In antenna theory, the non-radiative or reactive part of the near field is defined as "the region immediately surrounding the antenna wherein the reactive field predominates" [15]. Similarly to this definition, near field WPT non-radiative methods apply to when the distance between transmitter and receiver is several times smaller than the wavelength in question, as is the case of:

- Inductive coupling;
- Resonant inductive coupling;

- Capacitive power transfer;

Inductive Coupling

Two conductors are considered to be electromagnetically coupled when the variation of current flow in one of them, which creates a varying electromagnetic field, induces an electromotive force across the other party. An example of the interaction of the coils through magnetic fields is presented in Figure 2.5.

This is possibly the simplest method of WPT currently in use and is the basic working principle of common transformers.

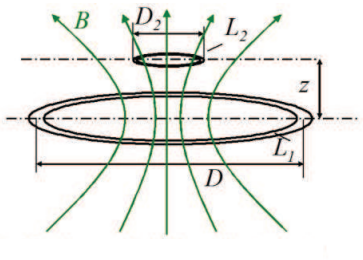

Figure 2.5: Coil arrangement for inductive coupling [16].

As the frequency of operation rises so does the hysteresis and Eddy current losses. Therefore this method shows to be highly efficient when dealing with low frequencies at short distances, which might be appealing for a handful of solutions given it implies a fairly small cost to implement [14].

Resonant Inductive Coupling

Applying the effects of resonance to the inductive coupling method one is able to increase the range and efficiency of power transmission. When two objects resonate at the same frequency they tend to exchange energy efficiently and dissipate little energy to objects with different resonance frequencies. In this way it is expected to preform power transfer with low interferences and losses into environmental objects [17].

Capacitors can be used in series and parallel with coils in order to build such resonant circuits, which can be tuned at a desired frequency.

Various coil link types might be used in order to increase the Power Transfer Efficiency (PTE) of these systems, that is, the ratio between the DC power delivered to the load and the DC power available from source. Transformers usually present 2-coil links, still 3-coil inductive links have presented PTE's of about 79 % at a distance of 10 mm and a working frequency of 13.56 MHz [18].

In [17] a 4-link, strongly coupled, self-resonant coil system is used in order to demonstrate nonradiative transfer of 60 watts, with an efficiency of 40%, through a distance of 2 meters (8

times the coil radius). Each coil pair is composed by two coils: the drive and transmitter coils, at the transmitter, and the receiver and load coils, at the receiver. This setup is presented in Figure 2.6.

The drive and load coils which only possess 1 turn each. They are inductively connected to the transmitter and receiver coils, respectively, which are the ones tuned to resonate.

The transmitter drive coil in this system was connected to a Colpitts oscillator, tuned at 9.9 MHz, this coil transfers power to the helical transmitter coil, tuned at that same resonant frequency but with a slightly larger diameter, which then induces current to the receiver coil (tuned at the same resonant frequency). Energy is then transferred to the receiver's charging coil and used to power a lightbulb.

Figure 2.6: MIT's demonstration panel for wirelessly powering a 60 W lightbulb through resonant inductive coupling [19].

This method has also proven to be a feasible solution for the charging of implantable medical devices at short distances. By using a 3-coil resonance-based wireless power transfer system, tuned a frequency in the medium band (2.46MHz), it has been shown that it is possible to obtain a PTE of 78% at a separation of 10 mm and of 44% at 20 mm [20].

Systems of this type are not extremely costly but, besides the copper needed to fabricate the coils, require an oscillator, power amplifier and capacitors to tune the coils. They show a fairly wide spectrum of applications, from short to medium distances (from 1 mm to 2 m) and versatile working frequencies (from 20 KHz to 13.56 MHz), as can be better seen in the figures of **Appendix C**.

Capacitive Power Transfer

Also known as electrostatic induction, capacitive coupling refers to the transmission of electrical energy through a given dielectric material, such as occurs with in a common capacitor. Dry air, for example, is a very efficient, commonly used dielectric in variable capacitors [21]. Figure 2.7 exemplifies the use of parallel metallic plates for power transfer.

Back in May 20th, 1891, at Columbia College, Tesla proposed before the American Institute of Electrical Engineers the use of high frequency alternating currents, passing through two vertical metal sheets, in order to create a powerful electrostatic fields between. This electrostatic field could then pass through the glass of a lamp thus keeping the its filament at incandescence [22]. Liu, et al., in [23], demonstrated that it is possible to obtain a PTE of 90 %, at a working frequency of 1 MHz, through a distance of 1 mm.

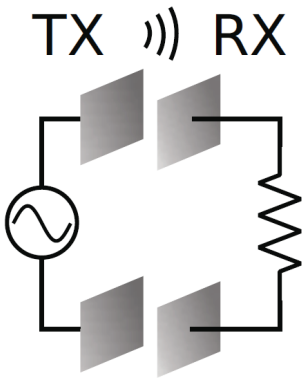

Figure 2.7: Depiction of power transfer through parallel metallic plates [21].

More recently, a novel technique entitled resonant electrical coupling has been recently presented at the 2014 IEEE Wireless Power Transfer Congress. This approach proposes, in its simplest configuration, that 4 conductive plates and 2 inductor coils be used as a tunable resonator and has shown to carry a balance between the PTE, distance and variations of orientation between the boards[24]. With this method it was possible to obtain an efficiency of 40 % through a distance of 4 m, at a frequency of approximately 14 MHz.

2.2.2 Far Field Methods

The far field methods refer to ways of transferring energy wirelessly through distances usually larger than the wavelength, in other words, means to transfer energy over long ranges.

Laser

Similarly to harvesting solar light, it is possible to transform electricity into a laser beam and aim it to a receiver made of photovoltaic cells, thereby controlling the amount of power being transmitted.

Regarding the conversion efficiency of photovoltaic cells, a new world record was achieved in September 2013 by the German Fraunhofer Institute for Solar Energy Systems with an obtained power efficiency of 44.7 %, and gradual improvements are to be expected [25].

The use reserved for laser beams varies with the power and divergence the lasers present, their usage may imply ranges from a couple of meters to a few kilometers. Still, the elements

required to implement a system of this type imply a fairly large investment.

Companies, such as LaserMotive, who was created after they had won the NASA Power Beaming Challenge back in 2009 [26], are already developing wireless power application based on this method, having already been able to fly a UAV for 150 times its battery life [27]. Besides the UAV power links, their products currently encompass optic fibre capable of performing power transfer and point-to-point, ground based, wireless power transfer links.

Microwaves

This method refers to the transmission of power using radio waves with significantly small wavelength, in the centimeter range, and is usually used to transmit power through the atmosphere into outer space.

Microwave power transmission is divided into 3 steps. First, power must be converted from DC to Radio Frequency (RF), then it must be transmitted through a given mean, usually air or vacuum, and, finally, collected by an antenna in order to be turned again into DC power at the receiving point [7]. Each step implies loss in efficiency, and the overall efficiency of the system is equal to the product of the efficiencies of each stage.

In [28], Brown claims to have measured a DC-microwave-DC conversion efficiency of 54 % and the currently recorded maximum RF-to-DC conversion efficiency refers to approximately 90 % efficiency at 2.45 GHz at 8 W input [7].

2.2.3 Wireless Power Reception

Besides the distinct means of emitting electromagnetic energy it is possible to group the means of reception and further DC power conversion into three main categories: scavenging, harvesting and power transmission [29].

Energy scavenging encompasses also energy harvesting and conversion. However, this form of energy reception thrives on the leftover available energy regarding the source and handles transfers in the range of microwatts. While for **energy harvesting**, handles RF power in the order of milliwatts. Both these methods take advantage of the energy produced by "unintentional" transmitters, that is, e.g. not used Digital Terrestrial Television (DTT) or Wi-Fi signals already available in the spectrum [29].

The third category regards **dedicated power transmission** of RF waves. With this method, the power source is flexible enough so that the direction and amount of power it transmits can be modified accordingly to the needs of the receiver at any given moment. Given the control upon the the power feed to the transmitter, and direction of the beam, this method is capable of converting watts of power.

2.3 Currently available Products

There are many major industry associations dedicated to the standardization of WPT regulations in order to potentiate the development of generic wireless charging ecosystems. From this group three associations can be underlined: the WPC, the Power Matters Alliance (PMA) and the Alliance for Wireless Power (A4WP).

The WPC, the oldest and probably most mediated of these associations, started its work in 2008 with the definition of its inductive electrical power transfer standard for distances up to 4 cm. The *Qi* standard (pronounced "Chee" from the Chinese word for spiritual energy flow) is aimed at becoming globally used, so that every device carrying its logo might work with *Qi* chargers, making it so that the user be able to charge his devices wherever it is, having no need for separate chargers, cables or adapters when travelling.

The last version from the WPC's interface definition for wireless power transfer, regarding low powers, was released in June 2013. These specifications guarantee the delivery of 5 W to *Qi* receivers, at a working frequencies between 100 and 205 kHz, at 50 mm of distance [30].

Currently, the WPC is working on extending its power delivery to 10-15 W, providing faster phone charging, an plan to later extend their program to 120 W and ultimately reach 2 kW. On of their main goals is making it possible to build the first wirelessly powered kitchen, in which common appliances will become cable and connector free, making them more convenient and safer to use.

This consortium currently counts with 657 products (last revised in November 8^{th}, 2014) mostly from mobile device manufacturers, like Sony, Google and Samsung, that are now *Qi* compliant.

2.3.1 Consumer Electronics

The number of *Qi*-complaint products increased from 36, at the end of 2011, to 657, at November, 2014. It is thus possible to claim that the market for wireless charging devices presents the tendency to grow. This is no surprise given that in 2009, just in the United States of America, around 57.9 million households possessed from 1 to 3 rechargeable electronic devices, and 7.9 million possessed more than 8 [31]. Therefore, it is expected the comfort that these wirelessly powered gadgets bring will make them broadly popular.

After a swift search on companies devoted to the development of wireless charging application, one is currently confronted with a wide range of enterprises with products of all shapes and sizes.

Duracell Powermat, a PMA certified company, possesses a wide range of charging solutions for top of the line cellphones, such as the iPhone 5, iPhone 4/4S, Samsung Galaxy SIII and even other USB adapters to charge small mobile devices. Their product list offers powermats (see Figure 2.8) capable of charging up to 3 devices simultaneously, being sold from $39.99

up to $69.99, and universal USB receivers in iPhone charging cases.

Powermat's solutions promise to reach a wide number of Americans with their "National Rollout" resultant of their most recent agreement. 100,000 "Powermat Spots" were deployed throughout New York and Seattle in participating Starbucks and Teavana Fine Teas + Tea Bars [32].

Figure 2.8: Powermat for 3 devices [33].

On the other hand, regardless of the the efforts of the above mentioned association to standardize wireless charging systems, even reference companies such as the MIT spin-off WiTricity are not complying to either of the available options. Still, as an exclusive MIT licensee, this companies has issued over 70 patents worldwide [34] and possesses product solutions from consumer electronics to industrial, medical, military and automotive applications. This company has even launched a Computer Aided Design (CAD) software, the WiCAD, editor, in order to make it easier to develop wireless charging applications and to reduce a company's time to market, this can be a very valuable tool for start-up companies that wish to enter de world of wireless power transmission.

These companies are devoted to the use of inductive or resonant inductive coupling in order to create wireless power links between devices, but other methods are also trying to find their way in the market. For example, the Murata capacitive coupling wireless power transmission modules have been used by Hitachi Maxell, Ltd. to create their AIR VOLTAGE wireless charger for the iPad 2 [35].

2.3.2 IC focused Companies

Besides low power fully functional wireless charging mechanisms there has also been developments regarding the market on Integrated Circuits (IC) for wireless power applications.

For example, Linear Technology's have launched their LTC4120 (see Figure 2.9). This device is a high performance wireless power receiver and buck battery charger that enables electrical engineers that are new to the field of WPT a faster development of their own receiver applications.

If the consumer, or developer, is searching for a wider range of solutions then he might come across Integrated Device Technology (IDT)'s products for wireless power transmitter

and receiver solutions [36]. They offer solutions compliant to the WPC and PMA standards for inductive coupling and the A4WP Rezence standard for inductive resonant coupling.

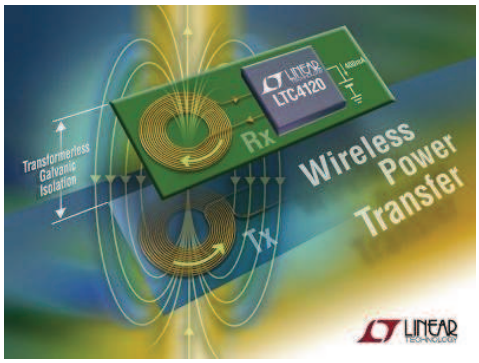

Figure 2.9: Linear Technology's LTC4120 wireless power transfer IC [37].

2.3.3 Automotive aimed

Also the automotive industry has pursued its share of the wireless power transfer market, presenting solutions as simple as integration of wireless charging mechanisms into the deck of a car in order to enable the driver and passengers to charge their devices on their way to work or even proposing a complete shift from the typical, extremely polluting, combustion engines to wirelessly powered electrical motors.

Drayson Racing Technologies, established in 2007, is a motorsport company dedicated to the development of solutions focused on performance improvement, enhancement of energy efficiency and reduction of carbon emissions. This company has been an adviser for the Federation Internationale de l'Automobile (FIA)'s Formula E championship, a new category of car racing composed entirely of electrically powered vehicles, which will have its inaugural edition between September 2014 and June 2015.

Besides their investments in Formula E, Drayson Racing Technologies have united forces with Qualcoom Incorporated and launched the Qualcomm Halo This device is capable of providing up to 40 kW of inductive power for any typical electrical vehicle, enabling it to be charged in less than an hour.

Bombardier has also found their way into this market with their PRIMOVE concept. PRIMOVE will be the first publicly available wirelessly charging system for buses and cars, its concept relies the use of inductive coupling through the periodical spacing of charging coils, buried underground, so that the vehicle is able of charge quickly and conveniently when not in use [38].

2.4 Academic Research on Drones and WPT

The academic world as also aimed part of its efforts to study and bring forward new concepts and applications based on drones.

Georgia Tech, for an instance, has its own UAV Research Facility, headed by Professor Eric N. Johnson, that is completely focused on UAV related research. Its current research topics encompass mainly subjects related to control theory, as vision aided navigation, obstacle avoidance, and management of mobile networks, applied to systems of several devices [39]. This research topic as lead to some protesting in the city of Atlanta because of the populations concern on the use of this data in warfare.

The Technical University of Delft, in the Netherlands, as been focusing strong efforts in the development of its DelFly, which, in its last version, as been entitled the "smallest flying ornithopter carrying a camera in the world" [40].

Specifically regarding WPT for drones, the University of Purdue as picked up on its history regarding the Wireless Power Helicopter and in 2010 demonstrated a small model helicopter taking flight, powered by means of a flared horn antenna on the transmitter end and two dipole antennas on the receiver end. Also the research group led by Professor Zoya Popovic, of the University of Colorado, is working now on a means of wirelessly powering a micro-drone in flight, of enabling it to charge in confined environments and even the ability of charging several drones simultaneously.

Nebraska Intelligent MoBile Unmanned Systems Lab, from Nebraska-Lincoln University, have focused their efforts the other way around. They have been developing a adaptive and autonomous energy management system that used drones to charge sensor networks via inductive coupling [41]. In this way, the drone is no longer the target but the energy transmitter.

2.5 Conclusions

From the numerous companies and products focused on wireless power transmissions components and application that have appeared in the 21st century, it is observable that there has recently been an increase in the focus and investment in this area.

From Tesla's giant coil implementations to William C. Brown's wirelessly powered helicopter, and the most recent developments of companies such as WiTricity, one can conclude that transferring electrical power without the need of cables can have an extreme diversity in its implementation methods, be it short ranged capacitive or inductive coupling or long range microwave power transfer. Each of these methods varies with regards to the power transfer efficiency needed at a given distance and the price that comes with implementing the required hardware.

This field fits the requirements of innovation perfectly and hasn't yet to reach the knee of

the commonly observed logarithmic development of innovative and profitable concepts, and so it still has much room to grow and many ideas to bring forth in years to come.

As a contribution to these developments we propose to bring forth a novel system based on microwave power transmission capable of making a small batteryless quadcopter take flight. Given the typical frequencies of operation of the resonant inductive methods are set in the MHz range this would imply great size and weight for the transmitter and receiver. So that these devices can be placed in the frame of the quadcopter without reducing its aerodynamics the GHz frequencies seem more appealing. Therefore, contrarily to the current major focus on resonant inductive coupling for charging solutions, the method of microwave power transmission was chosen. This system's architecture will be more thoroughly described in Chapter 4.

Chapter 3

Antennas

Antennas are passive devices characterized by their ability to radiate. They are transducers capable of turning electrical signals propagating in guiding devices, such as transmission lines, into electromagnetic waves propagating in free-space and vice-versa. Any conductive material (e.g. a single wire) can radiate in the presence of oscillating charges or, if the charges are moving with uniform speed, through a discontinuity or bend in the wire [15].

Over the last 60 years these devices have played a major role in the structure of typical wireless communication systems, such as television, radio, radar and satellite communications. We can group them by shape and geometry into the following:

Nowadays there are a countless different types of antennas, being that, given their geometry and shape, they usually fall into 3 major groups:

- **Wire antennas**, e.g. dipoles (see Figure 3.1), monopoles, helical, etc.

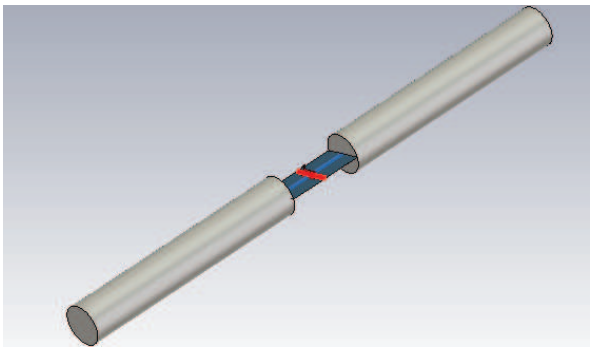

Figure 3.1: Half-wave dipole antenna.

- **Aperture antennas**, e.g. several shapes of horns (see Figure 3.2) or waveguides and slotted antennas.

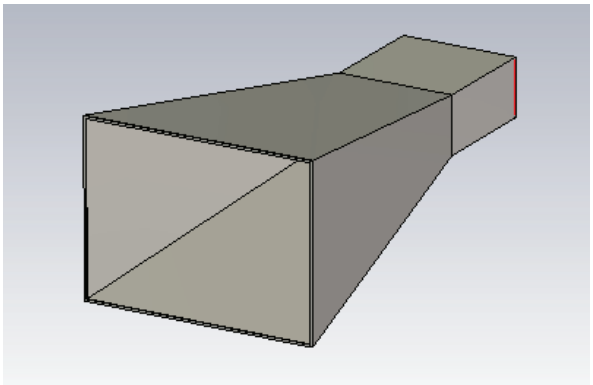

Figure 3.2: Horn antenna.

- **Microstrip Antennas**, e.g. circular and square patches (see Figure 3.3).

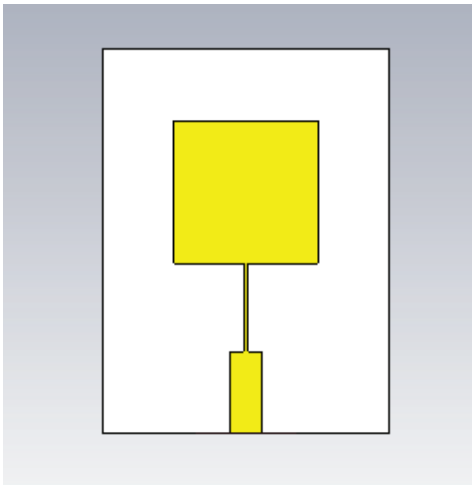

Figure 3.3: Square microstrip patch antenna.

Defining a few parameters it possible to describe their performance and differentiate antennas with regards to their utility for different solutions. The most important fundamental parameters of antennas are their: radiation pattern, directivity, gain, efficiency, bandwidth, voltage standing wave ratio, input impedance and polarization, and are briefly described throughout this chapter. This chapter serves as a theoretical introduction to the most relevant characteristics that define the working principle of antennas and how they can be applied in order to gain versatility for microwave power transmission.

3.1 Fundamental Parameters of Antennas

3.1.1 Radiation Pattern

An antennas' radiation pattern is the graphical representation, or mathematical description, of the variation of the power radiated by it given the overall spacial deviation from the element. [15]

This graphical representation enables a clear and more intuitive interpretation of how the antenna is expected to radiate in the far-field region, thus making it possible so it can be designed in a flexible way to fulfil a project's requirements.

Theoretically, radiation might occur in the same manner in every direction. These radiators are denominated as isotropic and are taken as reference to measure the directivity of other antennas.

Radiation patterns are usually represented using spherical coordinates, being that the azimuthal and elevation angles can be varied in order to analyze in which direction power is being mainly radiated. This coordinate system makes it very intuitive to scan the area around the antenna given that, for example, just fixing θ at 90^o and varying φ between 0 and 360^o a full representation of the horizontal plane is obtained. The vertical variation of radiation in a given direction is observed by simply keeping a constant value of φ and varying θ between 0 and 180^o.

A 3 dimensional representation of radiations patterns can be plotted as seen in Figure 3.4.

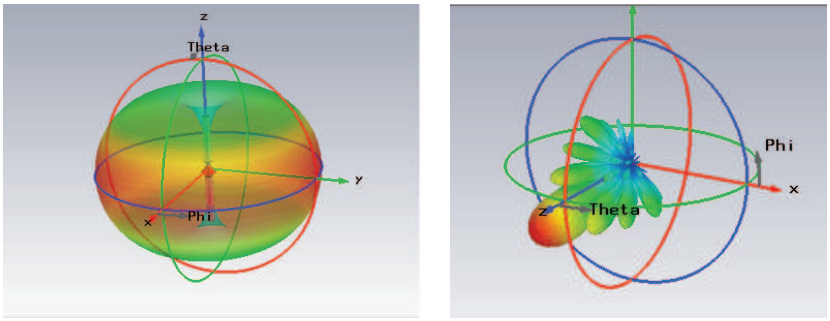

Figure 3.4: On the left, the radiation pattern of an omnidirectional antenna and, on the right, the radiation pattern of a directive antenna.

The image on the left of Figure 3.4 presents an antenna that is non directional in one plane, having maximum power radiating to the sides, while having a directive behaviour in the other, where little power is transmitted. The radiation pattern thus presents a doughnut like shape and is called omnidirectional.

On the other hand, antennas might present maximum power in a single direction. These antennas, are entitled as directional and typically present a single major lobe that is significantly larger then the subsequent minor lobes. The segment containing the direction of maximum radiation is entitled as the major lobe, or main beam, while any other lobe is con-

sidered as minor. Minor lobes are usually present in unwanted direction but can be minimized in order to obtain maximum radiated power in the main beam.

There is currently a wide choice with regards to CAD tools with electromagnetic solvers, making it fairly easy to visualize 3-D representations of an antenna's radiation pattern. However, sometimes it can be easier to interpret the variation of radiated power by bi-dimensional representations with fixed azimuthal or elevation angles (see Figure 3.5).

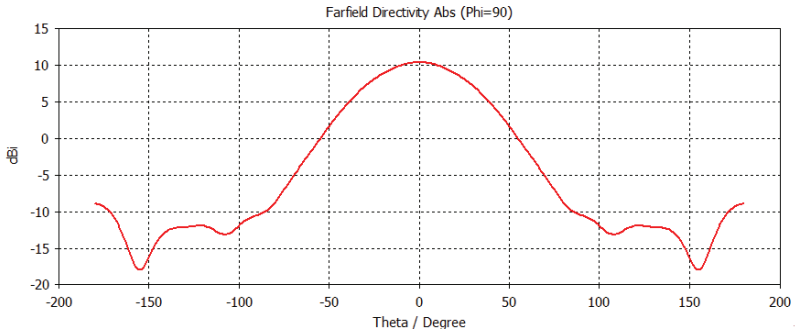

Figure 3.5: 2-D representation of the radiation pattern of the Horn Antenna presented in Figure 3.2.

3.1.2 Directivity, Gain and Efficiency

The directivity of an antenna gives information about how the antenna radiates, that is, if the antenna is extremely directive it will radiate with most intensity in a smaller solid angle, but if it is weakly directive then it will have a wider angle of radiation.

Directivity can thus be defined as the ratio between the amount of radiation in a given direction, $U(\theta, \varphi)$, and the radiation of an isotropic antenna in that same direction. We can write this relation in spherical coordinate system as:

$$D(\theta, \varphi) = \frac{U(\theta, \varphi)}{U_0} \tag{3.1}$$

where U_0 is the power radiated by an isotropic antenna and is defined in 3.2.

$$U_0 = \frac{P_{rad}}{4\pi} \tag{3.2}$$

In practice, directivity is usually refereed to has being the direction at which the radiated power of the antenna is maximum (U_{max}). With this in mind, by combining equations (3.1) and (3.2), one obtains:

$$D(\theta, \varphi) = 4\pi \frac{U_{max}}{P_{rad}} \tag{3.3}$$

Antennas are affected by mismatch losses and power dissipation. Therefore, two antennas

with equal directivity might radiate different amounts of power. The power radiated by each antenna depends on its gain.

To define the **gain** of an antenna, the radiated intensity is compared to that of an isotropic, lossless, antenna feed with the same amount of power. This relation can be mathematically written using (3.1), considering the power contribution of the isotropic antenna U_0 with regards to the total input power, P_{in}, as:

$$G(\theta, \varphi) = 4\pi \frac{U(\theta, \varphi)}{P_{in}} \tag{3.4}$$

Gain is thus directly related to directivity while taking under consideration the power losses in the antenna. This can be mathematically described as:

$$G(\theta, \varphi) = e_t D(\theta, \varphi) \tag{3.5}$$

where e_t is the **efficiency** of the antenna. In other words $e_t = \frac{P_{rad}}{P_{in}}$.

3.1.3 VSWR and Input Impedance

The input impedance of an antenna is the ratio between the current and voltage at the input of said antenna and plays an important role in regards to its efficiency. The impedance of an antenna varies not only with its geometry but with the frequency as well.

An antenna's input impedance usually presents an imaginary and real part, just as in 3.6.

$$Z_a = R_a + jX_a \tag{3.6}$$

Where the real part R_a represents the power that is radiated or absorbed by the antenna and the imaginary part jX_a the power stored in the near field of the antenna. An antenna is resonant once the imaginary part of its input impedance crosses zero, meaning that the current is in phase with the voltage and all the stored power is turned into into radiated power.

At high frequencies, the feed mechanisms used to excite the antennas can be analyzed as transmission lines. It is necessary that these lines be properly matched so that maximum power can be delivered to the antenna.

From equation 3.7 one can derive that if the antenna is properly matched to the transmission line, that is, if the characteristic impedance Z_0 of the transmission line is equal to the load Z_L, the input impedance will be equal to Z_0 independently of the length of the line.

$$Z_{in} = Z_0 \frac{Z_L + jZ_0 tan(\frac{2\pi f}{c} L)}{Z_0 + jZ_L tan(\frac{2\pi f}{c} L)} \tag{3.7}$$

When a load, in this case the antenna, is poorly matched waves are reflected back to the source creating standing waves with different amplitudes of those who are being introduced

into the transmission line, this interaction can be constructive or destructive in certain points of the transmission line.

If an antenna is perfectly matched to the transmission line then it will present a Voltage Standing Wave Ratio (VSWR) of 1. This measure, VSWR, can be used to better understand to which extent the antenna if rightfully matched, given that the higher its value, the higher will be the mismatch losses.

3.1.4 Bandwidth

The bandwidth of an antenna is the frequency range where it can be considered to function with an acceptable performance. From the literature, as a thumb rule, a reasonable definition of bandwidth can be the range where the return loss of the antenna is over 10dB [42][43].

3.1.5 Antenna Polarization

The polarization of an antenna refers to the polarization of plane-wave electromagnetic fields radiated by the antenna in the far field region. Several types of wave polarization are presented in Figure 3.6.

Antennas might be classified as linearly polarized, when presenting E-fields that only oscillate in one plane along the direction of propagation, or as circularly polarized, when the E-field presents two orthogonal components with equal magnitude and 90 degrees out of phase one from the other. Circularly polarized E-fields might rotate with right hand or left hand polarization.

If the perpendicular components don't present equal magnitude the E-field will not be circular polarized but elliptically polarized. This characteristic can be more easily interpreted throughout the frequency response of an antenna if the orthogonal components of the E-field are represented through their ratio, which is known as the axial ratio. For an antenna that radiates circularly polarized waves, the axial ratio must be close to 0 dB, being that as a thumb rule for their measurements a maximum value of 3 dB might be acceptable.

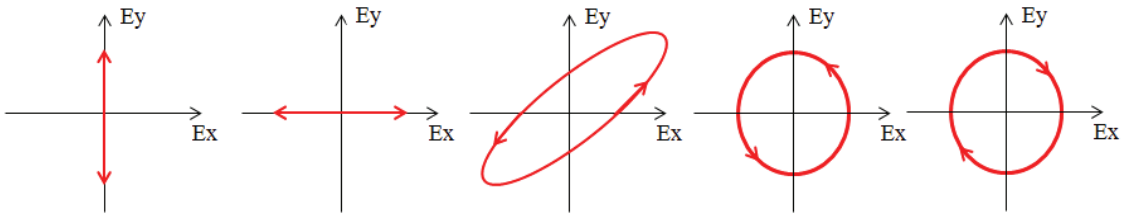

Figure 3.6: Variation of the E-field components for linear, elliptical and circular wave polarizations.

Regarding wireless communications, antennas presenting vertical polarization are not able to communicate with a horizontally polarized antennas, and vice-versa. Two vertically po-

larized antennas that are rotated a given θ one from the another imply that there will be a polarization mismatch, which can be described by the Polarization Loss Factor (PLF):

$$PLF = cos^2(\theta) \tag{3.8}$$

So in order for there to be no power losses due to polarization mismatch, both linearly polarized antennas must present a rotation angle of zero between their E-fields.

On the other hand, if placed parallel to one another, two circularly polarized antennas do not suffer from losses due to polarization mismatch due to rotation. On the other hand, when combined with linearly polarized antennas they imply a PLF of 3dB.

3.1.6 Friis Transmission Equation

It is possible to calculate the amount of received power if two antennas are in the far field from one another. The far field region is only reached once the distance from the antenna is greater than $\frac{2D^2}{\lambda}$, where D is the largest physical dimension of the antenna.

The Friis transmission equation (3.9) relates the gain of each antenna, free space path loss and wavelength to the received and transmitted powers.

$$P_R = P_T G_T G_R \left(\frac{\lambda}{4\pi d}\right)^2 \tag{3.9}$$

Where P_T is the transmitted power, G_T is the gain of the transmitting antenna, G_R is the gain of the receiving antenna, λ is the wavelength and d is the distance between the antennas.

Considering the variables in a logarithmic scale we get:

$$P_R = P_T + G_T + G_R + 20log\left(\frac{\lambda}{4\pi d}\right) \tag{3.10}$$

It must be underlined that this formula only takes under account the path losses of the system, making no reference to losses in the transmitter/receiver or due to polarization mismatch and therefore it is expected that the decrease in power received will be greater that that calculated.

3.2 Microstrip Antennas

Sometimes it is required to design radiating elements capable of being placed in irregular surfaces so that they can be applied without drastically changing the outline of the frame of the object. For this reason, conformable, low profile, antennas such as microstrip (patch) antennas usually come to mind, for they can be directly etched onto substrates using common printed-circuit techniques.

Microstrip antennas are three layer passive devices, of which the bottom layer is a ground plane, usually completely covered in a highly conductive material such as copper, and the top layer presents the patch itself, also made of a highly conductive material. These antennas might present a wide variety of shapes depending on the desired current distribution and resulting radiation characteristics. Between these two layers stands a sheet of dielectric material, commonly referred to as substrate. The structure of a microstrip antenna is presented in Figure 3.7.

Besides being low profile and conformable, these antennas present large versatility with regards to their polarization, input impedance and resonant frequency, and therefore by just adding loads, e.g. varactor diodes, between the patch and ground they can be transformed into adaptive elements [15], as is the case of smart antennas.

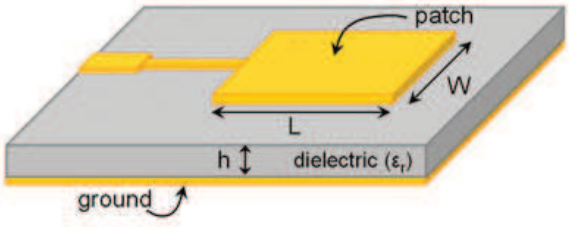

Figure 3.7: Microstrip patch antenna. [44]

However, these antennas also present a few disadvantages. Having usually a high Q, which might be wanted for some applications, might hamper their design at high frequency. At high frequencies, slight dimension differences between the design and printed element might lead to a frequency slip between the antenna's simulation and measured values. Microstrip antennas typically present low efficiency, low power handling and poor polarization purity [15].

The current distribution within the rectangular patch presents a null value at the edges and maximum typically in the middle, while the voltage is 90 degrees out of phase, presenting peak and minimum at opposite edges. Given this behaviour, besides the electrical field lines between the conductor of the top layer and the ground, there will be fringing fields on the edge of the microstrip antenna. The horizontal components of these fringing fields add up and give rise to radiation.

Resonance can be obtained when the input impedance is duly matched, preferably reducing the amount of power reflected back to the feed. Depending also, for the case of a rectangular patch, that equation (3.11) is met. With this equation it is deducible that for the patch to resonate its length must be equal to half a wavelength within the dielectric medium.

$$f_r = \frac{c}{2L\sqrt{\epsilon_r}} \tag{3.11}$$

Where c is speed of light, L the length of the patch and ϵ_r the relative permittivity of the

substrate.

The width of the patch, on the other hand, has little effect on the frequency of operation but can be varied to control the impedance at the edge of the antenna and increase its bandwidth. The larger the width of a rectangular patch, the larger the bandwidth and the lower the impedance at its edge.

The substrates used for these applications typically range from having a dielectric constant between 2.2 and 12 [15], being that using a thick substrate with low dielectric constant results in antennas with better efficiency and wider bandwidth, at the cost of having larger antennas.

Depending on the shapes of the patch and the dielectric constant of the substrate, a single element microstrip patch antenna usually presents a directivity between 5 and 9 dBi [45]. These values might be significantly improved by building an antenna array and being careful with possible coupling effects between the different elements.

Microstrip patch antennas are not only vastly used in aeronautical applications and satellites but also in commercial GPS and Mobile solutions.

3.2.1 Feeding Networks

Microstrip antennas can be feed using multiple configurations, of which the most common rely on feeding through inset feeds, coaxial cables or probe feeds, coupled feeds and aperture feeds.

Inset Feed

Possibly the simplest configuration to fabricate it consists on creating a small opening in the patch's conductor strip, an inset, and directly matching the microstrip transmission line to that point, as can be seen in Figure 3.8. A single transmission line can be directly matched to the input impedance or be composed of various quarter-wavelength impedance transformers.

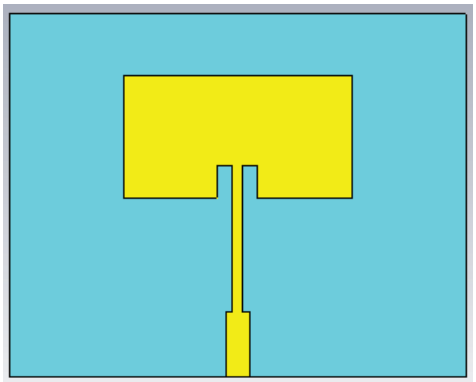

Figure 3.8: Rectangular patch antenna with an inset feed.

In this case, not only will the antenna radiate, but the feed line might also do the same. This might alter the radiation pattern of the patch. Therefore, using this method it is required to take under consideration that the substrate must be chosen so that the antenna can still radiate with the desired characteristics but also spurious feed radiation must be reduced.

Probe Feed

These antennas can also be feed with a coaxial cable placed underneath the patch, inside de substrate. An SMA connector is used, soldering its outer conductor to the ground plane and its inner conductor, through a via, to the patch. This feed configuration is presented in Figure 3.9.

It is possible to pinpoint the input impedance in the same extent as before by shifting the point were the probe is placed.

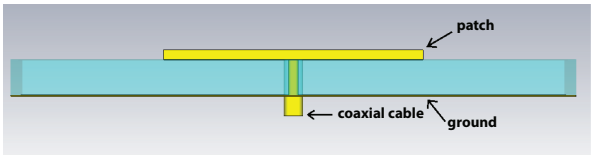

Figure 3.9: Probe feed patch antenna.

One must still take under consideration, especially when working with microwave frequencies, that when the substrate's height is electrically large then this probe will present an inductive behaviour.

In this case, given that the feed is not on the top layer, a substrate that favours radiation might be chosen without implying a degradation in the radiation pattern as found when feeding the patch through an inset. Still, the parasitic interference of the probe might result in radiation in undesirable directions and larger back lobes, which will imply power losses.

Aperture and Coupled Feed

It is possible to gain a degree of freedom by using the previous techniques but trimming the conductors so that the the probe or inset feed don't touch the patch, but are coupled to one another. The example for a coupled inset feed in presented in Figure 3.10.

In this case the gap between the feed and the patch creates a capacitance into the feed that can be used to better match both structures or even cancel the inductance created by the probe feed.

Aperture coupling refers to having two different substrates separated by a ground plane, which is responsible from shielding the transmission line placed in one of the substrates from the patch, placed on the other. A slot (aperture) is made in the ground plane in the point where it is desirable that the fields lines can pass from the feed to the antenna. The benefit of this method is that the substrate where the patch is placed might have a lower dielectric

constant, producing better radiation, while the other substrate might posses a higher dielectric constant, producing tightly coupled fields.

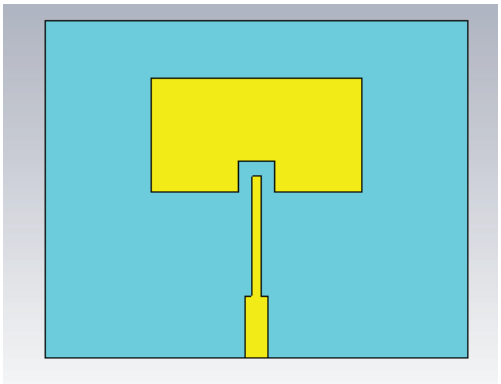

Figure 3.10: Coupled inset feed.

Even though aperture-coupled microstrip patch antennas present the benefit of optimizing independently the feed and antenna structure they are much more difficult to fabricate, aligning perfectly the slot, feed and patch.

3.2.2 Circular Polarization

So far the only pattern refereed to was the rectangular patch. If we consider that these antennas are being feed with the conventional methods, that where previously described, then they radiate primarily linearly polarized waves. However, by slightly varying their geometry or feed it is possible to obtain elliptical or even circular polarizations.

Circular polarization might be obtained by introducing asymmetries in the copper patterns, such as slots, insets or cuts. Possibly the most common way of doing so, in a square patch, is to cut opposite corners, as presented in Figure 3.11. In this way the patch might present a surface current that is circularly distributed throughout the copper, radiating circularly polarized waves.

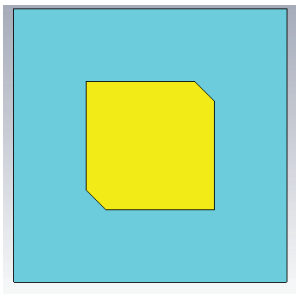

Figure 3.11: Square patch with cut corners.

It is also possible to obtain circularly polarized waves by feeding the patch in different points and thus exciting two orthogonal modes. This can be obtained, for example, by exciting two adjacent sides of a square patch through a power divider or a 90 degree hybrid.

3.3 Antenna Arrays

It is not always possible to obtain the desired radiation characteristics for a particular project using a single antenna. This limitation can be overcome placing simple and identical antennas in a given geometry, and exciting them, in order to direct the radiated energy as pleased. In this way it is possible to improve the directivity of the antenna, cancel interference in desired directions and even determine the direction of arrival of received signal. It is also possible to change the amplitude and phase of the current being feed to each element in real time and create adaptive radiation patterns. This ordered arrangement of two or more antennas is entitled as an antenna array.

Let us now take under account the electrical field of a single half-wavelength dipole which can be mathematically described, given an spherical coordinate system, as:

$$\boldsymbol{E_\theta} = \hat{\boldsymbol{a}}_\theta j\eta \frac{Ie^{-j\beta}}{2\pi r}\left[\frac{cos(\frac{\pi}{2})cos(\theta)}{sin(\theta)}\right] \tag{3.12}$$

If two of these half-wavelength dipoles were placed side by side with a given separation d and excited by currents that differ α in phase, but possess the same amplitude, then, in the far field, the total field would result of the sum of both these antennas' fields:

$$\boldsymbol{E_{Total\theta}} = \hat{\boldsymbol{a}}_\theta j\eta \frac{Ie^{-j\beta}}{2\pi r}\left[\frac{cos(\frac{\pi}{2})cos(\theta)}{sin(\theta)}\right]\left[2cos\left(\frac{\beta dcos(\theta)+\alpha}{2}\right)\right] \tag{3.13}$$

If we take our attention to the second part of equation equation (3.13) we can see how the total field radiated by the array varies with the separation between the antennas and the phase. This parcel is known as the array factor AF:

$$AF = \left[2cos\left(\frac{\beta dcos(\theta)+\alpha}{2}\right)\right] \tag{3.14}$$

From here it can be concluded that the resulting field depends on nothing else than the separation between elements and the way they are excited.

When analyzing an array in the far field, the description of the field of a single element can be simply multiplied by the array factor in order to obtain the mathematical description of the behaviour of the total field.

Arrays come in all shapes and sizes, depending on the end for which they are designed for, be it for commercial, military or personal use. They might be constituted by loop antennas, dipoles, aperture antennas or even microstrip patches, and be arranged from simple planar

structures to irregular surfaces. In this section the behaviour of the field radiated by half-wavelength uniform linear and planar arrays will be analyzed. The currents available to each element will be considered to have the same amplitude and phase difference between consecutive elements, and the coupling between elements and feed networks will be ignored [15].

3.3.1 Linear Arrays

A linear array refers to having all the elements placed along the same axis.

Considering once more the half-wavelength dipoles, but increasing the arrangement from 2 to N antenna elements, also equally spaced by d and with a phase difference of α between each consecutive element, it is possible to predict de behaviour of this topology for an infinity of solutions.

Given the array factor doesn't depend on the directional characteristics of the radiating elements themselves then these can be seen as isotropic sources [15]. Each element will thus present an $E - field$ with current $\mathbf{I}$ such as:

$$E = \boldsymbol{I}\frac{e^{-j\beta r}}{4\pi r}, \qquad \boldsymbol{I} = Ie^{j\phi} \tag{3.15}$$

Because the array is uniform then the current at each element can be described as

$$\boldsymbol{I_1} = Ie^{j\phi_1}; \qquad \boldsymbol{I_2} = Ie^{j\phi_2}; \qquad ... \qquad \boldsymbol{I_{N-1}} = Ie^{j\phi_{N-1}}; \qquad \boldsymbol{I_N} = Ie^{j\phi_N} \tag{3.16}$$

with $(\phi_2 - \phi_1) = (\phi_3 - \phi_2) = ... = (\phi_N - \phi_{N-1}) = \alpha$. And therefore the field for each element will be

$$E_1 = Ie^{j\phi_1}\frac{e^{-j\beta r_1}}{4\pi r_1}; \;\; E_2 = Ie^{j\phi_2}\frac{e^{-j\beta r_2}}{4\pi r_2}; \;\; ... \;\; E_{N-1} = Ie^{j\phi_{N-1}}\frac{e^{-j\beta r_{N-1}}}{4\pi r_{N-1}}; \;\; E_N = Ie^{j\phi_N}\frac{e^{-j\beta r_N}}{4\pi r_N} \tag{3.17}$$

Here the phase might be simplified as

$$\begin{aligned}
&\phi_2 = \phi_1 + \alpha \\
&\phi_3 = \phi_2 + \alpha = \phi_1 + 2\alpha \\
&\phi_N = \phi_{N_1} + \alpha = \phi_1 + \text{(N-1)}\alpha
\end{aligned}$$

and

$$\begin{aligned}
&r_2 \approx r_1 \text{ - } d\cos\theta \\
&r_3 \approx r_2 \text{ - } d\cos\theta = r_1 \text{ - } 2d\cos\theta \\
&r_N \approx r_{N_1} \text{ - } d\cos\theta = r_1 \text{ - (N-1)}d\cos\theta
\end{aligned}$$

As previously refereed, in section 3.3, the interaction between electrical fields radiated by each element, in the far field, can be added together in order to obtain the total field, as seen in equation (3.18).

$$E_{Total} = Ie^{j\phi_1}\frac{e^{-j\beta r_1}}{4\pi r_1}\left[1 + e^{j(\beta dcos\theta+\alpha)} + ... + e^{j(n-1)(\beta dcos\theta+\alpha)} + ... + e^{j(N-1)(\beta dcos\theta+\alpha)}\right] \tag{3.18}$$

Once again it is observable that the array factor only depends on the separation between the different elements, the phase difference of their excitation and the geometry by which they are distributed (or, in this case, the number N of elements).

Simplifying the array factor as a series we obtain:

$$AF = \sum_{n=1}^{N} e^{j(n-1)\Psi}, \Psi = \beta dcos\theta + \alpha \tag{3.19}$$

The array factor for an uniform linear array is nothing other than a geometrical progression and can be even further simplified as

$$AF = \frac{\sin\left(N\frac{\Psi}{2}\right)}{\sin\left(\frac{\Psi}{2}\right)}, \Psi = \beta dcos\theta + \alpha \tag{3.20}$$

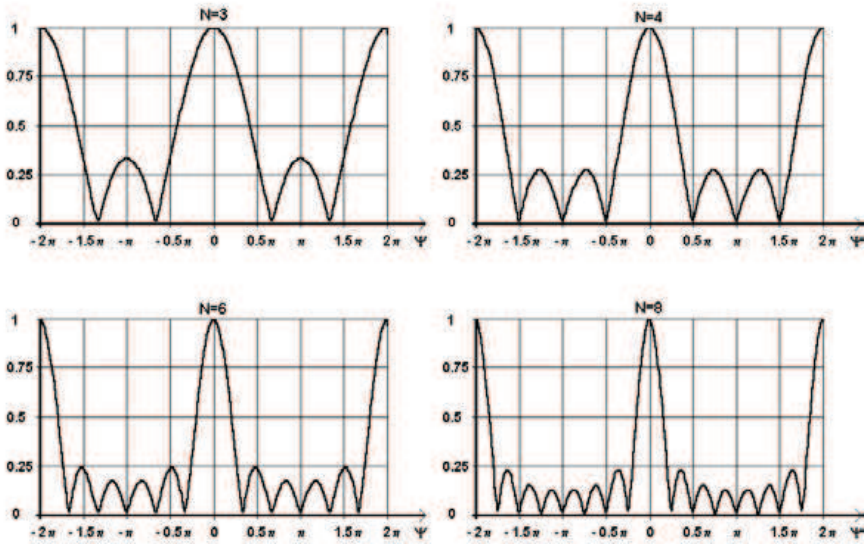

Figure 3.12: Amplitude of the array factor of a linear array for 3, 4, 6 and 8 elements [46].

Besides the obvious increase in the power density of the major lobe of the array as the number of elements increases, which is a result of the beam becoming narrower, also the side lobes suffer changes as their number increases and their power level decreases with the same change in geometry. Theses changes are visible in Figure 3.12).

3.3.2 Planar Arrays

A planar array can be seen as a 2 dimensional linear array in which instead of having only antennas placed in the same axis, e.g. the $x - axis$, they are found throughout a plane, e.g. $xoyplane$. Therefore, in this case it is possible to consider and analyze the array factor of the 2 different axis as linear arrays and then multiply each other, and the respective field of a single element, to obtain the total field.

To make this notion clearer, consider the array factor of the $y - axis$ as:

$$AF_y = \frac{\sin\left(N_y \frac{\Psi_y}{2}\right)}{\sin\left(\frac{\Psi_y}{2}\right)}, \Psi_y = \beta_y d cos\theta_y + \alpha_y \tag{3.21}$$

and the same for the $x - axis$

$$AF_x = \frac{\sin\left(N_x \frac{\Psi_x}{2}\right)}{\sin\left(\frac{\Psi_x}{2}\right)}, \Psi_x = \beta_x d cos\theta_x + \alpha_x \tag{3.22}$$

If both uniform linear arrays have the same length, the complete geometry will have a squared shape. The total array factor of a planar array is the product between the 2 linear arrays as presented in equation (3.23).

$$AF_{Total} = \left[\frac{\sin\left(N_x \frac{\Psi_x}{2}\right)}{\sin\left(\frac{\Psi_x}{2}\right)}\right]\left[\frac{\sin\left(N_y \frac{\Psi_y}{2}\right)}{\sin\left(\frac{\Psi_y}{2}\right)}\right], \qquad \Psi_x = \beta_x d\cos\theta_x + \alpha_x \qquad \Psi_y = \beta_y d\cos\theta_y + \alpha_y \tag{3.23}$$

3.4 Conclusions

Antennas are passive electromagnetic filters capable of being designed to meet the needs of an infinity of applications. As such, microstrip antennas, which present the advantage of being conformable to irregular surfaces and relatively straightforward to design and build, are suitable for this particular application.

At high frequencies these antennas present small enough sizes to be placed in any part of a drones and can even be designed using non-conventional substrates, such as cork, which are low-cost are fairly resistant to complicated climate conditions. These antennas do not imply severe changes in the outline of the drone and can allow it to maintain its aerodynamics.

Also the transmitting antenna will be devised using microstrip patches in a planar array configuration. Arrays of these antennas, once again, are fairly simple to print and design with high directivity, diminishing the effects of path loss to the transmitted power. It is also possible, in future applications, to apply beamforming algorithms to antenna arrays in order

to change the direction of the lobes of the array so that it can "follow" the drone, always supplying to it the maximum amount of power.

Circularly polarized antennas present the benefit of being practically immune to polarization mismatch, still for the transmitting antenna array vertical polarization will be used to make the design of the array more straightforward. While the receiver's efficiency will be compared with regards to both circularly and linearly polarized single patches.

Chapter 4

From Radio Frequency to Direct Current

Rectifiers are electrical devices frequently used in DC power supplies to convert alternating currents into direct currents. Due to their non-linear behaviour, the most commonly used devices for this end are the pn-junction semiconductor diodes.

In this chapter the behaviour of semiconductor diodes will be introduced as well as the benefits they bring to high frequency rectification. Also a few circuit topologies will be presented.

4.1 Semiconductor Diodes

Semiconductors, as the name suggests, are materials characterized by having conductivities between those of conductors and insulators. These can be divided into two general classifications, which are the elemental semiconductors found in group IV of the periodic table (e.g. Silicon (Si) and Germanium (Ge)) and the compound semiconductors which are alloys of group III and V of the periodic table (e.g. Gallium Arsenide (GaAs) or Indium Phosphide (PIn)) [47].

Silicon, for example, is currently the basis of almost all integrated-circuit technology [48]. Its atoms possess four valence electrons, resulting that its first four subshells are completely occupied while the 3p subshell lacks four electrons in order to be filled. To complete its outermost shell these atoms can share one of their valence electrons with each of their four neighbour atoms, thus forming covalent bonds between them.

In solid materials, e.g. crystal, electrons can only take discrete energy values [47], which are gathered into energy bands. Semiconductors present a narrow energy gap between the valence band and conduction band enabling a certain amount of electrons to be excited to the conduction band. At absolute zero temperature, all electrons are below an energy threshold called Fermi level. In these circumstances no electrons are available to conduct

electric current and so, intrinsic (i.e. undoped) semiconductors, behave as insulators. When temperature increases an electron can leave its corresponding atom, provided that sufficient thermal energy exists to break some of the covalent bonds [48], becoming a free electron that is available to conduct electric current. The positive net charge, or "hole", left behind by the electron may attract an electron from a neighbouring atom thus creating a new hole, so for each electron released we get two carriers: an electron and a hole.

This thermal spontaneous generation of hole-electron pairs results in an increase in the conductivity of silicon. Still, these concentrations are far too small to conduct current at room temperature. Conductivity can be increased through doping, i.e. inserting into the semiconductor lattice atoms of the III or V group of the periodic table. Being that for group V an additional electron per atom is added while for the group III an additional hole is added, resulting respectively in a n-type and a p-type semiconductor [47].

A diode is nothing less than a pn-junction, a p-type semiconductor in contact with an n-type semiconductor material [48]. Diffusion, i.e. the movement of charges from a region where their concentration is higher towards a region where their concentration is lower, of electrons occurs from the n-side to the p-side and of holes from the p-side to the n-side.

In an ideal diode, during the positive half-cycles of a sinusoidal input, when a voltage larger than zero is applied between the anode and the cathode the voltage barrier is decreased, diffusion prevails, and the diode behaves like a short circuit, conducting current and presenting an output voltage equal to the input. In this case the diode is said to be forward biased. On the other hand, in the negative half-cycles the diode is reverse biased, the voltage drop applied to the diode is negative, so no current will flow through it and the output voltage will be zero. In this case the voltage barrier is increased leading the holes from the n to the p-side and the electrons from the p to the n-side and the diode is said to be reversed biased.

If a diode is to be followed by a low pass filter made of a single capacitor and a resistor with the proper combination of values, that is, with a time constant high enough that it overcomes the source signal's period, then a DC output is obtained [48]. The higher the value of the capacitor used, the smaller the voltage ripple present at the output.

4.1.1 Schottky-Barrier Diodes

Regarding this project, the aim is to convert RF waves into DC with as greater efficiency as possible so that this received power can be used by a load, the drone. However, common pn-junction diodes present very high junction capacitances and are not suitable from high frequency application [49], thus other solutions must be taken under consideration.

To solve this problem, Walter Schottky devised another junction that could be used as a diode. The Schottky-Barrier Diode, or simply Schottky Diode, is based on a junction usually between a metal (aluminium) and a n-type semiconductor, presenting a much lower junction capacitance and dropout voltage [50]. Their conductivity is mostly due to the majority

carries (i.e. electrons), therefore, these diodes don't exhibit the effects of minority-carrier charge effect present in forward biased pn-junctions, making them able of switching on and off much faster, and much more appealing for high frequency applications [48].

4.1.2 Non-linear Behaviour

Unlike that which was presented in the introduction of this chapter, real diodes do not bear an ideal behaviour. Their I-V curve can be divided, not in two, but into three regions (see Figure 4.1). These regions are defined with regards to these diode's breakdown and threshold voltage's.

In the forward-bias region the current flow through the diode is proportional to the voltage and its I-V characteristic can be approximated by the Shockley diode equation:

$$I = I_S(e^{\frac{V}{nV_T}} - 1) \tag{4.1}$$

where I_S represents the saturation current the diode presents at a given temperature, V_T is the thermal voltage and is defined as $V_T = \frac{kT}{q}$, where k is the Boltzmann constant, T is the absolute temperature in Kelvins and q the magnitude of electronic charge, and n is the diode's emission coefficient, which commonly carries a number between 1 and 2, where 1 reduces the equation to an ideal diode behaviour. Given the exponential behaviour of this equation, current is only duly conducted once the threshold voltage is overcome.

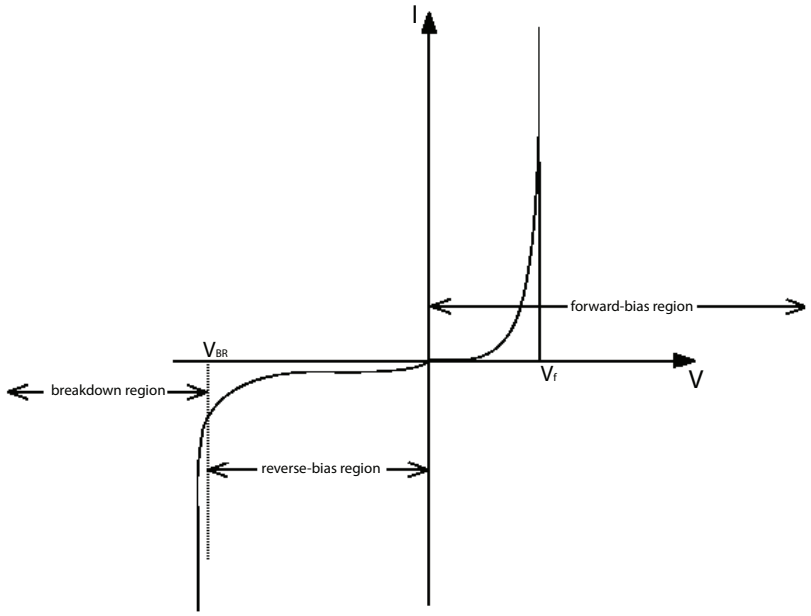

Figure 4.1: Diode's characteristic I-V curve.

When the voltage drop across the diode is negative then the diode is off but still exhibits relatively small reverse currents, this is the reverse-bias region.

The third region is designated the breakdown region and is only entered for voltages bellow the reverse breakdown voltage V_{BR}. In this region diodes conduct in the reverse direction and the current increases rapidly with small variation of the voltage [48].

4.1.3 Diode Model

In order to simulate non-ideal components, obtaining accurate enough results that they approach the values that will be acquired in practice, it is common to resort to a characterization of components through an equivalent model composed by linear elements.

The typical large-scale circuit model used to represent a diode's behaviour, be it *pn* or Schottky [50], is composed by the diode's junction capacitance C_j in parallel with a current source, being that both are in series with an ohmic resistance R_S of value typically between 0.1 and 20 Ω (see Figure 4.2). The typical junction capacitance of a *pn* diode at zero-bias is higher than that of a Schottky diode's, being that for the *pn* the zero-bias junction capacitance lies between 5 and 50 pF and for Schottky diodes between 0.2 and 5 pF [50].

Most diode manufacturers test their components in order to obtain enough parameters so that each batch's behaviour can be correctly modelled. These parameters are then presented in the datasheet of the component and can be used in common CAD software, such as Simulated Program with Integrated Circuits Emphasis (SPICE), to obtain more reliable simulation result. These SPICE parameters can then simply be introduced into RF and microwave simulators. The most important parameters are depicted in Table 4.1.

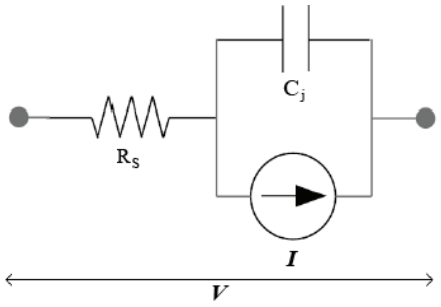

Figure 4.2: Typical large-scale model of a diode

SPICE	Typical Units	Description
B_V	V	reverse breakdown voltage
C_{J0}	pF	zero-bias junction capacitance
E_G	eV	bandgap energy
I_{BV}	A	current at B_V
I_S	A	saturation current
N		emission coefficient
R_S	Ω	ohmic resistance
$P_B(VJ)$	V	junction potential
$P_T(XTI)$		saturation current temperature coefficient
M		grading coefficient

Table 4.1: SPICE Parameters for the HSMS-286x family.

4.2 High Frequency Rectifiers

In a single diode rectifier configuration the maximum peak-to-peak voltage of symmetrical continuous waves, presented at the input, is limited to half the diode's breakdown voltage [51]. This then limits the maximum voltage drop across the diode $V_{O,DC}$ to:

$$V_{O,DC} = \frac{V_{BR}}{2} \tag{4.2}$$

If the peak-to-peak voltage surpasses the breakdown voltage then the diode will enter the breakdown region, current will flow in the reverse direction, and the DC level will no longer increase. The maximum DC power P_{DCmax} that can be dealt by the diode is thus given by:

$$P_{DCmax} = \frac{{V_{BR}}^2}{4R_L} \tag{4.3}$$

where R_L is the load resistance, which is typically 1.4 times the diode's intrinsic resistance in order to guarantee maximum efficiency [52]. This effect limits the conversion efficiency of the circuit at high powers ans is commonly labelled the "V_{BR} *effect*".

When rectifying high frequency signals the effect of higher order harmonics on the circuit's efficiency should be taken under strict consideration. If the circuit is poorly matched then the power available at higher order harmonics might increase, thus decreasing the total DC power.

In RF-to-DC converters it should be also taken under care the proper isolation and matching of the various segments of the circuit. For instance, DC isolation must be provided between the microwave source and the rectifying element, and the DC load isolated from RF power [53]. Also the input impedance, and the lines at the RF segment of the circuit, must be correctly matched to the microwave source or receiver antenna. In order to increase efficiency,

the circuit must possess DC feedback which enables it to properly deal with the DC power available to de diode.

4.2.1 Defining Conversion Efficiency

Probably the most important aspect of wireless power transmission, and energy harvesting, is the efficiency obtained when converting power back into DC. Although, there are several different definitions of efficiency found throughout the literature, making it somewhat difficult to find an agreement regarding which definition to take under account when describing an energy harvesting. In this subsection, the definitions found to be more common, and that were thus used throughout this project, will be presented.

The efficiency of energy-harvesting circuitry lies usually in two definitions: Power Conversion Efficiency (PCE) and Power Overall Efficiency (POE). These concepts serve as guidelines for the receiving end of a dedicated wireless power transmission system.

PCE is the ratio between the useful power delivered to the load and the power that is available at the input of the rectifier, subtracting any fraction of the power that was reflected previously to the diode, whilst POE relates the power that the rectifier output with the total received power. [54]

$$PCE = \frac{P_{outDC}}{P_{incidentRF} - P_{reflectedRF}} \tag{4.4}$$

$$POE = \frac{P_{outDC}}{P_{incidentRF}} \tag{4.5}$$

For WPT systems as a whole, the ratio between the power available at the transmitter, P_{inDC}, and at the receiver, P_{outDC}, can be taken under account to measure the total efficiency of the power transfer system. This relationship is defined as the PTE.

$$PTE = \frac{P_{outDC}}{P_{inDC}} \tag{4.6}$$

In [51] and [54] one can read a thorough analysis on the principles of energy harvesting circuits based on Schottky diodes. These documents present simulation results on the variation of the power conversion efficiency versus the input power obtained by altering the diode's SPICE parameters. From these references one can conclude that for a single diode rectifier:

- the efficiency curve presents a knee shortly before the diode's breakdown voltage is surpassed which leads to a rapid decrease;
- when the value of the series resistance of the diode increases there is an upward shift with regards to at which input power level the maximum efficiency, or knee, is located, but at a cost of a decrease in the obtainable maximum efficiency;

- if the breakdown voltage is increased the efficiency's maximum, or knee, increases and shifts upwards to a large input power;
- as the load resistance decreases so does the maximum power conversion efficiency, but the curves maximum is placed at a higher input power;

The typical variation of the PCE with the input RF power, for a fixed load, is plotted in Figure 4.3.

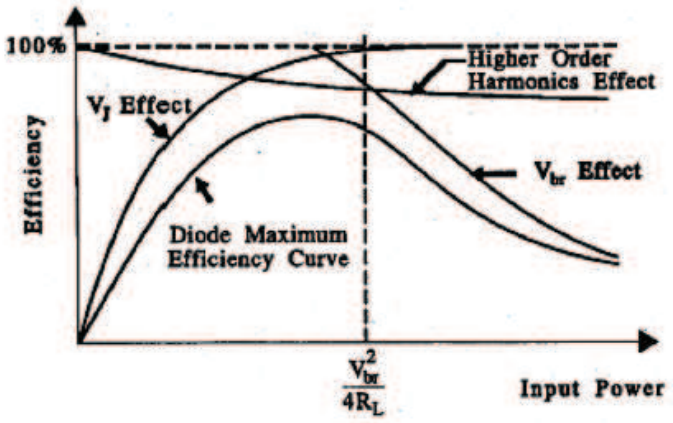

Figure 4.3: Relation of the efficiency with regards to the input RF power [55].

4.2.2 Circuit Topologies

As discussed at the beginning of this chapter, the simplest form of performing rectification is to use a diode followed by a low-pass filter. This topology is known as half-wave rectifier given that the diode is cut for half the period of the input Alternating Current (AC) signal, ideally only conducting the other 50 % of the signal. In practice, the diode can only output the AC signal subtracted by its threshold voltage.

Given that the signal is only rectified in the positive or the negative arches, never in both, the distance between the signal peaks that pass through the diode is larger than if all the waveform was use. Being that the distance between peaks is larger, it becomes more difficult to obtain small levels of output voltage ripple making the output signal less smooth.

Because the AC signal presents positive and negative arches it is possible to design two different topologies under this title, where the diode might be in series (see Figure 4.4) or in shunt (see Figure 4.5) with the input.

For the shunt topology, in order to guarantee that the received microwave power is properly rectified, it is common to place a quarter-wavelength transformer between the diode and the low-pass filter. The capacitor placed at the load of the circuit works as an RF short circuit,

connecting the RF signal directly to the ground. Using the quarter-wavelength transformer the diode sees, not a short, but a open circuit blocking the RF power from the DC load.

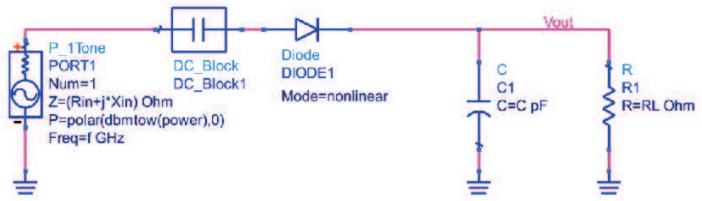

Figure 4.4: Series Half-wave Rectifier.

A DC blocking capacitor might be used to prevent DC reflections in the diode. However, if the rectifier is connected to an antenna, the antenna already provides this behaviour, letting only the RF signal through.

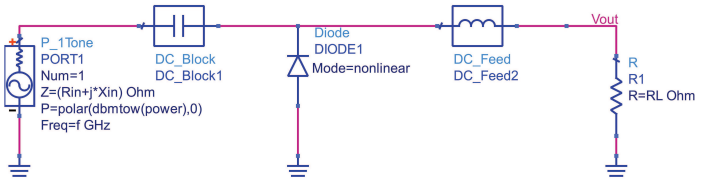

Figure 4.5: Shunt Half-wave Rectifier.

The input impedance of Schottky diodes change depending on the input power available, making it difficult to match them for a broadband of input powers.

As a result of their series parasitic resistances, diodes start to present a linear behaviour as the input voltage increases. This implies that at higher input powers the current and voltage that cross the diode are related by the series resistance R_S.

To use both halves of the waveform, obtaining greater efficiencies, it is common to use two or more diodes in a full-wave (see Figure 4.6) or bridge rectifier.

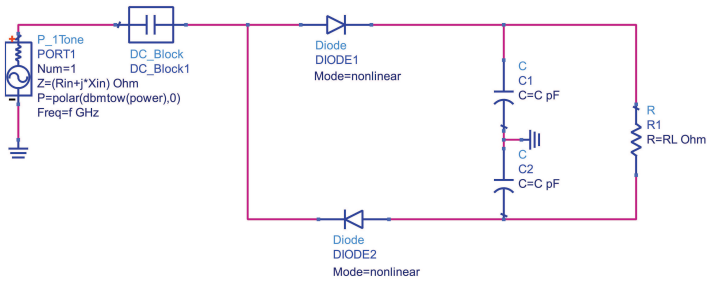

Figure 4.6: Full-wave Rectifier.

4.2.3 Voltage Multipliers

Although it is possible to convert RF into DC using a single diode, their dropout voltage, as small as it may be, will be different from zero and thus the output voltage will always be smaller than the input. In common energy-harvesting circuits, because they are aimed at receiving small values of power, voltage multipliers are needed so that the output is effectively increased.

The most mentioned voltage multiplier configuration in the literature is the Greinacher / Cockcroft-Walton multiplier [54] [56] which can be divided into 2 parts: a clamping circuit and a half-wave rectifier (see Figure 4.7).

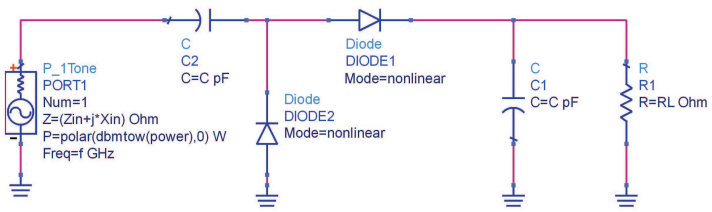

Figure 4.7: Voltage Doubler.

The capacitor and diode on the left, C_2 and $DIODE_2$, respectively, function as a clamping circuit. At the negative half-cycle of the AC input, $DIODE_2$ is forward biased and conducts current, charging the capacitor. During the positive half-cycle, $DIODE_2$ is reverse biased, the source voltage is added with the voltage available at C_2, and diode $DIODE_1$ is forward biased, conducting current. This will ideally result in having twice the amount of Volts available at the output. Because of this behaviour, the single stage Greinacher multiplier is also known as a voltage doubler.

The Greinacher multiplier can be easily extended to several stages simply by cascading various cells of clamping circuits and rectifiers. Given that efficiency is of major importance, then it must be taken under account how many stages are relevant to add to the circuit so that both the output voltage and PCE are increased. The multiplication factor that each stage implies varies with the power available to the circuit and is usually only beneficial until a limited number of stages, typically 3 or 4 [54].

4.3 Conclusions

In this chapter the behaviour of semiconductor diodes was briefly explained, leading to the description of the working principles of the most commonly used RF-to-DC circuit topologies.

Given their low threshold voltage and junction capacitance Schottky diodes seem to be the most straightforward solution in what regards rectification at high frequencies.

It was also discussed that the maximum efficiency of single diode rectifiers is not only limited by the power lost to higher order harmonics but also, at low input powers, by the their threshold voltage and, at higher powers, by their breakdown voltage. These devices show a variation of their input impedance with regards the available power.

Also, the voltage that energy-harvesting circuits are able to present at their output can be greatly and easily increased with resource to voltage multipliers, which can be extremely appealing when the input power presents low values. Given that in this case the amount of power dealt with will be high, at least relatively to common energy-harvesting applications, it is to be expected that a single diode will be enough to obtain the required voltage. However, obtaining the proper current drive poses as the major challenge for this application.

Chapter 5

System Architecture

In this dissertation it is proposed to design and develop a mean of wirelessly powering a quadcopter so that, in this way, its reduced autonomy can be improved.

The amount of power needed by its 4 rotors, so that the vessel may take flight, is not attainable using the inductive coupling methods without adding a significant amount of weight and change in shape to the target. Therefore, microwave power transmission is considered a feasible solution. Moreover, it is possible to build small antennas and circuits at high frequencies, flexible enough that they can be integrated on any part of the UAV's hull.

This chapter introduces the overall characteristics of the proposed system and describes the various components that were designed for it. The simulated values of each individual section of the system are presented.

5.1 System's description

The typical description of an energy harvesting system can be observed in right section of Figure 5.1. From left to right the blocks represent: a transducer, an impedance matching stage, a RF-DC converter, a DC-DC converter and the load. The overall efficiency of this part of the system is obtained by the product of the individual efficiencies of each of its stages. Therefore, the least number of stages must be introduced, and each of them must be carefully designed, for the overall system to present an efficiency as close to 100 % as possible.

In this particular project the receiver is thus divided into:

- The receiving antenna, described by Brown has needing to have a non-directive behaviour in order to make the target able to capture power even when subject to oscillation [6];

- An impedance matching network to reduce mismatch losses between the antenna and the rectifier;

- The RF-DC converter, responsible for rectifying AC RF power into DC;
- A DC-DC converter, to converter excess voltage into current;
- The load, a remote controlled drone;

Unlike the receiver, the transmitter should be composed by an extremely directive antenna so that the power available to the target is as greater as possible. Also it must comprise a power source and, if needed, a power amplifier capable of producing the required amount of power at the design frequency. Of this section only the antenna will be designed.

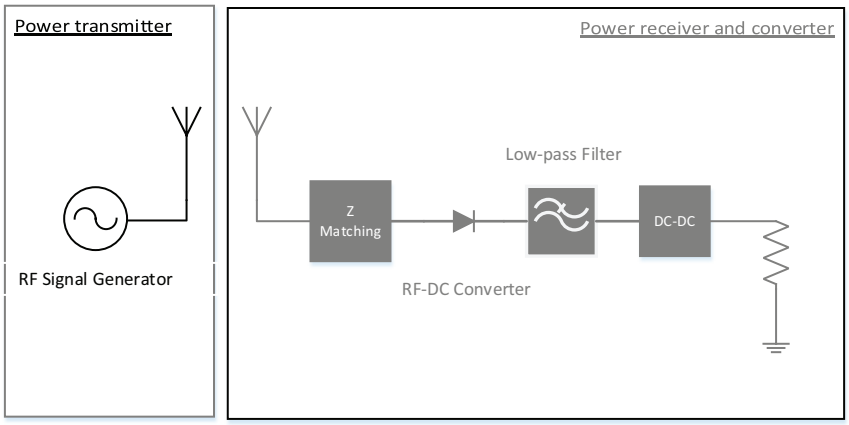

Figure 5.1: Wireless power transmission system architecture.

The Industrial, Scientific and Medical (ISM) radio band chart, presented in Table 5.1, shows the frequencies available worldwide from 13.553 MHz to 24.250 GHz. In order to obtain small antennas the frequency of operation chosen for this project was 5.8 GHz. At this frequency, conversion efficiencies up to 82 % have been demonstrated [52].

Frequency range		**Bandwidth**	**Center frequency**
13.553 MHz	13.567 MHz	14 kHz	13.560 MHz
26.957 MHz	27.283 MHz	326 kHz	27.120 MHz
40.660 MHz	40.700 MHz	40 kHz	40.680 MHz
2.400 GHz	2.500 GHz	100 MHz	2.450 GHz
5.725 GHz	5.875 GHz	150 MHz	5.800 GHz
24.000 GHz	24.250 GHz	250 MHz	24.125 GHz

Table 5.1: ISM radio bands.

5.1.1 The Drone

By a quick market search on the word “quadcopter” one is immediately faced with a great amount of models, available with various features and specifications.

In order to build this proof of concept, a drone small enough that it doesn't need excessive power to run, but is still capable of withstanding the payload of the *rectenna*, must be chosen. The model considered as the best solution, given it presents lower current specifications than the remaining available products, was the Hubsan X4 H107L, presented in Figure 5.2. The specifications for the chosen model can be observed in Table 5.2.

Figure 5.2: Husban X4 H107L

Model	Weight [g]	Battery	Max. Current [A]
Hubsan X4 H107L	27.8	3.7V 240mAh LiPo	1.8

Table 5.2: Hubsan X4 H107L specifications.

Such an electronic device can be modelled as either a variable current source in parallel with a resistor or as a variable resistor. This behavioural consideration is important so that the quadcopter can be considered during simulation and the remaining components designed for maximum power overall efficiency and, subsequently, transfer. For simplicity the device was thus considered to behave as a variable resistor.

5.1.2 Link Budget Analysis

As seen in Chapter 3, if the receiver and transmitter antennas are in the far field one from the other then it is possible to estimate the amount of received power using Friis' formula.

Given the wavelength is known and the power available for transmission will be limited by the available power sources and amplifiers, the main concern should be to design antennas with high gain, guaranteeing that they are as much directive as possible.

As seen in Table 5.2, to guarantee optimal working conditions for the drone it is necessary to provide it with approximately 3.7 V and 1.8 A of continuous current, which implies that 38.2 dBm (6.66 W) of power must be effectively converted.

Connecting a source directly to the drone and varying the voltage applied to it, it was measured, with a multimeter, that the drone is able to takeoff with at least 2.7 V, but still requires an average current of 1.5 A to do so. The minimum requirements for flight are

thus achieved with 36 dBm (4 W). Assuming that in a worst-case scenario the power overall efficiency at the receiver rounds 50 %, at least 40 dBm would be necessary at the receiver end. However, the maximum power available at the laboratory at the time was 35 dBm at 5.8 GHz.

The variation of the received power, in Watts, with the distance, in centimeters, given by equation (3.9), is observable in Figure 5.3. These values were calculated assuming that the transmitter antenna possesses a gain of 20 dBi, the receiver antenna presents a gain of 7 dBi and that 35 dBm are transmitted at 5.8 GHz.

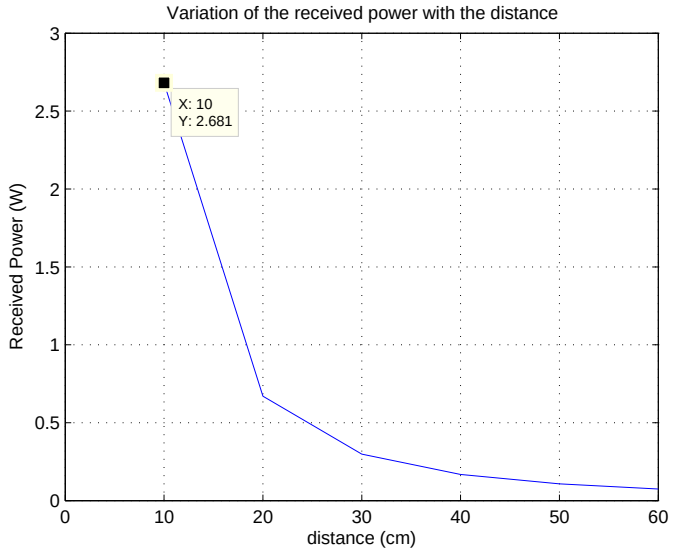

Figure 5.3: Variation of the received power with distance using a 35 dBm power amplifier.

Given such a high power component, that 40 dBm could be delivered to the *rectenna*, was not available at the time for the chosen working frequency, the individual parts of the system will be later validated for a realizable power (32 dBm).

5.2 Transmitter Antenna

There are several types of antennas, all with different characteristics that make them adequate for a wide range of solutions. Antennas might present omnidirectional or directional radiation patterns, conformable or rigid structures, and in some case be easily built and reproduced. In order to better understand the variation of these characteristics and correctness of different topologies for power transmission, the behaviour of several antenna configurations will be studied through simulation.

Unless otherwise stated the simulations made were run using the Transient Solver with the standard accuracy of -30 dB and a hexahedral mesh with 10 lines per wavelength.

5.2.1 Design of a Helical Antenna

The most commonly found transducers in the recent literature on wireless power applications are the coils used for inductive and resonant inductive coupling. Their structure suggests that these can be looked upon as non other than helical antennas (see Figure 5.4).

Moreover, a single helical antenna is a broadband antenna and can easily be designed to present an end-fire radiation pattern with great directivity and circular polarization, making it an appealing solution as a power transmitter.

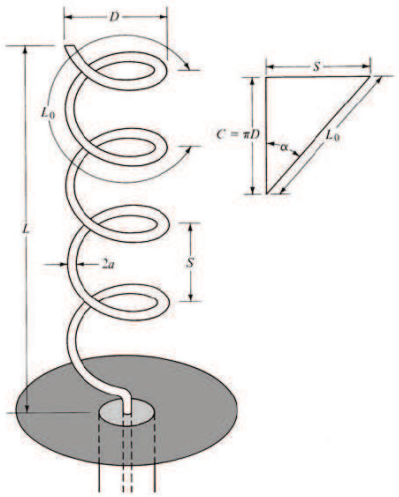

Figure 5.4: Helical Antenna [15].

As presented in [15], to achieve circular polarization in the end-fire mode of an helical antenna it is necessary that the circumference of the helix be in the range of $\frac{3}{4} < \frac{C}{\lambda_0} < \frac{4}{3}$ and that the spacing between turns be about $S \approx \frac{\lambda_0}{4}$. Furthermore it is typical for the antenna to present a ground plane with at least $\frac{\lambda}{2}$ of diameter and feed by a coaxial cable.

It must also be considered that optimally the ratio between the wavelength and the circumference of the structure must be approximately equal the unity [15] and that as the wire radius of the helix increases the resonance frequency decreases. With this in mind, the values in Table 5.3 were considered for simulation.

Parameter	**Value**
Circumference C	5.17 cm
Spacing S	1.3 cm
Pitch angle α	14 °
Ground diameter D	10.34 cm
Coil radius R	0.83 cm
Coil height L	13 cm
Number of turns N	10

Table 5.3: Helical antenna design parameters.

Designing this antenna using Computer Simulation Technology (CST) the object in Figure 5.5 was obtained. The material considered as the conductor was annealed copper and the reflector plane was made from etched FR-4 with a dielectric constant of 4.3 and loss tangent of 0.025.

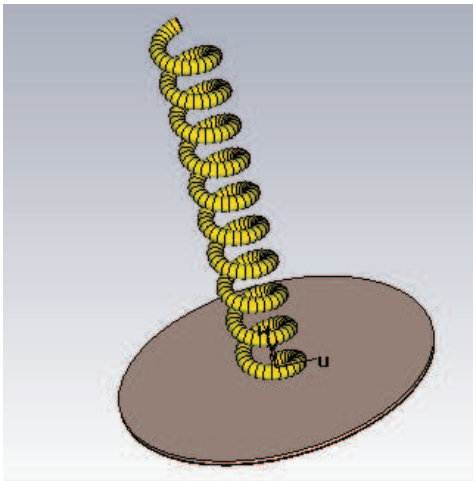

Figure 5.5: 5.8 GHz Helical Antenna.

A bandwidth of 3 GHz, between 3 and 6 GHz, and a directivity of 14.31 dBi at 5.8 GHz were obtained.

This solution presents great directivity and circular polarization as a result of a fairly straightforward design but it also presents the disadvantage of being complicated to reproduce with enough accuracy to fulfil the design specifications of pitch angle, spacing and circumference. Therefore other directive antenna topologies can be taken under consideration to conclude which better applies to this case.

5.2.2 Design of a Quasi-Dipole

The Yagi-Uda antenna is a very practical end-fire antenna array which consists of several dipole elements, given that only one is excited and the rest are parasitic elements feed through coupling. This configuration works exclusively as an end-fire array because the elements in the forward beam act as directors while the parasitic elements in the rear act as reflectors.

To make this antenna easily reproducible, given the tight tolerances at 5.8 GHz, a planar quasi-dipole as shown in Figure 5.6 is firstly proposed.

This single quasi-dipole presents a directivity of 3.9 dBi and return loss of 32 dB at 5.8 GHz.

It can be considered that the horizontal rectangular section at the bottom side of the antenna will behave as the reflector of the array. By adding a parasitic directors evenly spaced in front of the dipole it is possible to increase the directivity of the antenna.

However, even though this single quasi-dipole is simpler to replicate than helical antennas, it still does not present characteristics appealing enough so it can be applied to a microwave power transmission system, specially considering its low directivity and how difficult it would be to place the rectangular board of the array in order to point it to the power receiver.

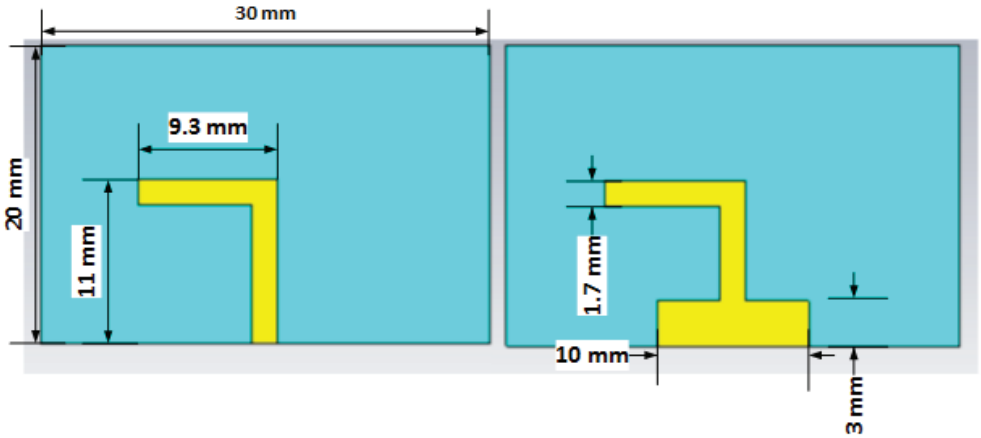

Figure 5.6: Quasi-dipole structure devised as possible element for the transmitter array, with the top layer on the left and the bottom on the right.

5.2.3 Design of a Microstrip Patch Antenna Array

Another solution that is simple to replicate and can easily be displayed in a planar array configuration, in order to gain greater directivity, are microstrip patch antennas. As presented in section 3.2, these antennas are conformable to planar or even nonplanar surfaces, are simple to manufacture with the same means of common printed-circuits and are versatile regarding their fundamental parameters.

Single Patch

The first step in the design of the full array is to design a single patch element. To keep the design simple, in this first approach, the array will be composed of rectangular patches with vertical linear polarization.

Using the design procedure presented in [15] for microstrip rectangular patch antennas, it is possible to calculate the dimensions of the a patch with regards to the resonance frequency of 5.8 GHz for a Rogers RO3006 substrate with 1.27 mm of height and a relative permittivity of 6.15.

The length (L), extended incremental length (δL), width (W), vertical distance of the feeding point from the edges (Y_0) and impedance at the edge of the patch (Z_{in}) obtained are presented in Table 5.4.

L	9.8 mm
δL	0.55 mm
W	13.3 mm
Z_{in}	232.379 Ω
Y_0	0.034 mm

Table 5.4: Patch Dimensions.

From these values the patch was designed using the CST Microwave Studio (MWS), and a frequency sweep from 4.8 to 6.8 GHz preformed, to verify if the variation of return loss and input impedance were as expected.

It was observable that the expected resonant frequency was placed around 5.59 GHz for the dimensions present in Table 5.4, and therefore, to obtain the desired resonant frequency, a parameter sweep was realized by varying the length of the patch antenna from 9.1 to 9.8 mm. The desired length was found at 9.3 mm.

Given that lines with characteristic impedances larger than 105 Ω designed with this substrate at 5.8 GHz imply a line thinner than 0.25 mm, making it impossible to print using the available methods, it is not possible to design a single quarter-wave impedance transformer to feed the patch directly through its edge and therefore it is necessary to excite it using a inset feed.

Through equation (5.1) it is clear that to obtain an input impedance of 50 Ω the feed should be at 3.4 mm from the center of the lower (or upper) edge of the patch, and to obtain a 100 Ω input impedance one should put the feed at a distance of 2.7 mm. A $\frac{\lambda}{4}$ transformer with a characteristic impedance of 70.71 Ω was thus placed at an inset of 2.7 mm to obtain the desired input impedance of 50 Ω.

$$y_0 = acos\left(\sqrt{\frac{Z}{Z_{in}}}\frac{L}{\pi}\right) \tag{5.1}$$

Increasing the mesh to 30 lines per wavelength and using CST's Transient Solver's Optimizer, by varying the antenna's width and the feed characteristics in order to obtain the best possible return loss, a patch antenna with characteristics on Table 5.5 was obtained.

L	9.35 mm
W	17.3 mm

Table 5.5: Optimized Patch Dimensions.

These values are relative to a feed with a width of 0.75 mm and 10.08 mm of length, placed 2.5 mm inside the patch.

In order to obtain a slightly larger bandwidth, a slight increase in the width of the antenna was preformed. In this way, problems that might occur if the printed patch suffers a slight

shift in its resonant frequency, due to printing tolerances, can be reduced. The final patch design can is shown in Figure 5.7.

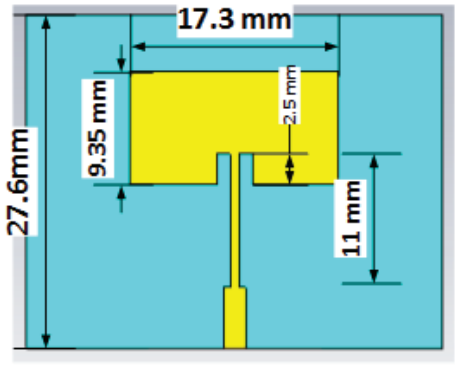

Figure 5.7: Rectangular microstrip patch antenna.

The simulated antenna presents a return loss of 21 dB at 5.8 GHz, as showed in Figure 5.8.

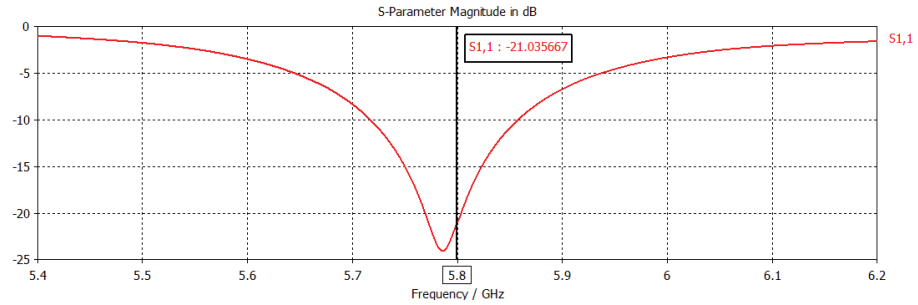

Figure 5.8: S_{11} of the optimized rectangular patch antenna.

The far field directivity of the antenna was also calculated, presenting 7 dBi at 5.8 GHz, and is presented in Figure 5.9.

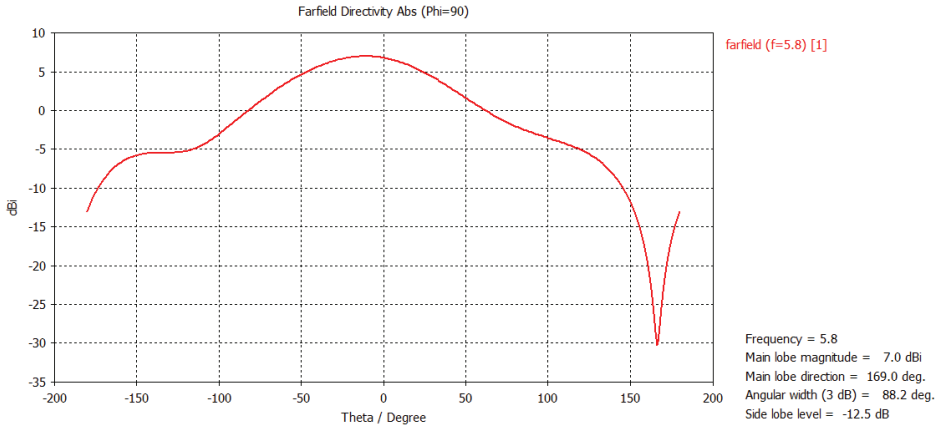

Figure 5.9: Radiation pattern of the individual element.

Once the individual patch element was finalized, the remaining array could be designed.

Array Design

CST's farfield post-processing tool enables a straightforward estimate of the the directivity and gain of a complete array. This tool can calculate the array factor depending on the spatial arrangement of the elements and the amplitude and phase of the current with which each element is being excited. After calculating the array factor, CST can produce a theoretical far field which can then be optimized by varying the spacing between elements to obtain the desired radiation pattern.

Optimizing the distance among array elements between 0.5λ and λ it was verified that the maximum theoretical gain was obtained at 0.7λ distance between patches. Also, by varying the number of antennas in the array, it was observable that the linear value of the gain doubles as the number of antennas also double, as presented in Table 5.6.

Array Configuration	**Gain (dBi)**
1x1	≈ 7
1x2	≈ 10
2x2	≈ 13
2x4	≈ 16
4x4	≈ 19

Table 5.6: Variation of the gain with the number of antenna elements.

Although the Array Factor post-processing tool can quickly produce an approximation of the farfield of the array, it considers the array to be ideal and leaves aside coupling effects between elements and feed lines, and losses in the feed network. Therefore, it is required to design and simulate the full array to account for all discrepancies.

The number of elements was increased symmetrically, in an iterative fashion, to adjust and optimize the dimensions of the antennas and feed lines so that the antenna's parameters would stay close to the desired values. The final configuration is a 16-element array as seen in Figure 5.10.

The feed network of the complete array was composed of quarter-wavelength transformers and lines of 100 Ω of characteristic impedance connected by T-junctions. The array is symmetrical so that the antennas can be excited with the same amplitude and phase. The final quarter-wavelength transformer ends in a line with 50 Ω of characteristic impedance, guaranteeing the matching for external connections.

For this array, a simulated return loss of approximately 18.19 dB was obtained at 5.8 GHz, as can be seen in Figure 5.11, being that the antenna presents a bandwidth of 130 MHz.

The radiation pattern presents a directivity of 19.6 dBi in the main lobe and side lobe level of -15.7 dB. The pattern for a azimuth angle fixed at 90° can be observed in Figure 5.12.

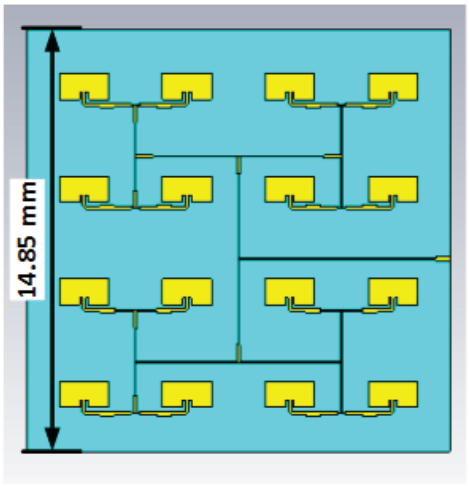

Figure 5.10: 4x4 Rectangular Patch Antenna Array.

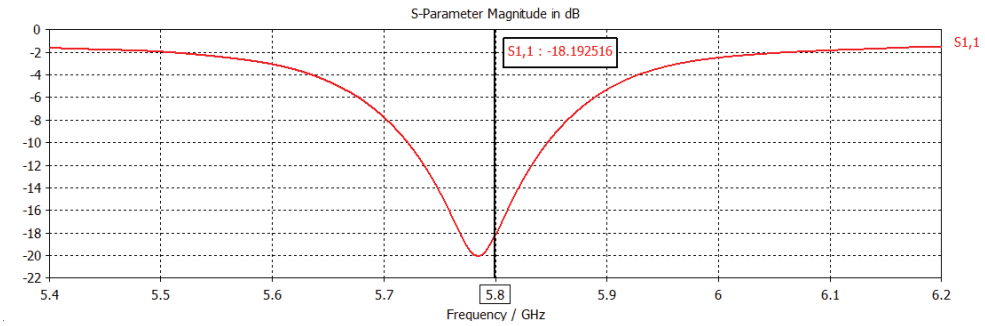

Figure 5.11: S_{11} results of the 4x4 patch antenna array.

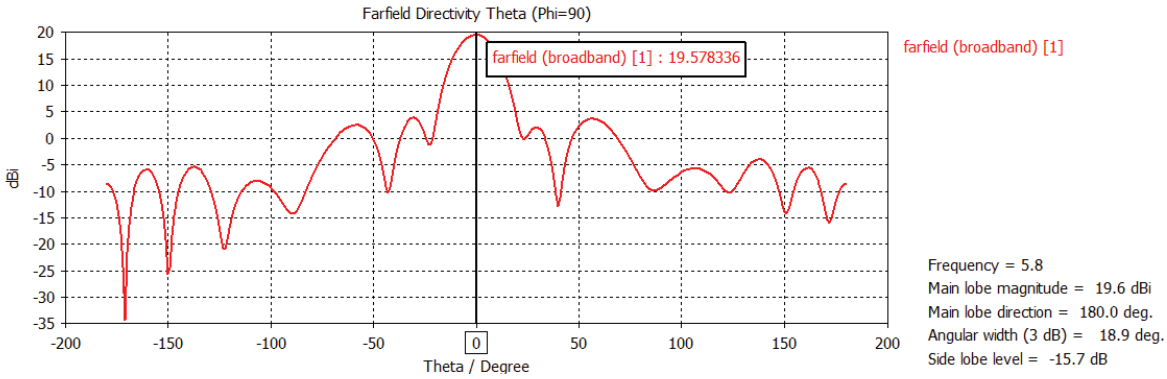

Figure 5.12: Radiation pattern for the 4x4 patch antenna array.

5.3 Receiver

The chosen drone presents a small length and width, approximately 6 cm both ways. Given that the RF-DC converter should not introduce a great impact on the aerodynamics of its hull, and become a significant payload, it must be as compact as possible.

The proposed *rectenna* architecture to be used regards overlapping two different substrates with a ground plane in between them, as presented in Figure 5.13, placing on one face the circuit and on the other the antenna, connecting them through a via. In order to maintain the low profile of the circuit, the antenna used should be a patch. This double layered topology reduces the area occupied by the circuit.

To decide on which substrates to use it is necessary to make compromises regarding the bandwidth, line dimensions, efficiency and field bounding. Therefore, it is proposed for that the top layer, where the rectification circuitry is located, be designed on a thin substrate, $h < 0.8\ mm$, with a low ϵ_r and the bottom layer be designed on a thicker substrate, with $h > 0.8\ mm$, in order to increase the bandwidth of the antenna, and higher dielectric constant to decrease the size of the antenna.

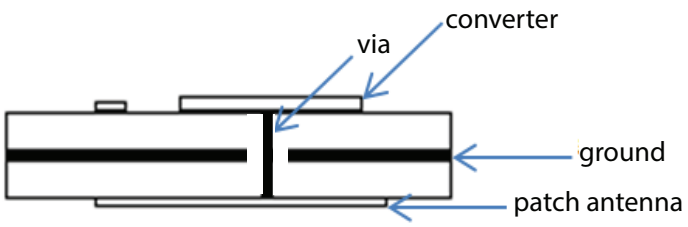

Figure 5.13: Proposed layout for the RF-DC converter.

The substrates chosen for the design of the above described circuits and antennas were the Rogers RO3006 of 1.27 mm of height, with a dielectric constant of 6.15, and the RO3003 with 0.73 mm of height and a relative permittivity of 3.

5.3.1 Antenna

To later test the effects of polarization mismatch between with linearly and circularly polarized antennas two patch antennas were designed.

Using the same equations as before, considering the Rogers RO3006 substrate, two different designs were made. In one case the patch was left with a square geometry and on the other its corners were cut so that the surface current distribution on it could be tuned to result in Right Hand Circularly Polarized (RHCP). The outline of these patches can be observed in Figure 5.14.

The position of the probe feed was then tuned to optimally match the antennas to 50 Ω, increasing their return loss at 5.8 GHz to the maximum value, without losing the desired

polarizations.

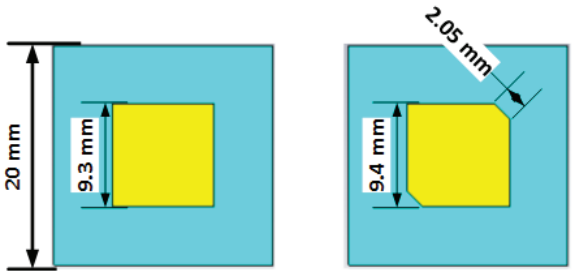

Figure 5.14: Linear vertical polarized square patch antenna and RHCP patch with cut corners.

For the square patch, the optimal length found for the was of 9.3 mm, with the coaxial feed placed 1.65 mm from the center. The results from the simulation of this patch are plotted in Figure 5.15, presenting a return loss of 42 dB at 5.8 GHz and a bandwidth of 162 MHz.

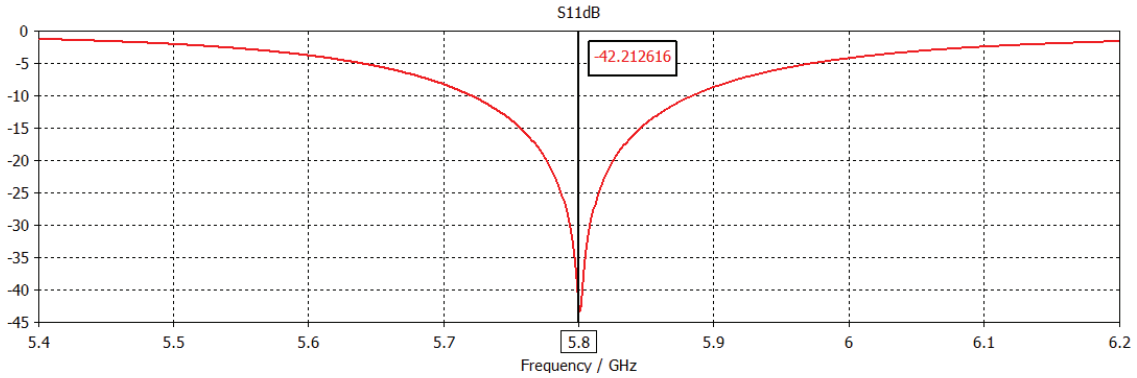

Figure 5.15: S_{11} results for the simulation of square patch antenna.

The patch with cut corners was slightly more difficult match but ended up presenting a simulated 13 dB of return loss at the desired frequency. The simulated values of its return loss can be observed in Figure 5.16.

Even though the return loss is close to the 10 dB thumb rule limit it can be considered a good result given that the antenna presents a S_{11} under -10 dB between 5.69 and 6.05 GHz, adding up to a bandwidth of 315 MHz. Therefore, for any frequency shift lower than 157 MHz the S_{11} of the antenna is still a valid result. The radiation pattern of the antenna presented a directivity of 5.7 dBi and a axial ratio of 0.35 dB at 5.8 GHz, as seen in Figure 5.17. These results were obtained for a patch length of 9.4 mm, with 1.45 mm cuts and the feed shifted 2.15 mm vertically from the center.

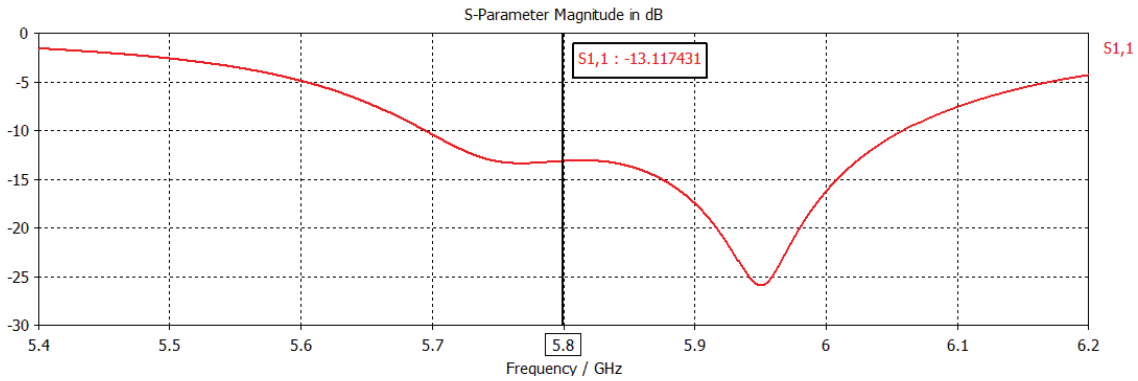

Figure 5.16: S_{11} results for the simulation of circularly polarized patch antenna.

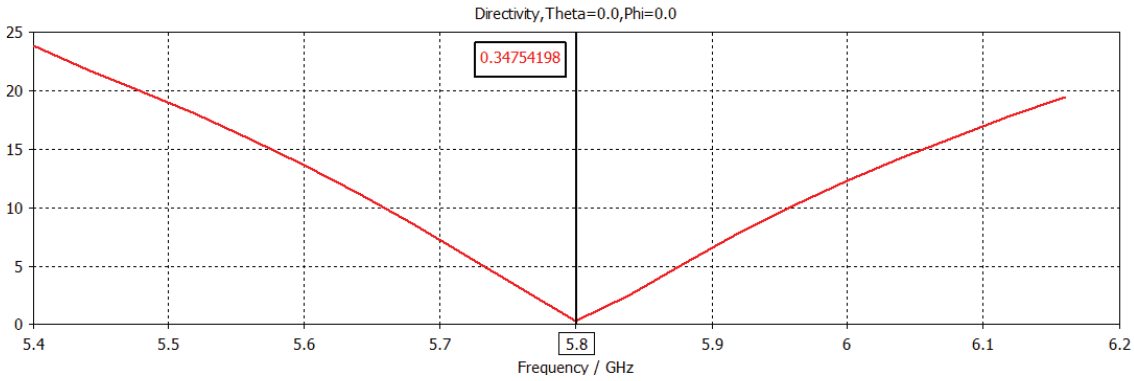

Figure 5.17: Axial ratio of the RHCP patch antenna.

5.3.2 RF-DC Converter

Avago Technologies provides a wide variety of Schottky diodes that differ in specifications and package layout, making them a flexible choice for different designs of RF-DC converters.

Considering that in ideal conditions the drone will need 3.7 V and 1.8 A to fly, which represents 6.66 W of power, that the maximum power conversion is limited to an input power of $\frac{{V_{BR}}^2}{4R_L}$ and that the maximum POE expected from an half-wave rectifier, with high powers at the input, will be around 50 % then the breakdown voltage of the diode should be at least greater than 10 V, as can be seen in(5.2).

$$\frac{{V_{BR}}^2}{4R_L} > 13.32 \Leftrightarrow {V_{BR}}^2 > 106.56 \Leftrightarrow V_{BR} > 10\ V \tag{5.2}$$

The diodes chosen for this project will be the HSMS-2810, which present a minimum breakdown voltage, V_{BR}, of 20 V, a series resistance of 10 Ω and a maximum forward voltage of 400 mV. This diode was chosen also because the alternative with greater breakdown voltage states its value at 70 V which would shift the maximum efficiency to a too large value. It

should also be noticed that at 32 dBm the peak-to-peak voltage of the sinusoidal signal, for a 50 Ω system, will be 25.175 V, meaning that diodes with lower V_{BR} cannot be considered.

For 40 dBm of input power, which implies a peak-to-peak voltage of 63 V, the HSMS-2800 would be the better choice for it presents a minimum breakdown voltage of 70 V.

In order to implement this diode in Advanced Design Systems (ADS), the SPICE parameters that are presented in the datasheet [57] were used. These parameters are displayed in Table 5.7.

Parameter	Units	Value
B_V	V	25.0
C_{J0}	pF	1.1
E_G	eV	0.69
I_{BV}	A	1e-5
I_S	A	4.8e-9
N		1.08
R_S	Ω	10
$P_B(VJ)$	V	0.65
$P_T(XTI)$		2
M		0.5

Table 5.7: SPICE Parameters for the HSMS-281x family.

The model of the parasitic components of the diode's package, up to 3 GHz, is described in the application note AN 1124 [58]. Even though this model is not described for 5.8 GHz it will be taken under consideration given it is still the closest behavioural approximation available.

For the low pass filter the value of the capacitor chosen was 100 pF so that it would present the behaviour of a short-circuit at 5.8 GHz and guarantee that the RC time constant would be lower than the period of the RF wave. Given the variable impedance of the drone, the load value used will be optimized, during simulation, so that the power conversion efficiency is maximized.

Moreover, to obtain maximum power transfer, the power source's output impedance must usually be matched to the conjugate of the loads input impedance, however, the input impedance of the Schottky diodes varies with the available power. This implies that even if the impedances are perfectly matched, at a given input power, the variation of power, due to shifts in distance between the drone and transmitting antenna, will make it so that the receiver circuit will be prone to losses from impedance mismatch. Source pull will be performed to the rectifier with regards to a fixed input power, at which POE is maximum, in order to verify which is the optimal source impedance and the matching network will be designed accordingly.

In the remainder of this subsection, rectifier circuits based on Agilent's HSMS-2810 diode, and its parasitic elements, will be simulated using ADS. Unless otherwise stated, the simulations will be done with input power sweeps from -20 to 40 dBm at a frequency of 5.8 GHz.

Single shunt rectifiers

Single diode rectifiers can present higher RF-DC conversion efficiencies than bridge rectifiers because they only imply the loss factor of the series resistance of one diode [59]. Therefore, and given that the power levels being transferred in this case make it so it is not necessary to implement voltage multiplication, the topology chosen to be implemented was the single shunt rectifier. Harmonic Balance simulations were performed to obtain the variation of output voltage, current and POE with regards to the input power, while the Large-Signal S-Parameter (LSSP) solver was used to find the circuit's input impedance.

Firstly the circuit was simulated using the HSMS-2810 SPICE parameters, in nonlinear mode, and using ideal RF chokes and DC blocks to optimize the output load, thus obtaining the maximum POE for input powers close to 30 dBm.

The microstrip lines were carefully designed for the Rogers RO3003 substrate using ADS's LineCalc tool. They were added to the circuit and optimized to imply a lower decrease of the expected POE. Because the drone behaves as a variable resistor, and the RF-DC converter can only be optimized for a single load, the load was continuously tuned to maintain the POE maximized.

Besides using the low pass RC filter, two radial stubs were implemented to create RF short-circuit for 5.8 GHz at the output of the circuit. In this way, the effect of the high-frequency parasitic components of the filter's capacitor could be neglected, serving as extra guarantee that the power at the fundamental tone and second harmonic would not affect the load. The final layout can be observed in Figure 5.18.

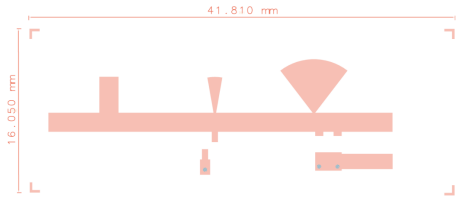

Figure 5.18: Single shunt rectifier circuit layout.

To overcome the fact that it would not be expected that powers greater than 30 dBm would be received in the far field of the transmitting antenna, the optimization of the circuit was done with regards to the point of maximum POE closer to a power input of 30 dBm. As the power at the input increases so does the value of the output voltage, until a certain point. Once the output voltage saturates, the diode will eventually come close to the reverse

breakdown region, making it no longer capable of producing proper rectification. If the circuit is designed to reach high levels of output voltages, by adjusting the maximum power conversion point, then the unneeded excess of voltage can later be converted into current using a DC-DC Buck converter.

Source pull was applied, considering the input power which presented the maximum POE, and then a single-stub matching circuit was designed, using ADS's Smith Chart utility, so that the output would present 50 Ω of input impedance for that same power and could be matched to the antennas.

An optimal load of 270 Ω was obtained through tuning and the matching stage was design in order to match the input to 50 Ω at 27 dBm. The simulated POE and output voltage variation is presented in Figure 5.19.

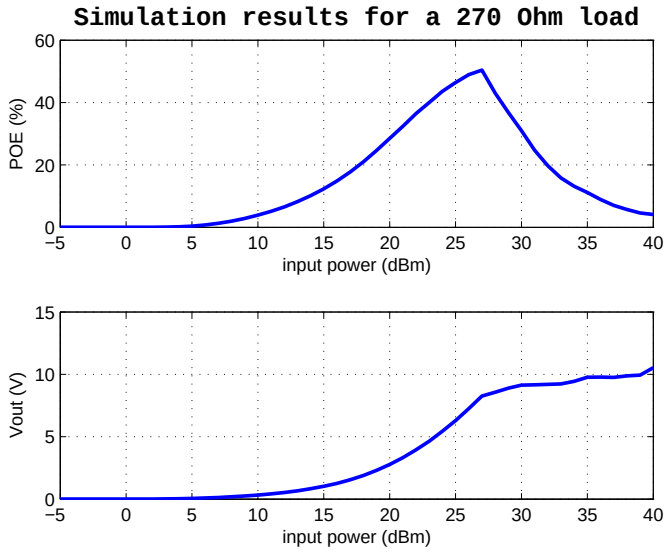

Figure 5.19: Simulation results of the POE and output voltage of a single shunt rectifier considering a 270 Ω load.

Given that the ADS LSSP Schematic solver does not account for additional parasitics of the geometry of circuit, the circuit was also optimized by adjusting the microstrip lines with regards its Momentum simulation. For this case the optimal load obtained was 100 Ω and the circuit was matched at 29 dBm. The obtained POE and output voltage variation with regards to the input power is showed in Figure 5.20.

This distinction was made in order to later compare the accuracy of the solvers present in the Schematic window of ADS and the Momentum solver. In this way it can be possible to understand if for RF-DC converters Momentum simulation is in fact needed or if the Harmonic Balance and LSSP solvers are sufficient.

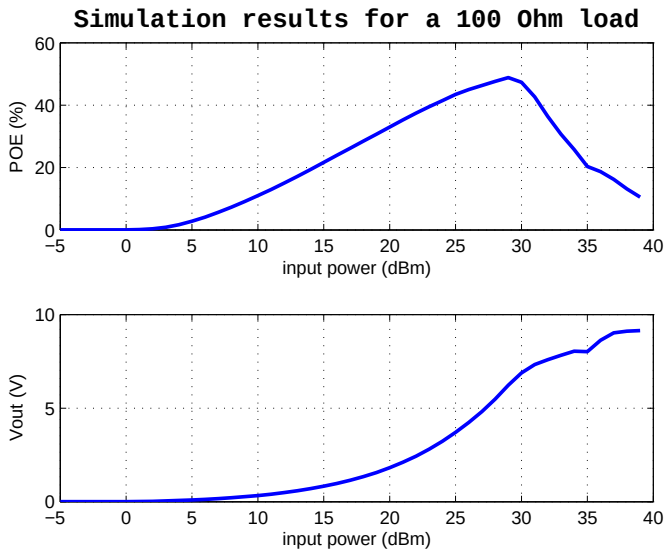

Figure 5.20: Simulation results of the POE and output voltage of a single shunt rectifier considering a 100 Ω load.

5.3.3 DC-DC Converter

To keep the size of the circuitry to a minimum, this section should not depend on external microcontrollers to assure the voltage regulation. An IC Buck Converter, the SEMTECH SC4215A, was chosen for the DC-DC conversion section of the power reception stage. This step-down converter can present a maximum output current of 1.5 A and its output voltage can be set using a simple voltage divider. The designed layout is presented in Figure 5.21.

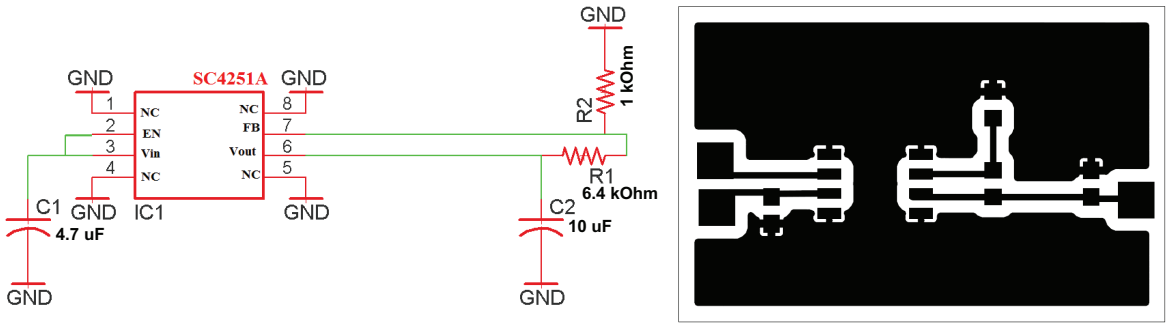

Figure 5.21: The schematic, on the left, and the layout, on the right, of the DC-DC converter.

5.4 Conclusions

A microwave power transmission system was described and the frequency of operation chosen at the beginning of this chapter, being that the design of each part of the system, and

expected results, were later presented.

The only element designed for the transmitter end was a 16-element microstrip antenna array. Microstrip antennas were chosen given their low-profile and easy reproduction which makes it simple at higher frequencies to design an array with the needed radiation characteristics with fair precision. The antennas present linear polarization and are slightly wider than the initial theoretical values to improve the bandwidth of the antennas. The simulated array presented a total of 19 dBi of directivity and 18 dB of return loss at 5.8 GHz.

On the other hand, all the elements of the receiving section were described. Both a linear and circularly polarized patch antenna were simulated with satisfactory results and a single shunt rectifier was designed.

The POE of the rectifier varies with the load of the circuit and with the available input power. Therefore, it becomes complicated to optimize the rectifier for a variable load, such as the drone, and for variable input powers, such as does implied by the movement of the drone. The circuit was thus maximized considering as input power a point, close to 32 dBm, where maximum POE and output voltage were obtained.

If the rectifier is not capable of solely providing the drone with its current and voltage requirements, the DC-DC converter is also available to guarantee the voltage provided to the drone is kept at a stable level and that the current can be stepped-up.

Since all the segments of the microwave wireless power transmission were designed and their expected behaviour demonstrated through simulation, the circuits and antennas could be printed and properly tested.

Chapter 6

Implementation and Experimental Results

Once built, the developed antennas and RF-DC converter were subjected to experimental testing to evaluate their performances and find the level of agreement between predicted and practical results.

In this chapter, the behaviour of each component is individually analyzed. The first section describes the results obtained for the transmitter's microstrip patch antennas while the second section deals with the data obtained from the patches for the *rectenna*. The behaviour and further experiments on the designed RF-DC converter are presented in the three following sections. The final section summarizes the results and main conclusions drawn from each experiment.

6.1 Microstrip Antenna Array

6.1.1 Return Loss

To evaluate the proximity of the simulations with the practical values before printing the full 4x4 array, a single rectangular patch antenna was printed and measured with an E8361C PNA Microwave Network Analyzer, calibrated for a frequency between 5.3 and 6.3 GHz. Figure 6.1 presents the corresponding results compared to the expected simulated values.

The antenna presented a downwards shift of its S_{11} minimum of 94 MHz from the desired resonant frequency, being that its maximum return loss is very similar to the desired value, 22.5 dB, but at a frequency of 5.7 GHz. At the intended resonant frequency this antenna does not comply to the requirements given that its return loss is only 8.1 dB.

In order to bring the simulation results closer to the ones obtained with the network analyzer the relative permittivity considered was changed from 6.5 to 6.7. The dimensions of the array were once again tuned to fulfil the requirements. The full 4x4 array, presented in

Figure 6.2, was then printed and its S_{11} parameter measured.

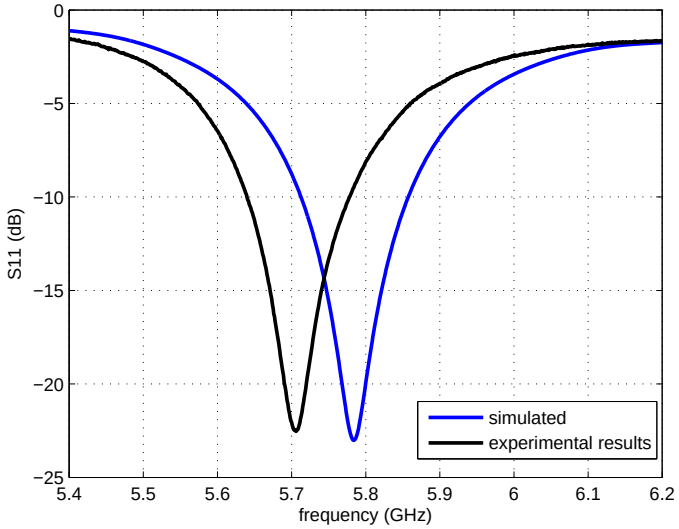

Figure 6.1: Simulated and measured S_{11} parameters of a single rectangular patch.

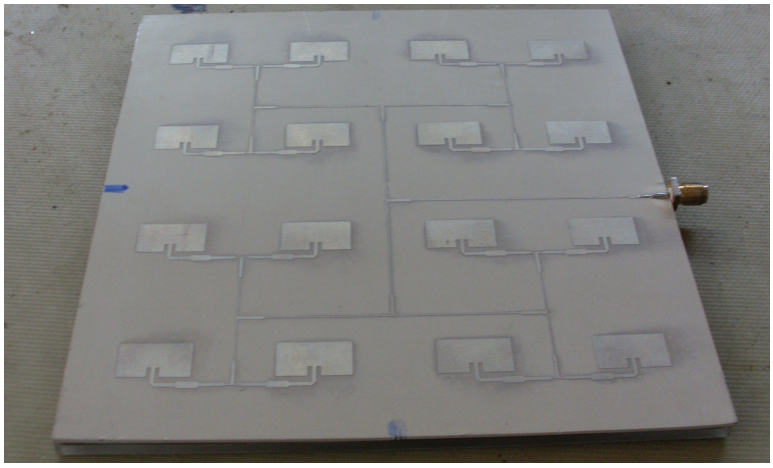

Figure 6.2: Photograph of the printed antenna array.

It can be observed, in Figure 6.3, that the shape of the measured return loss is slightly different from that of the simulated antenna and that the minimum of the S_{11} suffered an upwards shift of approximately 64 MHz from the desired frequency. The change in resonant frequency could maybe have been predicted with a finer mesh refinement. The original mesh used 1,959,694 tetrahedral mesh cells, however, by using 3,913,175 mesh cells a resonant frequency of 5.83 GHz is obtained, which comes even closer to the measured results but implies a much longer simulation time. Still the antenna presents a S_{11} of approximately -10 dB at the desired frequency making it acceptable for the project's requirements and still

within the ISM band.

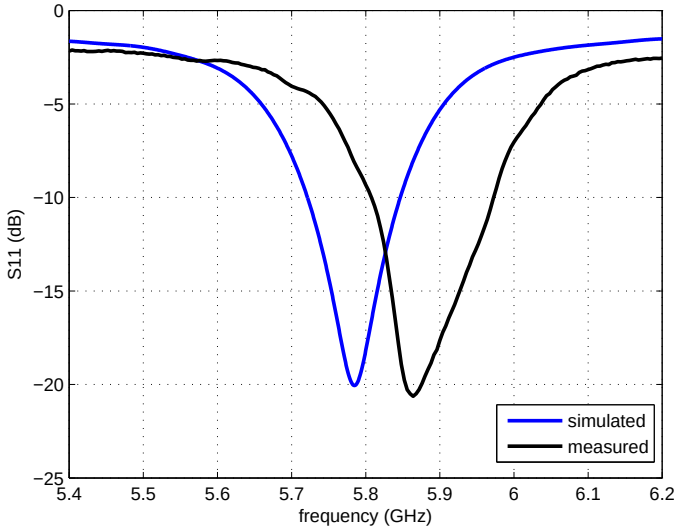

Figure 6.3: Simulated and measured S_{11} parameters of the full 4x4 array.

6.1.2 Gain and Radiation Pattern

Given the S_{11} values of the antenna array were considered acceptable, the antenna's gain was measured with resort to a hybrid tapered/rectangular anechoic chamber, that possesses a working frequency between 1.7 and 18 GHz, capable of performing angular steps of 0.01°. The antennas were distanced 4 m from each other which, considering that the maximum dimension of the array is 15 cm, places them in the far field.

By measuring the S_{21} values of the array, using a Rohde&Schwarz ZVB20 Vector Network Analyzer, at different rotation angles and comparing the results to those of a reference horn antenna with a known gain at 5.8 GHz, an ASYSGH-5480, a two-dimensional radiation pattern corresponding to the plane perpendicular to the rotation axis (vertically oriented in this case) could be obtained.

The measured values at 5.8 GHz, for both vertical and horizontal planes, are presented in Figure 6.4.

This array presented a gain of 16.8 dBi at 5.8GHz, and of approximately 18 dBi at 5.86 GHz. The measured radiation pattern, compared simulated results at 5.8 GHz for Phi = 0°, is presented in Figure 6.5.

Using Kraus' approximate formula [15] it was also possible to verify that the array presented a directivity of 20.8 dBi.

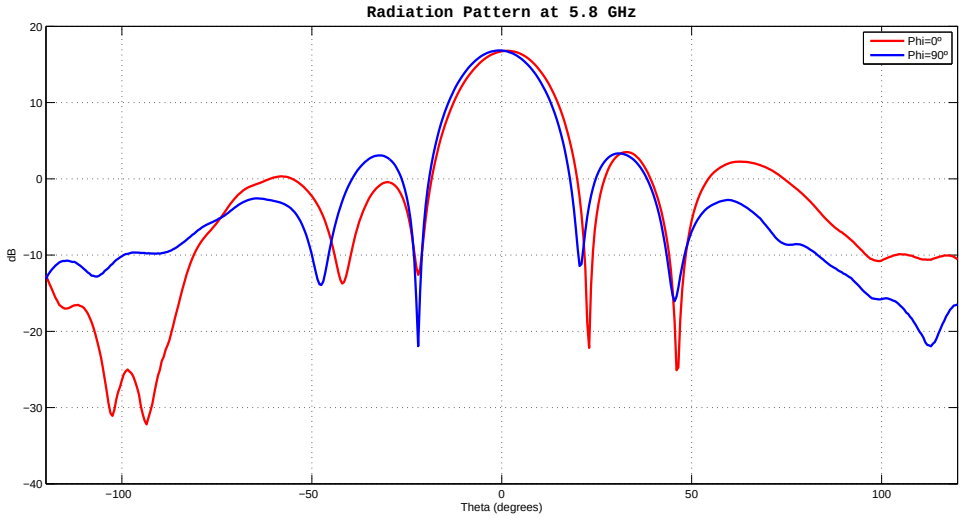

Figure 6.4: Radiation pattern of the antenna array at the vertical and horizontal planes.

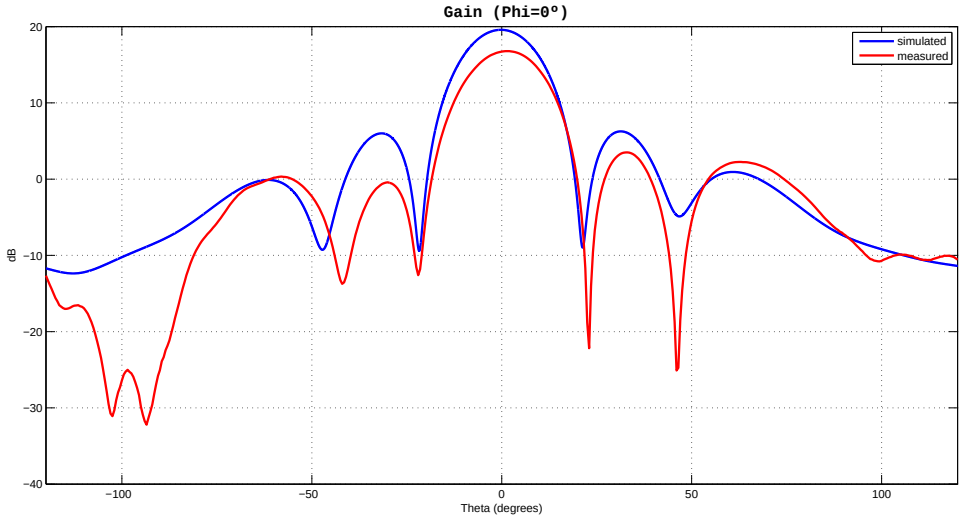

Figure 6.5: Simulated and measured gain of the 4x4 patch antenna array for Phi = 0° .

6.2 Receiver Antennas

Once both receiver patch antennas were printed, drilled and soldered, their S_{11} parameters were measured and compared to the previously displayed simulated results. The antennas are presented in Figure 6.6.

The measured and simulated S_{11} for these patches can be seen in Figure 6.7, for the square patch antenna, and Figure 6.8, for the RHCP antenna. These results shifted from

those that were expected but both antenna present acceptable return losses at the desired work frequency, 14.7 dB for the linearly polarized patch and 13.2 dB for the RHCP one.

This shift between the simulated and measured results is believed to be a consequence either of milimetric shifts in the position of the feed, due to the fact that the drilling was made by hand, or from the presence of solder to secure the feed, which was not accounted for in the simulations.

Later, the supposedly RHCP patch was measured to verify if the antenna truly possessed an acceptable axial ratio at 5.8 GHz. This antenna ended up presenting a directivity of 6.8 dBi, regarding Kraus' formula, while the linearly polarized one presented a directivity of 7.6 dBi. The remaining relevant behaviour of the radiated energy from the RHCP antenna is plotted in Figures 6.9 through 6.12.

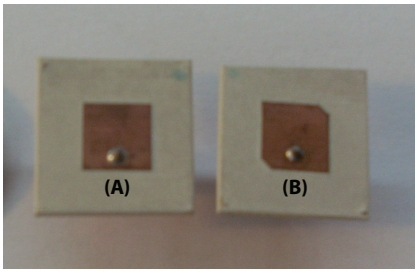

Figure 6.6: Linearly (A) and circularly (B) polarized antennas for the receiver.

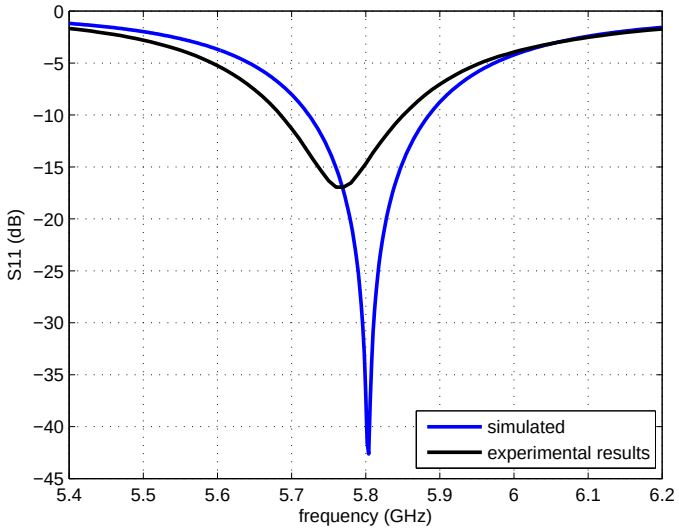

Figure 6.7: Measured and simulated S_{11} of the 5.8 GHz square patch antenna.

In Figures 6.9 and 6.10, it is visible that, for both the horizontal and vertical planes, the axial ratio of the antenna is bellow 3 dB, which confirms that it radiates in a circularly polarized mode.

Moreover, given that between $\pm 30^{\circ}$ the antenna presents a cross polarization rejection of approximately 20 dB, as seen in Figures 6.11 and 6.12, it can be concluded that, successfully, the antenna presents right hand circular polarization.

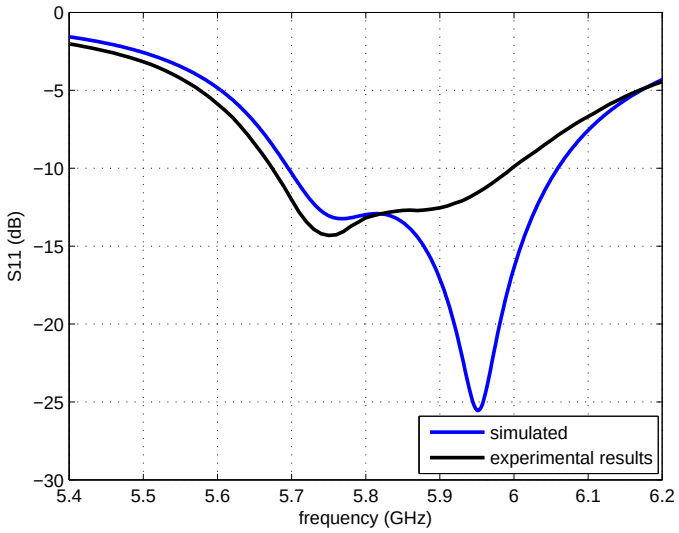

Figure 6.8: Measured and simulated S_{11} of the 5.8 GHz RHCP patch antenna.

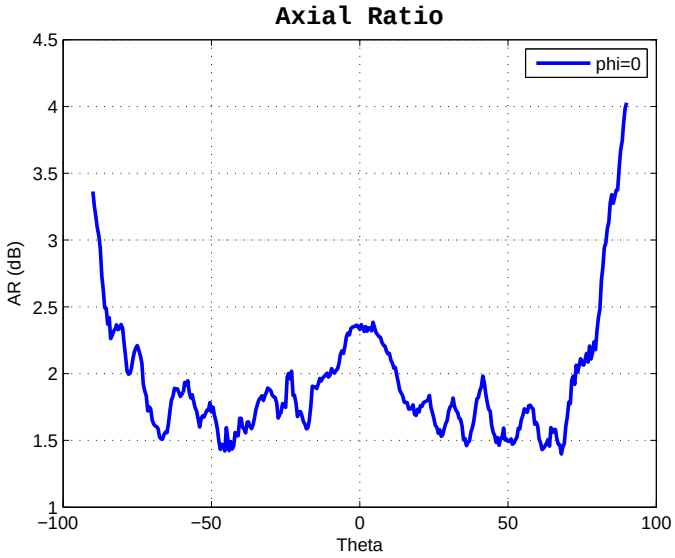

Figure 6.9: Axial ratio of the RHCP patch antenna for Phi = 0° measured at 5.8 GHz.

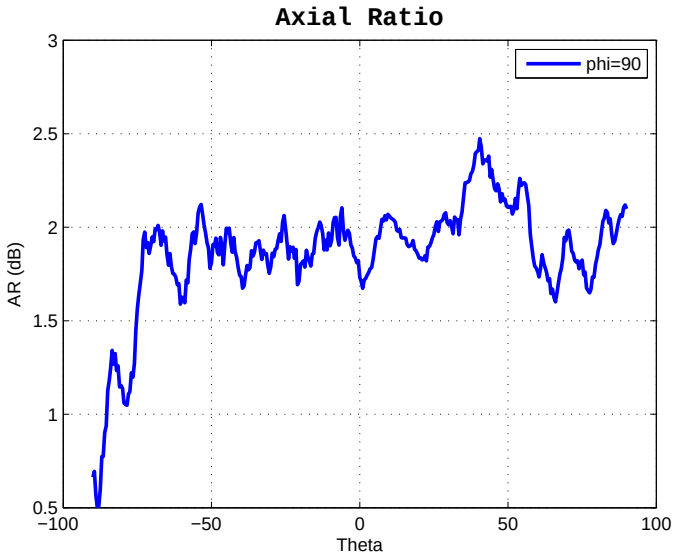

Figure 6.10: Axial ratio of the RHCP patch antenna for Phi = 90° measured at 5.8 GHz.

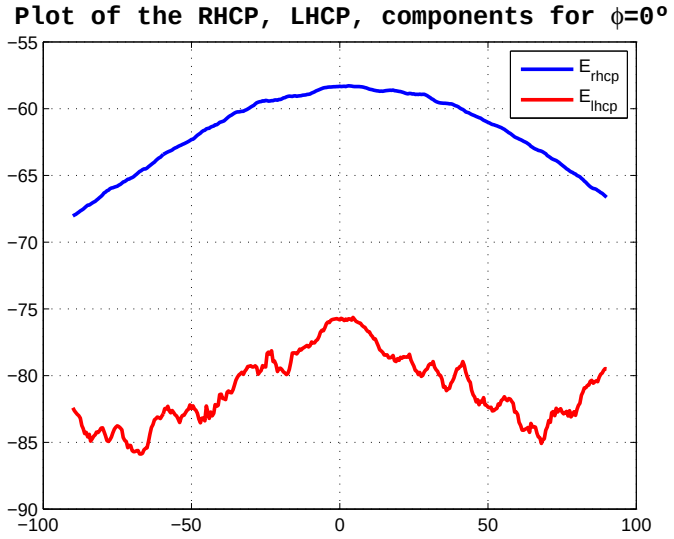

Figure 6.11: RHCP versus right hand circular polarization of the 5.8 GHz RHCP patch antenna for Phi = 0°.

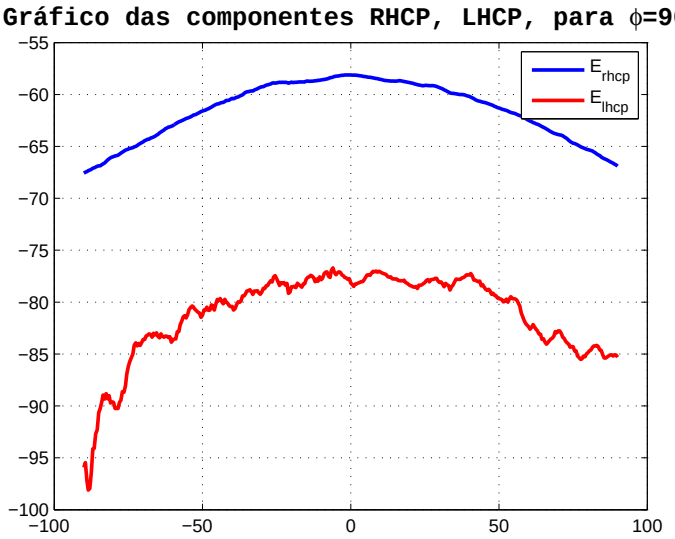

Figure 6.12: RHCP versus right hand circular polarization of the 5.8 GHz RHCP patch antenna for Phi = 90°.

6.3 Single Shunt Rectifier

Both RF-DC converters were printed on a RO3003 substrate. However, due to the low density of this substrate some boards were bent during manufacturing leading to slight cuts in the copper lines. This may lead the results to diverge from what is expected. The circuit based only on ADS simulation is visible in Figure 6.13.

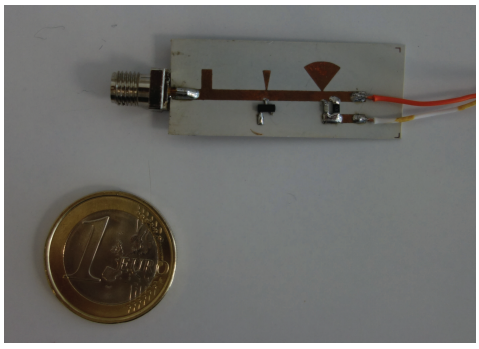

Figure 6.13: Printed RF-DC converter.

One of the relevant parameters to measure from an RF-DC converter is its S_{11}, and in this way verify if the circuity is correctly matched at the desired input power. However, given that the available VNA possessed an output power range of only -19 dBm to 0 dBm it was not possible to directly measure the input voltage reflection coefficient of the circuit for the relevant input power span.

The obtainable output voltage was still measured, and the POE response calculated, regardless of the circuits input impedance at the design range.

To measure the DC output voltage variation of the RF-DC converter, a SMU200A vector signal generator combined with a ZVE-8G+ Power Amplifier (PA) from Mini-Circuits, which presents a 32 dBm output power at 1 dB compression, were used. This combination was necessary because the vector signal generator presented the capability of producing a maximum output power of 20 dBm.

To confirm the power at the output of the PA, a 8593E spectrum analyzer from Hewlett-Packard was used. The output power was measured to be between 1.5 and 30.4 dBm, considering a range from -30 to 0 dBm at the signal generator.

Given that the gain of the PA depends of it being properly matched, and that the input impedance of the RF-DC converter varies with the power applied to it, it is not possible to predict the power that the amplifier will provide to circuit if directly connected. An isolator could be used to prevent reflected power from returning to the PA's output but the components available worked only for a maximum frequency of 4 GHz.

In order to measure the output voltage of the converter, trying to guarantee proper matching to the amplifier, the device was connected directly to the 4x4 antenna array, which presented a reasonable return loss at the desired frequency, and the power at the signal generator was varied from -30 to 0 dBm.

To guarantee maximum received power on the receiver end, a wideband SGH-2575 horn antenna, which possesses a gain of 11.87 dBi at 5.8 GHz, was connected to the RF-DC converter. A multimeter was used to measure the voltage at the 270 Ω output resistor. This complete experimental setup is presented if Figure 6.14.

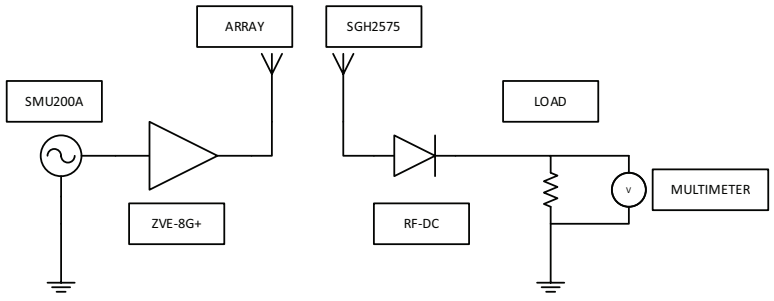

Figure 6.14: Diagram of the experimental setup.

In the midst of the measurements the transmitter 4x4 array broke at the point where the SMA was soldered. The substrate was realigned and strengthened so that the connector could be soldered again. The change in return loss presented by the antenna at this point can be seen in Figure 6.15.

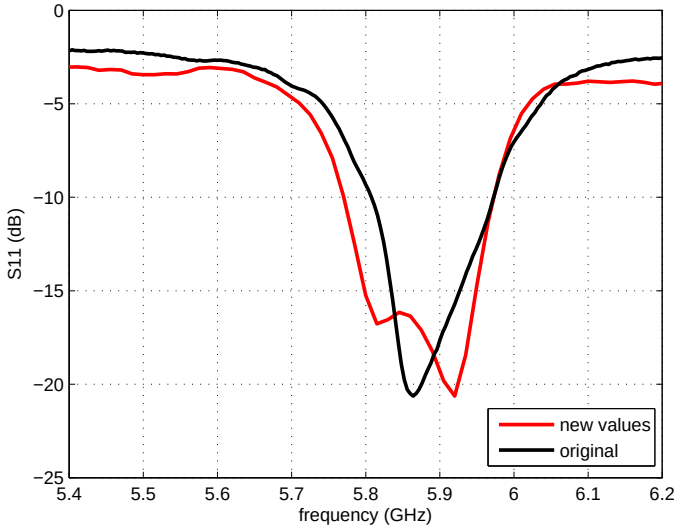

Figure 6.15: $S11$ values of the array after the SMA connection pad was soldered again.

However, to verify the efficiency of these circuits the array was considered to be no longer be in condition to be part of the experiments. An ASYSGH-5480 antenna, which presents a gain of 19 dBi at 5.8 GHz, was used for the power transmission. The antennas were distanced 20 cm for one another.

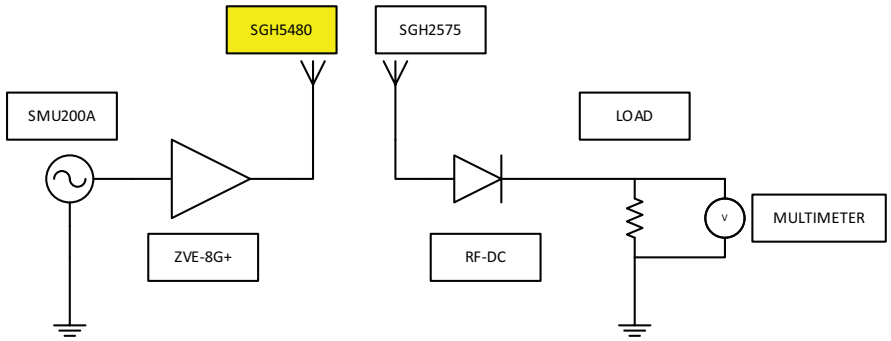

Figure 6.16: Diagram of the experimental setup for the measuring of the output voltage of the 2nd batch of RF-DC converters.

At 20 cm the antennas are not in the far field. Given the biggest dimension D of the antennas is the 14.85 cm width of the array, for them to be in the far field they should be at a distance greater than, approximately, 85 cm. However, given the reactive behaviour of the field do to this proximity, larger power, in absolute value, than that predicted by the Friis' transmission equation is expected to be obtained, which is convenient to obtain a larger input power span at the RF-DC converter.

The power obtained at the receiver end was measured with an HP 437B Power Meter so that after the voltage was measured the efficiency could be calculated. Even with such

high gain antennas it was only possible to obtain a maximum of 20.6 dBm of power at the considered distance.

The values of the power measured at the PA, P_{outPA}, the power measured at the receiver antenna, $P_{received}$, the measured output voltage, V_{out}, and the POE are presented in Table 6.1, for the ADS simulated circuit, and in Table 6.2, for the Momentum simulated one. The measured variation of the POE can be better observed in Figures 6.17 and 6.18.

P_{outPA} **(dBm)**	$P_{received}$ **(dBm)**	**Vout (V)**	**POE (%)**
3.4	-7.4	0	0
4.3	-6.4	0	0
5.3	-5.4	0.001	0.001
6.2	-4.5	0.001	0.003
7.2	-3.6	0.002	0.024
8.2	-2.5	0.006	0.103
9.4	-1.5	0.014	0.353
10.4	-0.5	0.028	1.173
11.4	-0.7	0.061	2.657
12.4	1.7	0.103	4.903
13.4	2.7	0.157	8.285
14.4	3.7	0.229	12.532
15.3	4.7	0.316	17.921
16.3	5.7	0.424	23.453
17.3	6.6	0.538	28.999
18.3	7.7	0.679	35.674
19.3	8.7	0.845	42.345
20.3	9.7	1.033	48.013
21.3	10.6	1.22	53.8731
22.3	11.6	1.45	60.1434
23.3	12.6	1.719	64.475
24.3	13.6	2.322	69.241
25.3	14.6	2.67	72.721
26.3	15.6	3.041	75.282
27.3	16.6	3.42	76.302
28	17.6	3.819	76.943
29	18.5	4.205	76.980
30	19.3	4.559	79.223
31	20	4.899	82.924

Table 6.1: Measured values for the LSSP and Harmonic Balance simulated RF-DC Converter.

P_{outPA} **(dBm)**	$P_{received}$ **(dBm)**	**Vout (V)**	**POE (%)**
3.4	-7.4	0	0
4.3	-6.4	0	0
5.3	-5.4	0.001	0.003
6.2	-4.5	0.002	0.010
7.2	-3.6	0.004	0.033
8.2	-2.5	0.009	0.131
9.4	-1.5	0.021	0.566
10.4	-0.5	0.038	1.473
11.4	-0.7	0.071	3.900
12.4	1.7	0.104	6.648
13.4	2.7	0.144	10.124
14.4	3.7	0.191	14.147
15.3	4.7	0.246	18.641
16.3	5.7	0.309	23.363
17.3	6.6	0.373	27.671
18.3	7.7	0.456	32.102
19.3	8.7	0.549	36.962
20.3	9.7	0.656	41.919
21.3	10.6	0.767	46.580
22.3	11.6	0.9	50.944
23.3	12.6	1.054	55.500
24.3	13.6	1.224	59.453
25.3	14.6	1.414	63.024
26.3	15.6	1.626	66.200
27.3	16.6	1.855	68.438
28	17.6	2.093	69.206
29	18.5	2.345	70.614
30	19.3	2.583	71.262
31	20	2.799	79.753

Table 6.2: Measured values for the Momentum simulated RF-DC Converter.

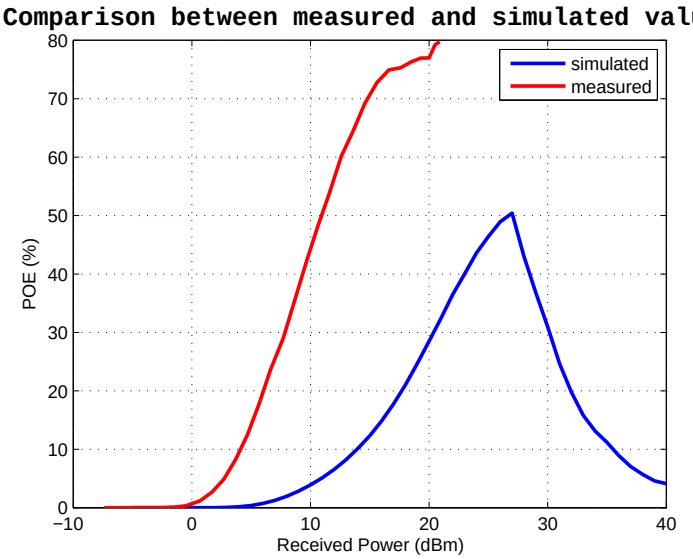

Figure 6.17: Simulated versus measured POE of the LSSP and Harmonic Balance simulated RF-DC Converter.

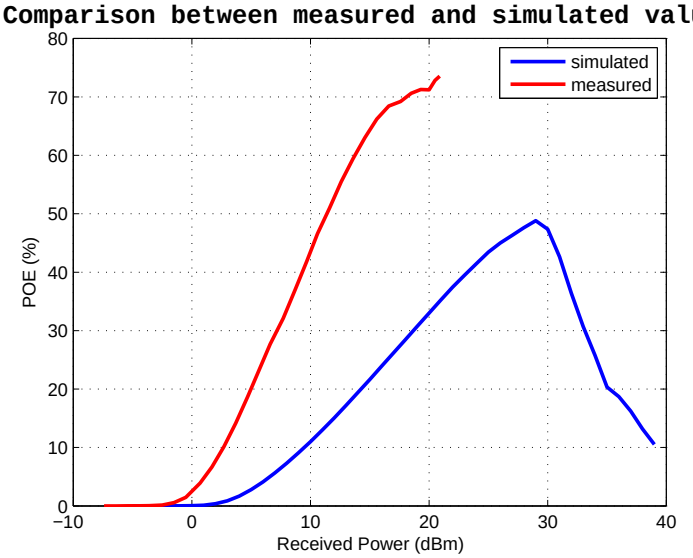

Figure 6.18: Simulated versus measured POE of the Momentum simulated RF-DC Converter.

Considering that the maximum efficiency predictable for a half-wave rectifier is 50 % it is observable, in the previous Figures, that the preformed measurements cannot be conclusive.

The shift observed in the obtained results can be justified through the mismatch of the antenna used at the receiver. If the impedance of the antenna is not 50 Ω at 5.8 GHz, then the measurements at the power meter, which is matched for 50 %, might present values lower than those that are actually being received by the antenna. If this is the case, then the POE

is less than what was measured.

The variation of the received power through the Friis' transmission equation for the 19 dBi of gain of the transmitter, 11.87 dBi of the receiver, and a transmitted power of 30 dBm is plotted, is compared to measured values in in Figure 6.19.

Even if the Friis' transmission equation only applies in the far field, a difference of 3 dB can be observed at this region, i.e. after 85 cm. By adding these 3 dB to the received power in Tables 6.2 and 6.1, Figures 6.20 and 6.21 are obtained.

Changes in the impedance of the antenna will also imply that the matching stage of the RF-DC will match the circuit for an input power other than that which was intended.

Moreover, parasitic elements of the diodes can change the input impedance of the circuit, and given the model for 5.8 GHz is not available then it becomes difficult to accurately predict their weight on these results. If the series resistance, or the minimum breakdown voltage, of the real diode shift from the supposed values it will imply also a change in the shape of the efficiency, as presented in [51]

Even with these values, at a 30 cm of distance between the antennas, the drone was directly connected to the RF-DC converter to verify its behaviour and it was observed that its LED's would light up with tenuous shine.

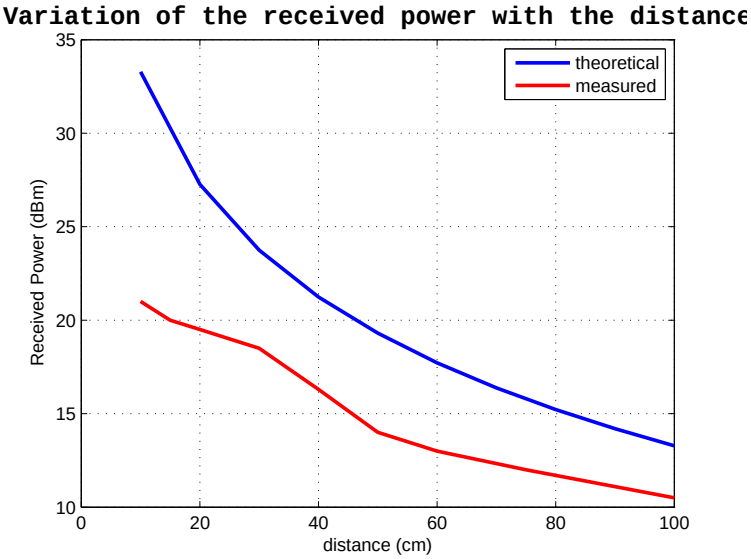

Figure 6.19: Measured and calculated link budget.

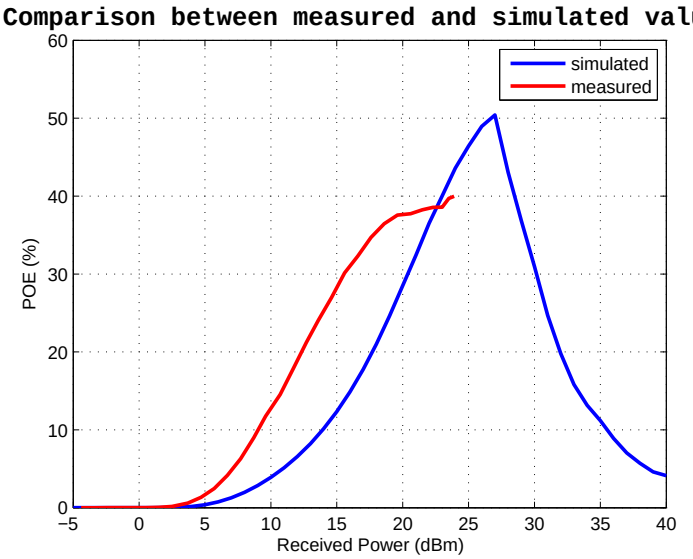

Figure 6.20: Simulated versus measured POE of the Momentum RF-DC Converter, considering a 3 dB compensation to the input power.

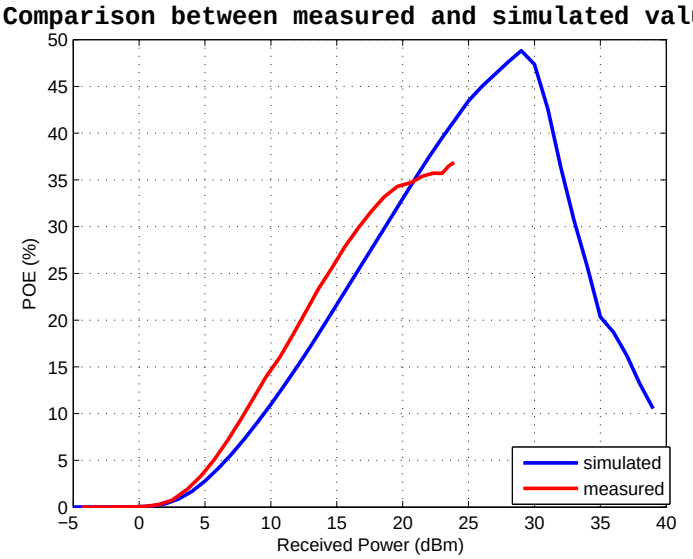

Figure 6.21: Simulated versus measured POE of the Momentum RF-DC Converter, considering a 3 dB compensation to the input power.

6.4 Powering the Drone

It was also desirable to verify the behaviour of the drone once connected to the RF-DC converter. The measurements presented in this section were made by connecting the PA through a DC-Block to the RF-DC converter and connecting the converter directly to the drone. This was done to qualitatively verify to which length the drone could function whilst connected to the converter.

For this part of the experiment the PA used was one designed for a master's dissertation project at the University of Aveiro, capable of a maximum output of 35 dBm at 1 dB compression.

Using a multimeter it was possible to measure the current and voltage that was being produced by the RF-DC converter. Measurements were done to compare the behavior with, and without, the DC-DC converter. Both the measured output voltage and current variation, regarding the PA, are presented in Figures 6.22 and 6.23.

It must be noted that given the variation of input impedance of the RF-DC converter with the available power it was not possible to accurately measure the power delivered to the converter. However, the output powers measured directly with a Power Meter were considered in order to plot the variations of output voltage and current.

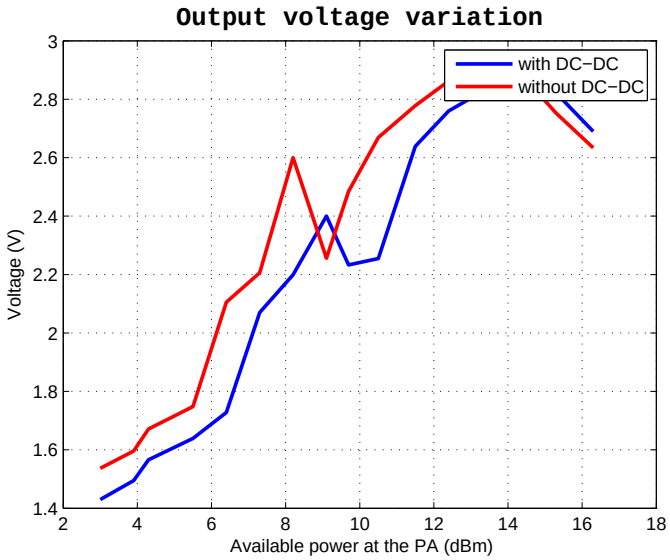

Figure 6.22: Variation of the output voltage, directly link the PA, RF-DC converter and the drone, with and without the DC-DC converter.

It was possible to observe that the drone's LED's would light up with maximum brightness when the power at the PA ranged from 8.2 to 16.3 dBm. It was possible to establish the link between the drone and its remote control, but once the throttle was pushed upwards, and more current was required from the drone, the LED's would blink, a signal to warn the user

of low battery levels. The drone would eventually restart, meaning that too much current was being required.

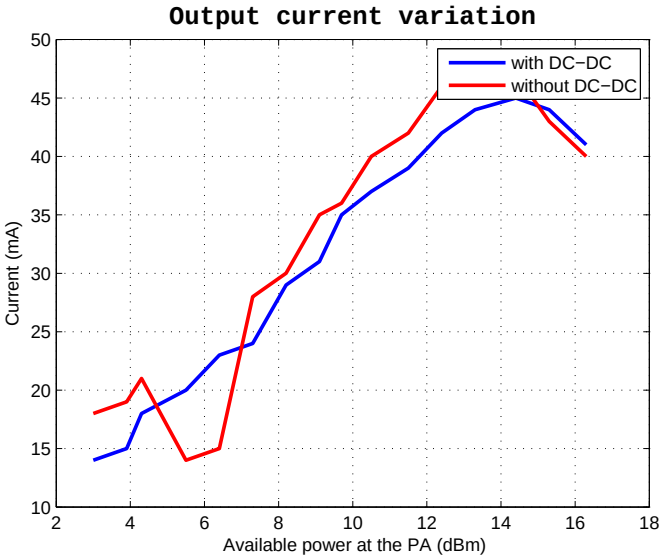

Figure 6.23: Variation of the output current, directly link the PA, RF-DC converter and the drone, with and without the DC-DC converter.

6.5 Conclusions

A 4x4 rectangular microstrip patch antenna array for a working frequency of 5.8 GHz was successfully designed and printed being that the antenna presented a directivity of 20 dBi, with regards to Kraus' formula, a return loss of 10 dB at desired frequency and gain of 16.8 dBi and 18 dBi at 5.8 GHz and 5.86 GHz, respectively.

Both receiver patches present adequate return losses, being that the square patch for linear polarization presents a return loss of 14.7 dB, and a directivity of 7.6 dBi, at 5.8 GHz and the RHCP polarized square patch presents 13.2 dB of return loss, and 6.8 dBi of directivity, for the same frequency.

The RHCP antenna presented also an axial ratio below 3 dB for both the horizontal and vertical planes and a cross polarization rejection of approximately 20 dB which implies that it radiates, as expected, with right hand circular polarization at 5.8 GHz.

Measuring the RF-DC converters in order to obtain conclusive results becomes a complex task given the high frequency of operation and the non-linear behaviour of a seemingly simple circuit. Any shift in the delivered power or impedance of the circuits in the measuring chain can lead to inconclusive or not easily interpretable results. For example, given that the antennas don't present exactly 50 Ω of input impedance at 5.8 GHz the designed impedance matching circuit does not ideally match the input impedances, which explains the shifts in

POE.

It was not possible to generate enough current for the drone to take flight with the available power and a system designed to convert for 40 dBm should be considered for future developments. Still, given that it is possible for power to reach the drone, and be converted, then it can also be considered to try different approaches, e.g. using supercapacitors to increase the drones running time.

The DC-DC converter used possesses a large input impedance, which shifts the maximum efficiency to a lower value of the input voltage, and is not capable of producing the voltage step-down current step-up. DC-DC converters, capable of stepping-up current, typically depend of microcontrollers to obtain high efficiencies. Given this added weight, and complexity, this stage should not be necessary to power the drone.

To conclude, the designed system converts just enough power to allow the used quadcopter to boot and link with its remote control. However, this architecture can be adapted for other purposes and further improvement.

Chapter 7

Conclusions and Future Work

In this chapter, a general summary and the most important conclusions extracted from this work will be displayed and various research directions that can be followed, in order to improve the current system, will be pointed out. Besides this, the final section will present some final remarks on the importance of wireless power transmission and its application to powering drones.

7.1 General Analysis

At the beginning of this work it was established as main goal to design a wireless power transmission system that could enable a drone to be charged while in flight so that it could present a superior running time and from this overall goal smaller tasks were determined, such as a literature study to determine the best wireless power method to implement and how do design each independent segment of the system.

By researching the state of the art on wireless power transmission it could be observed that this field has currently a great focus on it and several companies are investing to increase their knowledge on the subject to hit the markets with innovative ideas. There is some research specifically considering wireless power transmission applied to drones but it is focused on using them as power sources and only has the group of Colorado University started doing its research being that the are still no publications on the matter.

From the various methods of transmitting power wirelessly analyzed it was concluded that the method to better fit the requirements of this project be that of microwave power transmission given it has proven to be capable of handling considerable amounts of power and is constituted by elements that can be very flexibly designed.

With this in mind, the structure of antennas and their characteristics were reviewed to identify the topology that better suited the needs of the envisioned system. Microstrip antennas were chosen because of the fact that they can be conformed to almost any surface, be easily printed different substrate and have a relatively straightforward design. These antennas

can also be easily altered in order present different radiation polarizations and be set into arrays to increase their gain. The fact that these antennas can be simply etched onto a substrate makes them also easily reproducible.

Once the means of power transmission and reception were established it was necessary to study the circuitry that enable the conversion of RF signals in to DC, RF-DC converters. The most important behaviour these circuits is without a doubt their POE, which made it necessary to analyze which parameters that tinker with their efficiency and led to the realization that they are limited, in higher power, at $\frac{{V_{BR}}^2}{4R_L}$. A single diode topology was chosen to be implemented given the high power that has to be dealt with to power a drone and also to diminish the effect of losses through dissipation that would be presented if more diodes were added.

With all the architectures to be implemented chosen, it was the possible to design and simulate the different elements. Several compromises were taken with regards to the RF-DC converter stage, given the available power, so that it would be possible to at least demonstrate successfully power being transmitted, received, converted and used by the drone.

The antennas were functioning as expected and so this part can be considered to be successfully validated. The RF-DC converters did not present the expected behavior which may have come from divergences from 50 Ω of input impedance of the receiver antenna used for testing, changes in the characteristic impedances of the lines printed because of some tolerance shift or even because the real parasitic model of the diode's package at 5.8 GHz could not be considered. Even though the RF-DC converters did not behave as expected they functioned quite well at the received power, at 20 cm distance between the antennas, and enabled the drone to light up and connect with its controller, but once the throttle was needed there was not enough current to power the drone and so it was automatically reseting itself.

The input impedance of DC-DC converters is usually high, as was the case of the one tested here, and this implies that the efficiency of the receiver circuitry will be limited to a small input power which does not suit this type of applications. To overcome this shortcoming it might be possible to use Maximum Power-Point Tracking circuits, as seen on solar panels, so that the the RF-DC converter is always transferring power to an optimal load. Also, the DC-DC converter used in this case was not adequate for this power handling and a Buck converter with larger efficiency should be procured, but this will imply gravely enlarging the circuit and maybe the need of inserting an external source because high efficiency DC-DC usually depend on a microcontroller to function.

In summary, the system designed throughout this dissertation creates the wireless link at a frequency of 5.8 GHz between transmitter and receiver, considering a small distance between them, and converts enough power to allow the used quadcopter to boot and link with its remote control. Even though it was not possible to remove the battery from the drone and

make it fly through wireless power transmission, the circuits and antennas designed show potential to be adapted for other purposes.

7.2 Future Work

As any research topic, once some questions are answered, new questions and ideas arise. From these ideas, the following were those that seemed more interesting for further developments.

- Instead of trying to make the drone fly without a battery, a supercapacitor could be added to the receiver of the microwave power transmission system in order to make the battery's discharge slower thus increasing the flight time;
- Development of a 2x2 patch array for the reception being that each antenna would be isolated from the others by a maximum power point tracking circuit or by a DC-DC converter that would guarantee that they all possessed the same output voltage. In this way the current produced by each antenna could be added;
- Use a 40 dBm output power at 1 dBm compression 5.8GHz Power Amplifier to guarantee that more power reaches the drone and use a HSMS-2800 diode for the reception;
- Possibly reduce the project frequency to 2.4 GHz which would imply larger antennas but less attenuation, a larger efficiency for the RF-DC converters and cheaper power amplifiers;
- Turn transmitter antenna array into a phased array to enable power to be transmitted with two degrees of freedom;
- Study the need to provide electromagnetic shielding to the remaining circuitry of the drones.

7.3 Final Remarks

As stated at the beginning of this document the *Internet of Things* will create a complete dependence of self-sufficient electronic system and drones will undoubtedly be used as a means of collecting information and powering independent wireless sensor nodes so surely effective means of powering them or simply increasing their battery life will in soon appear.

It is with certainty that I state the in the next couple of years we will be amazed with how far this topic will evolve.

Appendices

Appendix A

Article for the 8th Congress of the Portuguese Committee of URSI

Wireless power transmission and its applications for powering Drones

António Carvalho[1], Nuno Carvalho[1], Pedro Pinho[2], Ricardo Gonçalves[1]

[1]Instituto de Telecomunicações, Dep. de Electrónica, Telecomunicações e Informática, Universidade de Aveiro, Portugal
[2]Instituto de Telecomunicações, ISEL, Portugal

***Abstract*—Unmanned aerial vehicles or drones, as they are commonly referred to, suffer from a few drawbacks of which their short flight time can be underlined. For most commercial applications the maximum flight duration falls around a total of 15 minutes. In order to solve this limitation a microwave wireless power transmission system, working at 5.8 GHz, aimed at enabling drones to be charged in flight will be proposed and described in detail. The development of the antennas used, and corresponding rectifiers, will be thus discussed and suggestion for further work will be presented. With the architecture used it was possible to enable the drone to turn on and establish a link with its remote control by transmitting 32 dBm of power. The designed RF-DC converter did not reach its efficiency peak at the desired input power, still it presented a power overall efficiency of 70 % for 20 dBm of input power.**

***Keywords*—Microwave antenna array, Microstrip antennas, Rectennas, Unmanned Aerial Vehicles.**

I. Introduction

Unmanned Aerial Vehicles (UAV), commonly referred to as drones, are non-crewed aircrafts that can either be autonomous or remotely controlled. These devices have become massively used in the military, commercial and academic fields for several ingenious applications.

Several successful applications have arisen from the use of drones. These devices have been used to create a 3-D mapping of the Matterhorn, guide MIT students around campus and even to aid the American police in drug busts. Amazon has also recently announced they plan to create a UAV delivery service. However, this section will only present the research made specifically on wireless power transmission for drones.

A major drawback of these devices comes from their dependence of external power connections or batteries in order to function. These elements can lead to a rapid degradation of the hardware given that the pins connected to these devices get lax over time and can prevent proper battery charging after some use and also batteries have limited lifespans. It is thus necessary to make them able of being powered in a more effective and versatile way.

Lasermotive is the only company thus far to have presented a functional mean of wirelessly charging a drone at distance. It first got its financing after winning the NASA Centennial Challenges Power Beam challenge and their approach is based on a laser power beaming, where light is sent from the ground to the device and is then converted into useful electricity [1].

Another way of looking at wireless power transmission is seeing the drones not as receivers but as the power transmitters. Nebraska Intelligent MoBile Unmanned Systems Lab, from Nebraska-Lincoln University, have focused their efforts the other way around and have been developing a adaptive and autonomous energy management system that used drones to charge sensor networks via resonant inductive coupling [2]. This application can be very helpful, for example, for powering and transferring information with sensors in large or remote crop fields.

The University of Purdue as picked up on its part regarding the Wireless Power Helicopter and, in 2010, demonstrated a small model helicopter taking flight, powered by means of a flared horn antenna on the transmitter end and two dipole antennas on the receiver end. Also the research group from the University of Colorado is working now on a means of wirelessly powering a micro-drone in flight, enabling it to charge in confined environments and even charge several drones simultaneously, but there are still no publication on the matter.

In this article a wireless charging system will be proposed detailing the transmission, reception and power conversion architectures used. Section II presents a summary of the history of wireless power transfer, underlining some of the most relevant feats obtain so far. From that point forward, a full description of the proposed system and its elements is displayed, given that Section III regards the overall system while Sections IV and V show in more detail the current development of each section of the system.

The final section underlines the most relevant conclusions and obtained results.

II. History of Wireless Power Transmission

The idea of transferring electrical energy without the means of wires is not new. For the past century several scientists and engineers have thrived on the idea of building a truly wireless world by getting rid of the need for cables.

Nikola Tesla, probably the first and most frequently mentioned supporter of the concept of wireless power transmission, is said to be responsible for the first ideas and experiments on this field. This inventor, famous for his support of alternating currents, dreamt of wireless communications and power transfer and dedicated a considerable amount of effort to the development of these fields [3]. In 1893, Tesla was able to

demonstrate the wireless illumination of phosphorescent lamps at the World's Columbian Exposition, Chicago, and between 1900 and 1917, he focused his efforts to the development of the Wardenclyffe tower, a tower that would work as an antenna for wireless transatlantic telephony and demonstrate the transmission of power through long distances without cables. Yet, given the difficulty to find further financial support for this project, the tower was demolished during the 1st World War [4].

Almost half a century later a noticeable feat was accomplished by an electrical engineer from the Raytheon Company. William C. Brown devised a somewhat entertaining experiment as proof of concept for his developments in rectifying antennas ($rectennas$) and succeeded in 1964 to fly a helicopter 15 meters in the air without use of an onboard power supply. Even though the helicopter required kilowatts of power to be transmitted in order for it to maintain flight this experiment proved the feasibility of microwave power transmission [5].

Already in the 21st century, several companies that are focusing their efforts on wireless power transmission systems have popped up. Of these, probably the most mediated would be WiTricity, a company that spun off from its homonymous Massachusetts Institute of Technology (MIT) project which was lead by Prof. Marin Soljačić. WiTricity is a company that manufactures devices for wireless energy transfer using "strong" inductive coupling and has already demonstrated a power unit powering simultaneously a television set and three cellphones at the TED Global Conference in Oxford, 2009.

Several major industry associations have been created in order to globally standardize wireless power transfer mechanisms. The first consortium to be established, back in 2008, was the Wireless Power Consortium. It includes already over 180 companies, industry leaders in the most various of fields, e.g. mobile phones, batteries and infrastructure [6] and has established their Qi norm, which defines interface for low power transfer (around 5 W), and is working on their standard for medium power (up to 120 W).

III. Description of the Proposed System

The typical wireless power transfer system can be divided into two major sections, the power transmitter and the receiver. In the transmitter, high frequency waves are generated with enough power to comply with the specifications of the project and are then directed and radiated at the receiver. The receiver end must then capture and efficiently convert this power to direct current (DC) so that it might be provided to a given load. These core components are better observed in Figure 1.

The transmitter must be capable of generating and radiating power at microwave frequencies. The choice of generator, which is typically between a magnetron or solid-state source, will vary with desired frequency, efficiency, signal purity and power, which will have the major weight on the overall cost of this section [**?**]. The antenna, as described in [5], should present an extremely directive radiation pattern.

The receiver's antenna on the other hand should be "non-directive" so that the target is able to capture power even when subjected to small movements. Following the antenna an impedance matching network is typically used to reduce

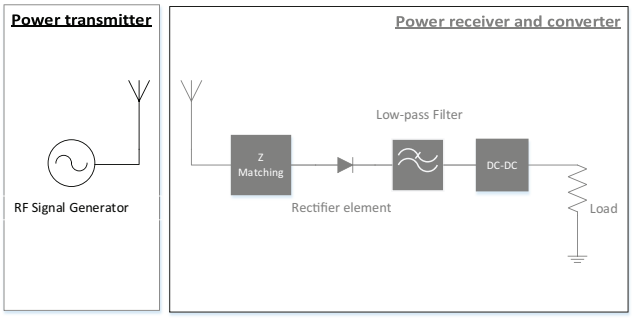

Fig. 1: Wireless power transfer system consisting of a transmitter and receiver section.

Fig. 2: Representation of a drone charging with resort to microwave power transmission.

mismatch losses between the antenna and the rectifier, this section might not be necessary if both the antenna and rectifier are designed to be already matched at the desired input power. Then comes the RF-DC converter and, if needed, a DC-DC converter to tune the output current or voltage's value. It should be noted that the power overall efficiency (POE) of the receiver is equal to the product of the independent efficiencies of each of its stages and thus to obtain maximum power conversion efficiency the number of stages needed must be minimum [7].

Schottky diodes are the most commonly used devices for high frequency rectifiers. These diodes present a much lower junction capacitance [8] and dropout voltage then common pn junction diodes. Their conductivity is mostly due to the majority-carriers (i.e. electrons), thus these diodes don't exhibit the effects of minority-carrier charge effect present in forward biased pn junctions, making it able of switching much faster between on and off [9], and much more appealing for high frequency applications. However, the input impedance of these diodes changes with the available power, making it somewhat difficult to precisely optimize the circuit given that with a moving target and antenna polarization mismatch there will be significant changes in the available power levels.

As in [10], the frequency chosen for this project was 5.8 GHz for it implies smaller components dimensions. This frequency is complaint with the Industrial, Scientific and Medical standards.

The load is of major importance for the receiver given that, for diode based rectifiers, it limits the conversion efficiency at higher input power levels [11]. For this project the load is a commercial HUBSAN X4 quadcopter.

Given the quadcopter acts as a variable load and that the power conversion efficiencies of RF-DC converter vary with the available input power and the load, several compromises will be taken when designing the RF-DC converter. A representation of the concept of wirelessly charging a drone is showed in Figure 2.

IV. Transmitter

For this section only the antenna will be designed. The specifications of this project are therefore limited to the available power at 5.8 GHz which is 32 dBm.

The type of antenna chosen for both the transmitter and receiver was microstrip patch given they are simple to replicate and can easily be displayed in a planar array configuration in order to gain greater directivity. These antennas are conformable to planar or even nonplanar surfaces, are simple to manufacture with the same means of common printed-circuits and are versatile regarding their fundamental parameters [12].

First, a single patch element was designed and then simulated using the Microwave Studio from the CST suite. The dimensions of the patch were tuned so that it would present a return loss over 20 dB at the desired frequency and a bandwidth sufficiently wide to have some safeguard regarding the implementation tolerances the dielectric constant and printing tolerances. The substrate used was a 1.27 mm high Rogers RO3006 substrate with a design dielectric constant of 6.15 and a loss tangent of 0.002.

The patch was excited using an inset feed composed of a quarter-wave impedance transformer from inside the patch to a 50 Ω line were the connectors would be soldered and resulted in a simulated return loss of 21 dB at 5.8 GHz. This single element antenna presented a directivity of 7 dBi.

The single patch antenna presented measured a return loss of 22.5 dB at 5.7 GHz instead of the desired frequency and so for remainder of the design of the array the dielectric constant was considered to have a slightly higher value. The comparison between simulated and measured S_{11} is presented in Figure 3.

After the dimensions of the patch were tuned to approximate the simulated and measured results, the array factor was derived with regards to distribution of the individual elements. For this case the array is symmetrical so that the antennas are excited with the same amplitude and phase, therefore only the spacing was optimized. A total of 16 elements were considered.

The feed network of the complete array is composed by quarter-wave impedance transformers and T-junction. The final design is presented in figure 4.

A directivity of 19.6 dBi for the main lobe was obtained through simulation, with a return loss is 18.19 dB at 5.8 GHz and a bandwidth of 130 MHz.

A return loss of 9.8 dB was measured at 5.8 GHz, being that its minimum value is presented at 5.864 GHz. Moreover,

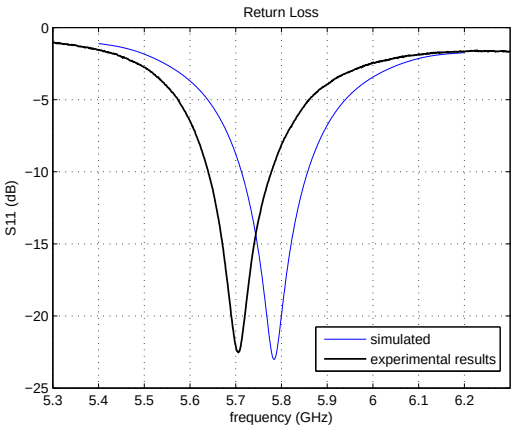

Fig. 3: Measured return loss of the patch compared with the simulated values.

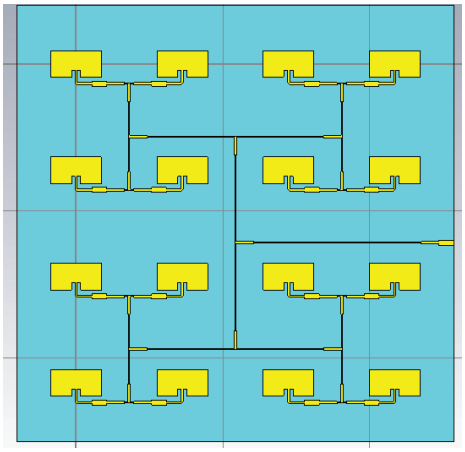

Fig. 4: Final array layout.

a gain of 16.8 dBi and 18 dBi were measured for the antenna array at 5.8 GHz and 5.864 GHz, respectively. The measured and simulated S_{11} and radiation pattern at 5.8 GHz are respectively presented in Figures 5 and 6.

The directivity of the radiation pattern was calculated using Kraus' formula [12] resulting in 20 dBi and this array can thus be considered as directive.

V. Receiver

A. Antennas

To verify the effects of polarization mismatch both a linearly and a right-hand circularly polarized patch antennas were designed. Both antennas were also design regarding a Rogers RO3006 substrate with a height of 1.27 mm. This dielectric of 6.15 is fairly high, given radiation is desired, but was used as a compromise to obtain smaller dimensions. The designs are presented in Figure 7.

For this case the antennas were designed with a coaxial feed so that the rectifier circuit could be added at the back o

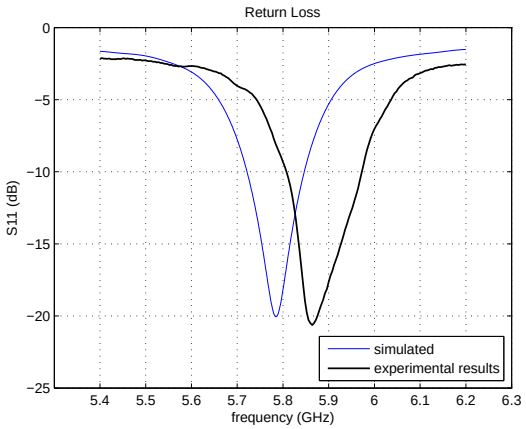

Fig. 5: Comparison between the measured and simulated S_{11} of the full array.

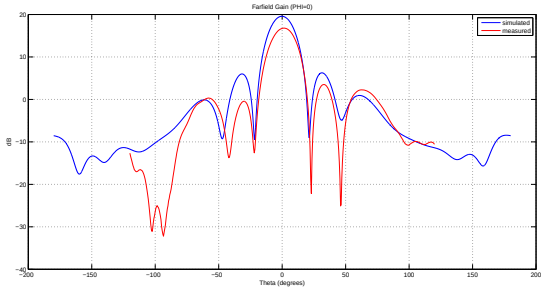

Fig. 6: Simulated and measured gain variation with theta of the 4x4 patch antenna array.

the antenna.

The simulated square patch presented a return loss of 42 dB at 5.8 GHz and a bandwidth of 162 MHz while the circularly polarized patch presented a return loss of 13 dB and an axial ratio of 0.35 dB. The S_{11} of the measured and simulated results for both antennas are presented in Figures 8 and 9.

The results shifted from the simulations for both antennas but still present themselves as acceptable at 5.8 GHz. These changes in frequency response can come from small shifts in

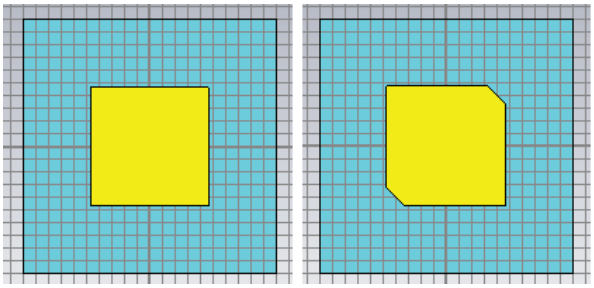

Fig. 7: Receiver antennas.

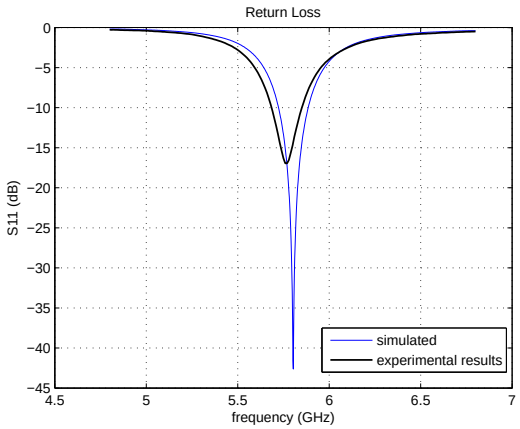

Fig. 8: Comparison between simulated and measured values for the linearly polarized square patch.

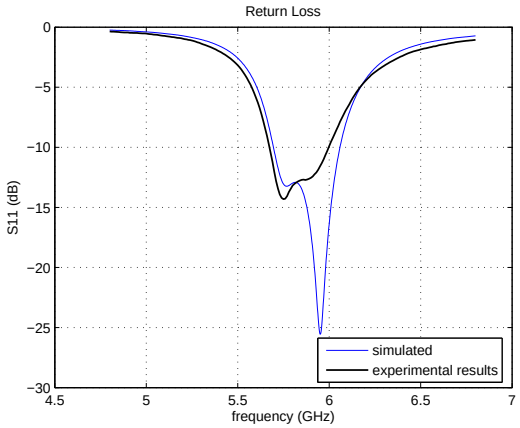

Fig. 9: Comparison between simulated and measured values for the right hand circularly polarized patch.

the placement of the feed, given this implementation was done by hand, and parasitic effects from the solder, which was not considered during simulation.

The linearly and circularly polarized antennas presented a return loss of 14.7 dB and 13.2 dB, respectively. The later presented a measured axial ratio under 2.4 dB for $\pm$ 30 degrees from mainbeam at 5.8 GHz making its polarization acceptable.

B. RF-DC

For the HUBSAN X4 to fly in ideal conditions it needs approximately 3.7 V and 1.8 A, which represent 6.66 W of power. However, the maximum power conversion is limited to an input power of $\frac{V_{BR}{}^2}{4R_L}$ [7] and that the maximum power conversion efficiency expected from a half-wave rectifier, with high powers at the input, will be around 50 $\%$ [10] given it is also limited by the diodes non-ideal behaviour. Given the available power is only 32 dBm and considering path, conversion and mismatch losses, it is predictable that the drone will not be able to fly depending solely on this system.

Fig. 10: Single shunt rectifier circuit layout.

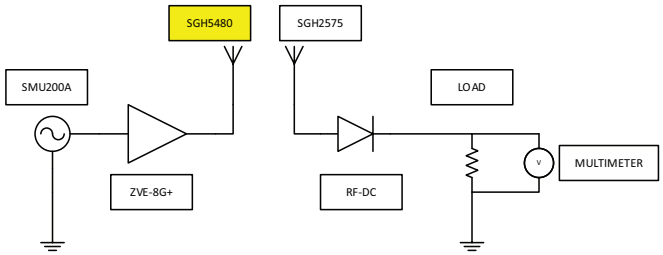

Fig. 11: Diagram of the experimental setup for the measuring of the output voltage of the RF-DC converter.

Considering that 32 dBm of received power would imply a peak-to-peak voltage of the sinusoidal signal, for a 50 Ω system, of 25.175 V the diodes chosen were the HSMS-2810 which present a minimum breakdown voltage, V_{BR}, of 20 V, a series resistance of 10 Ω and a maximum forward of 400 mV.

For the low pass filter following the diode a 100 pF capacitor was picked for it works as a short-circuit at 5.8 GHz and guarantees a RC time constant would be lower than the period of the RF wave. Given the drones behaves as a variable resistor, the considered load in the simulations is that which implies greater efficiency for the overall circuit.

A single shunt rectifier topology was thus designed and simulated using Advanced Design Systems, being that the lumped elements were tuned through Large Signal S-Parameters and Harmonic Balance simulations and the microstrip lines were optimized through Momentum Microwave simulation. Radial stubs were added to the circuit in order to attenuate the behaviour of power at undesirable frequencies. Also an impedance matching network was added to match the impedance of the antenna to the input impedance of the RF-DC converter that resulted in maximum power conversion efficiency at 32 dBm. The circuit layout is presented in Figure 10.

The circuit was measured using the experimental setup presented in Figure 11, where isolation between power amplifier and load is obtained using two references antennas. The antenna array designed previously was not used because it had suffered some damage to its connector due and was not operational at the time.

Even with such high gain antennas it was only possible to measure a maximum input power of 20.6 dBm and therefore, for the measured results, only efficiencies for input power of 0 do 20 dBm where considered.

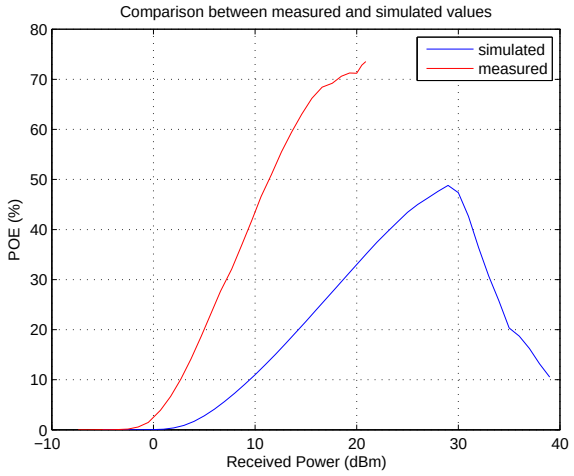

Fig. 12: Simulated versus measured POE of the Momentum simulated RF-DC Converter.

It can be observed in Figure 12 that the POE is reaching for its maximum value at input power level lower than that which was intended in the simulation. It is likely that this change in POE is either due to changes in the characteristic impedance of the lines, or due to shifts of the input impedance of the antennas which leads the matching circuit to reach 50 Ω at a lower input powers.

The efficiency at 20 dBm of input power is approximately 70 %, which is very close the the 75 % maximum found in the literature [13], and it is expected that at 30 dBm the circuit will have already passed the higher power threshold and will present low efficiencies.

VI. Experiments with the Drone

Given that not enough power could be converted in receiver so that the drone could take flight the power amplifier was connected to the RF-DC converter, with a broadband DC-Block between them, to verify the response of the device. For this case the battery was removed and the drones was directly connected to the RF-DC converter.

It was verified that once connected to the RF-DC converter the drone was able to fully light its four LED's and establish a link with the remote control. However, at this point the LED's would start blinking as a sign of low battery (lack of current). No measurements were devised in order to gather information on how much power was being transmitted from the power amplifier to the RF-DC Converter.

VII. Conclusion

A 16 element antenna array with a gain of 16.8 dBi at 5.8 GHz has been developed with the intent of being used for wireless power transmission while two single patch antennas, with different radiation polarizations, were designed for the receiver end. Although its results shifted from the simulations, a single shunt RF-DC converter was designed, obtaining an efficiency of 70 % for an input power 20 dBm.

Overall, the several sections designed present potential in being further implemented in fully or temporarily charging an unmanned aerial vehicle, tackling its reduced autonomy.

ACKNOWLEDGMENT

We would like to acknowledge the financial Support of COST IC1301.

REFERENCES

[1] Brooke Boen. After the Challenge: LaserMotive. http://www.nasa.gov/offices/oct/stp/centennial_challenges/after_challenge/lasermotive.html, November 2012.

[2] B. Griffin and C. Detweiler. Resonant wireless power transfer to ground sensors from a uav. *Proceedings of IEEE International Conference on Robotics and Automation (ICRA)*, 2012.

[3] Nikola Tesla. The transmission of electric energy without wires. *The thirteenth Anniversary Number of the Electrical World and Engineer*, 1904.

[4] Hugo Gernsback. U.S. Blows Up Tesla Radio Tower. *The Electrical Experimenter*, page 293, September 1917.

[5] William C. Brown. The microwave powered helicopter. *Journal of Microwave Power and Electromagnetic Energy*, 1(1):1–20, 1966.

[6] Wireless Power Consortium. http://www.wirelesspowerconsortium.com/about/.

[7] Christopher R. Valenta and Gregory D. Durgin. Harvesting wireless power. *IEEE Microwave Magazine*, 15(4):108–120, June 2014.

[8] R. Ludwig and P. Bretchko. *RF Circuit Design: Theory and Applications*. Prentice-Hall, Upper Saddle-River, N.J., 2000.

[9] Adel S. Sedra and Kenneth C. Smith. *Microelectronic circuits*. Oxford University Press, 2011.

[10] James O. McSpadden, Lu Fan, and Kai Chang. Design and experiments of a high-conversion-efficiency 5.8-ghz rectenna. *IEEE Transactions on Microwave Theory and Techniques*, 46(12):2053–2060, December 1998.

[11] Tae-Whan Yoo and Kai Chang. Theoretical and experimental development of 10 and 35 ghz rectennas. *IEEE Transactions on Microwave and Techniques*, 40(6):1259 – 1266, June 1992.

[12] Constantine A. Balanis. *Antenna Theory: Analysis and Design*. John Wiley & Sons, Inc., 2005.

[13] W. Tu, S. Hsu, and K. Chang. Compact 5.8-ghz rectenna using stepped-impedance dipole antenna. *IEEE Ante*, 6:282–284, June 2007.

Appendix B

Article for the 9th European Conference on Antennas and Propagation

5.8 GHz Microstrip Antennas and Array for Microwave Power Transfer

António Carvalho[1], Nuno Carvalho[1], Pedro Pinho[2], Apostolos Georgiadis [3] Alessandra Constanzo[4]
[1]Instituto de Telecomunicações, Dep. de Electrónica, Telecomunicações e Informática, Universidade de Aveiro, Portugal
[2]Instituto de Telecomunicações, ISEL, Portugal
[3]CTTC, Barcelona
[4]Universidad de Bologna, Italy

***Abstract*—Wireless power transmission presents itself as being a solution to some common problems of the extensive use of electronics devices such as the removal of parasitic components present in feeding pads and the constant charge of electronic devices without the need of wires. This solution becomes attractive, for example, as a means of increasing the flight time of battery dependent unmanned aerial vehicles. Microstrip antenna due to their ease of manufacturing, low fabrication cost, support of different polarizations and are conformable to irregular surfaces and different substrates, seem very advantageous in being used for microwave power transmission. This paper presents a linearly polarized 16-element antenna array with uniform amplitude and phase excitation proposed for power transmission with a with a gain of 16.8 dBi while both a linearly and circularly polarized single element patch are proposed for reception with a gain of 5.5 dBi and 5.3 dBi, respectively.**

***Index Terms*—Microwave antenna array, Microstrip antennas, Rectennas.**

I. Introduction

For the last century the concept of transferring energy without resorting to wires has been researched and several notorious demonstrations came of this idea [1]. Tesla was responsible for the first concrete ideas and experiments and, although he was not successful at implementing these for commercial use.

Halfway across the 20th century, Raytheon engineer William C. Brown demonstrated the flight of a helicopter powered solely by electromagnetic waves being transmitted by a 3 meter wide ellipsoidal reflector. Between 3 to 5 kW of power were beamed to the helicopter, which was capable of flying 10 hours straight and reach an altitude of 15 m. This was the first time the concept of a rectifying antenna was presented. The *rectenna* used in this experiment was a 0.2 m^2 half-wave dipole antenna array with around 4480 diodes [2]. Nowadays several companies are investigating the capabilities of resonant inductive coupling as a means of charging common household appliances. These systems can make devices capable of being remotely powered allowing for a greater freedom of movement and making them more compact by removing their battery [3].

Nowadays, this concepts of wireless power transfer can be envisioned to power unmanned aerial vehicles in midst flight. Using this method it could be possible to build wireless charging stations scattered across a wide area where the drones could power up at a distance.This concept is better observed in Figure 1.

Fig. 1: Depiction of a drone charging with resort to microwave power transmission.

For this specific application, techniques such as resonant inductive coupling seem disadvantageous given the extra weight that would be implied to the device, which would decrease even further its operational time, and the distance limitations, given most of the currently available wireless power charging docks require milimetric proximity between the transmitter and receiver coils to effectively transfer power.

Microwave wireless power seems an adequate solution given that with *rectennas* it is possible to have a high flexibility in the design of the different elements of the system. The radiating element, for example, can be any type of antenna such as dipoles [1] [4], Yagi-Uda [5] [6] and microstrip [6] [7].

The rectifier element, usually a Schottky diodes, can present various values of breakdown voltage making them desirable for different implementations. Conversion efficiencies from 34 % at 0 dBm input power [8] to 50 % at 10 dBm of input power [9] and even 71.4 % at 24.2 dBm of input power [10] have been obtained for microwave energy harvesters working at 5.8 GHz. The largest conversion efficiency accounted for so far was 90.6 % at 2.45 GHz in [11].

This paper is organized as follows. First the typical architecture of a wireless power transfer system is presented and each of its components is briefly described. The third and forth sections present the design and results of the transmitter and receiver antennas designed for a wireless power transfer

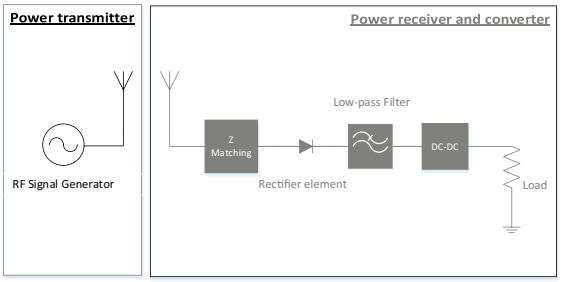

Fig. 2: Wireless power transfer system.

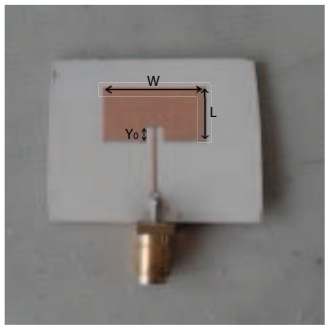

Fig. 3: Transmitter's patch antenna.

system intended to be implemented in a small quadcopter unmanned aerial vehicle. The final section draws some conclusions on the obtained results and possible implementation of the designed antennas for above mentioned system.

II. System's Description

Wireless power transfer systems consist of several fundamental components which enable direct current (DC) power to be converted into RF waves, transmitted between two points and once again back into useful DC. These core components can be observed in Figure 2 where they are divided into power transmitter and receiver.

On the receiver this power must be captured and efficiently converted. This section presents the typical energy harvesting structure, which frequently consists of the receiver antenna, an impedance matching circuit to properly match the antenna with the signal rectifier, a rectifying circuit with a low-pass filter which removes the fundamental from the output, as well as other unwanted harmonics, and finally the load. The most important aspect of this segment is without a doubt its overall efficiency which can be derived as the product of the efficiencies of each individual stage [3].

The frequency of operation and total transmitted power must be complaint with the Industrial, Scientific and Medical (ISM) radio bands and other local regulations. In this paper the chosen frequency was 5.8 GHz.

The load is of major importance for the receiver given that, for diode based rectifiers, it also limits the efficiency at higher power levels [11] and for active loads one should compromise on which range of input power levels maximum efficiency should be obtained.

III. Antenna for Power Transmission

On his experiments with the microwave powered helicopter, William C. Brown described the transmitter as being composed by an extremely directive antenna so that the power available to the target is as greater as possible without there being major losses to the side lobes [2]. To obtain such directivity an array of microstrip antennas, designed for linear polarization, is presented.

A. Single Element

The element of this array is a patch, printed upon a Rogers RO3006 substrate with a relative permittivity (ϵ_r) of 6.15, a loss tangent ($tan\delta$) of 0.002 and 1.27 mm height. The antenna geometry is presented in Figure 3, while the corresponding dimensions are in Table 1. The patch and a feeding microstrip line with a length of $\frac{\lambda}{4}$ which also matches the input impedance of the antenna to 50 Ω, are printed in the top face of the substrate. For simulation purposes Computer Simulation Technology's (CST) Microwave Studio (MWS) was used.

Figure 4 shows the simulated and measured return loss (S_{11}) for the proposed antenna. The simulated gain was 7 dBi.

The measured results showed a downwards shift in the return loss which implied that the ϵ_r considered in the simulation had to be changed and the dimensions of patch were thus tuned.

L	9.8 mm
W	13.3 mm
Y_0	0.034 mm

TABLE I: Patch Dimensions.

B. Full 16-element Array

Based on the element designed in the previous section a 4x4 antenna array with a directivity of 19.6 dBi for the main lobe and a side lobe level of -13.3 dB was designed . CST's post processing tools were used to obtain the optimal spacing between the independent elements.

As for the feed of the single patch, the feed network of the complete array is composed by quarter-wave impedance transformers and lines of 100 Ω characteristic impedance, except for the 50 Ω line at final transformer, which is responsible for output matching. The array is symmetrical for the antennas to be excited with the same amplitude and phase.

The return loss of the array can be observed in Figure 4. This antenna also presented a gain of 16.8 dBi at 5.8 GHz, as can be seen in Figure 6, and 18 dBi at 5.864 GHz.

IV. *Rectenna*

For power reception and conversion rectifying antennas, or "*rectennas*", are commonly used in wireless power transmis-

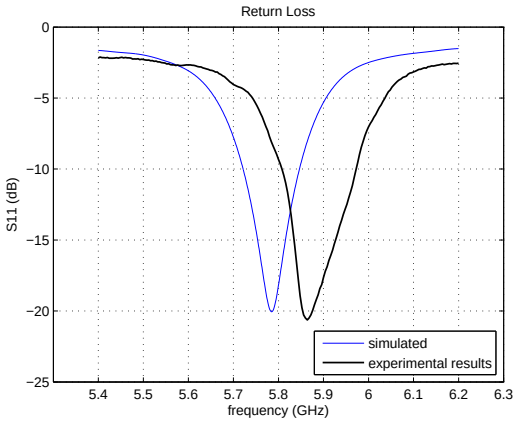

Fig. 4: Comparison between measured and simulated return loss of the full array.

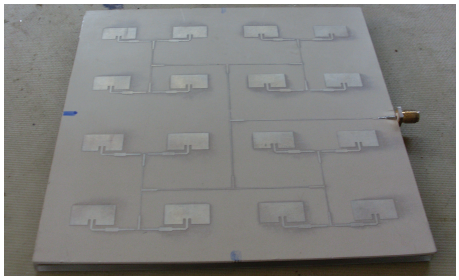

Fig. 5: Final 16-element array.

sion systems. This concept was first demonstrated in 1964 in William C. Brown's experiments with the microwave power helicopter. The first implementation of this concept consisted of a dipole antenna with a diode connected between its branches [2].

In our *rectennas* with microstrip patch antennas we propose a two layered circuit with overlapped substrates of different dielectric constant, separated by a ground plane, as shown in Figure 8. The circuits would be connected through a slot in the substrates and both RF-DC converter and antenna could be directly designed to be matched, in this way the impedance

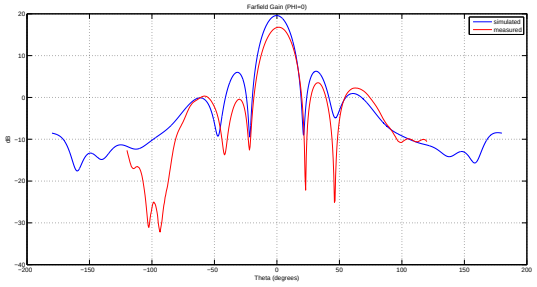

Fig. 6: Simulated and measured radiation patterns of the 4x4 transmitter array.

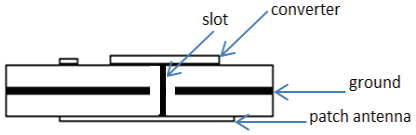

Fig. 7: Proposed layout for the substrate of the *rectenna*.

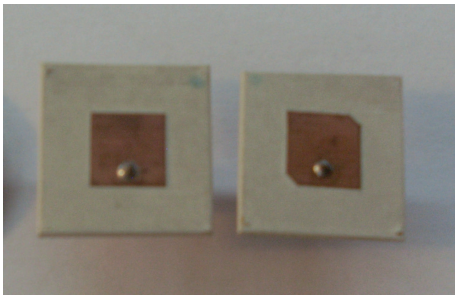

Fig. 8: Patch antennas for the receiver.

matching stage could no longer be necessary and greater efficiency could be obtained however given the variation of the input impedance of the diodes with the input power this task becomes intricate and for a matter simplicity, in this case, the antennas were designed and matched for 50 Ω.

The receiver antennas were designed for the same Rogers RO3006 substrate as presented before. In order to compare the effects of polarization mismatch in wireless power transfer, two antennas were designed with different polarizations and simulated with coaxial feeding in order to tune their dimensions and achieve the desired polarizations and return losses.

If both antennas are linearly polarized they must be oriented in the same direction for there not to be polarization losses. Antennas with different polarizations will be designed for this system to later verify the effect of polarization mismatch between transmitter and receiver and conclude which preforms better with the previously designed transmitter array.

Once again the Rogers RO3006 substrate with 1.27 mm of height was used to design these antennas. A substrate with a relative permittivity of 6.15, which is ordinarily high regarding the design of patch antennas, was chosen to obtain small sized antennas.

Once the patches were printed they presented the shape seen in Figure 8. Their S_{11} parameters were measured and compared to the simulations.

A. Results

The results shifted from the simulations for both antennas but still present themselves as acceptable at 5.8 GHz. These shifts can come from small shifts in the placement of the feed and from the effect of parasitic inductances introduced by the SMA's copper line placed within the substrate.

The measured and simulated return loss of both linearly and circularly polarized patch antennas can be observed, respectively, in Figures 9 and 10. The variation of the simulated axial

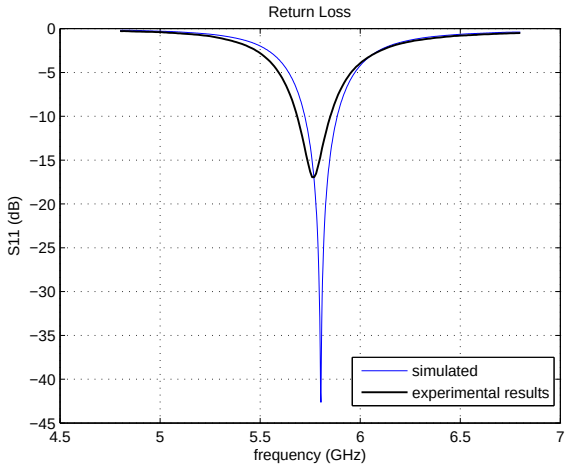

Fig. 9: Comparison between simulated and measured values for the linearly polarized square patch.

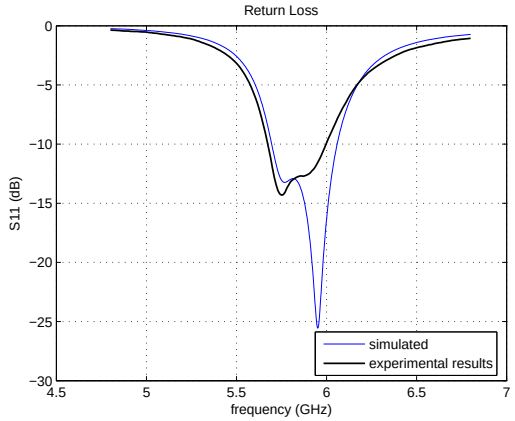

Fig. 10: Comparison between simulated and measured values for the right hand circularly polarized patch.

ratio of the circularly polarized antenna can be observed in Figure 11 and presented a value of 0.32 at 5.8 GHz. Moreover this antenna presented a gain of 5.3 dBi while the linearly polarized patch is expected to have a gain of 5.5 dBi.

V. Conclusion

Simulations and measurements were performed in different microstrip antenna topologies that are here proposed to be part of a microwave wireless power transfer system. The transmitter antenna array demonstrated a gain of 16.8 dBi at 5.8 GHz while the receiver antennas presented gains of 5.5 and 5.3 dBi. The circularly polarized antenna presented an axial ratio of 0.3. Given the high flexibility and simplicity to replicate and design these antennas, microstrip antennas present themselves as a good structure to apply in wireless power transfer systems.

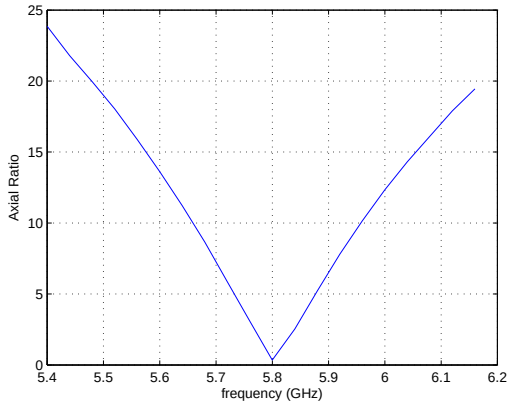

Fig. 11: Simulated value of the axial ratio of the circularly polarized patch antenna.

Acknowledgment

We would like to acknowledge the financial Support of COST IC1301.

References

[1] W. C. Brown. The history of power transmission by radio waves. *IEEE Transactions on Microwave Theory and Techniques*, 32(9):1230 – 1242, September 1984.

[2] W. C. Brown. The microwave powered helicopter. *Journal of Microwave Power and Electromagnetic Energy*, 1(1):1–20, 1966.

[3] C. R. Valenta and G. D. Dugin. Harvesting wireless power. *IEEE Microwave Magazine*, 2014.

[4] J. O. McSpadden, L. Fan, and K. Chang. Design and experiments of a high-conversion-efficiency 5.8-ghz rectenna. *IEEE Transactions on Microwave Theory and Techniques*, 46(12):2053–2060, December 1998.

[5] R. J. Gutmann and R. B. Gworek. Yagi-uda receiving elements in microwave power transmission system rectennas. *Journal of Microwave Power*, 14(4):313–320, 1979.

[6] H. J. Visser. Indoor wireless rf energy transfer for powering wireless sensors. *Radioengineering*, 21(4):963–973, December 2012.

[7] J. O. McSpadden and K. Chang. A dual polarized circular patch rectifying antenna at 2.45 ghz for microwave power conversion and detection. *IEEE MTT-S International Microwave Symposium Digest,*, 3:1749 – 1752, 1994.

[8] C. Chin, Q. Xue, and C. Chan. Compact of a 5.8-ghz rectenna incorporating a new patch antenna. *IEEE Antennas and Wireless Propagation Letters*, 4:175–178, June 2005.

[9] W. Tu, S. Hsu, and K. Chang. Compact 5.8-ghz rectenna using stepped-impedance dipole antenna. *IEEE Ante*, 6:282–284, June 2007.

[10] M. Furukawa, Y. Takahashi, T. Fujiware, S. Mihara, T. Saito, Y. Kobayashi, S. Kawasaki, N. Shinohara, Y. Fujino, K. Tanaka, and S. Sasaki. 5.8-ghz planar hybrid rectenna for wireless powered applications. *Asia-Pacific Microwave Conference*, pages 1611–1614, December 2006.

[11] T. W. Yoo and K. Chang. Theoretical and experimental development of 10 and 35 ghz rectennas. *IEEE Transactions on Microwave and Techniques*, 40(6):1259 – 1266, June 1992.

Appendix C

State of the Art of Resonant Inductive Coupling

The state of the art of projects that use resonant inductive coupling are presented in this section. The variation of power transfer efficiency for each project are presented in Figure C.1, regarding the distance, and in Figure C.2, regarding the frequency of operation.

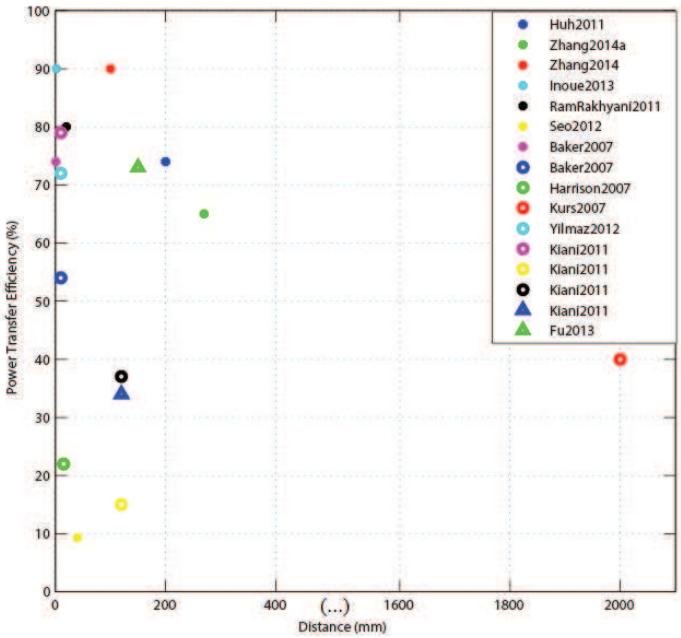

Figure C.1: State of the art resonant inductive coupling power transfer efficiencies versus distance.

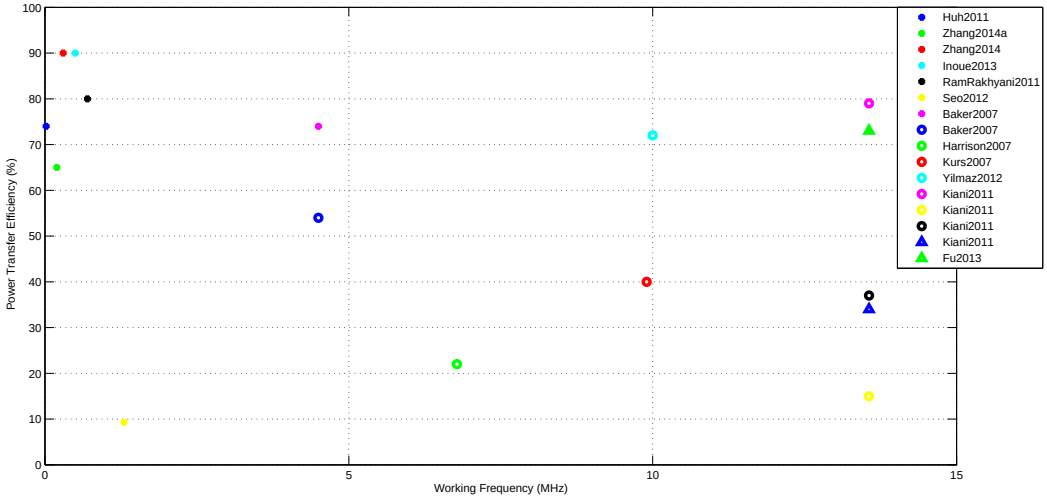

Figure C.2: State of the art resonant inductive coupling power transfer efficiencies versus frequency of operation.

The above mentioned results were obtained from: [60],[61], [62], [63], [64], [65], [66], [67], [17], [68], [18], and [69].

There are only a few publications regarding the other near field methods. Of which [70] can be underlined for inductive coupling, presenting a power transfer efficiency of 35 %, at 1 MHz, and 80 %, at 5 MHz, both for a distance of 10 mm.

Regarding capacitive coupling, a PTE of 40 % at a distance of 5 m was obtained at 14 MHz in [24] and of 90 %, at 1 MHz, for a distance of 1 mm, in [23].

References

[1] Richard Fitzpatrick. Ampère's Circuital Law. http://farside.ph.utexas.edu/, July 2007. The Univesity of Texas at Austin.

[2] John J. O'Connor and Edmund F. Robertson. Heinrich Rudolf Hertz. http://www-history.mcs.st-andrews.ac.uk/Biographies/Hertz_Heinrich.html, July 2007. School of Mathematics and Statistics University of St Andrews, Scotland.

[3] Wave Structure of Matter (WSM). A photograph of nikola tesla sitting inside a circular framework demonstrating the largest tesla coils ever built. http://www.spaceandmotion.com/Physics-Nikola-Tesla-Inventions-Resonance.htm.

[4] Nikola Tesla. The transmission of electric energy without wires. *The thirteenth Anniversary Number of the Electrical World and Engineer*, 1904.

[5] Hugo Gernsback. U.S. Blows Up Tesla Radio Tower. *The Electrical Experimenter*, page 293, September 1917.

[6] William C. Brown. The microwave powered helicopter. *Journal of Microwave Power and Electromagnetic Energy*, 1(1):1–20, 1966.

[7] William C. Brown. The history of power transmission by radio waves. *IEEE Transactions on Microwave Theory and Techniques*, 32(9):1230 – 1242, September 1984.

[8] Eric Giler. A demo of wireless electricity. http://www.ted.com/talks/, July 2009.

[9] Wireless Power Consortium. http://www.wirelesspowerconsortium.com/about/.

[10] Space Solar Power Institute Clean Baseload Energy. Photograph of william c. brown observing a panel of dipole antennas. http://www.solarsat.org/billbrown_memorial.htm.

[11] G. Goubau and F. Schwering. On the guided propagation of electromagnetic wave beams. *IRE Transactions on Antennas and Propagation*, 9(3):248–256, May 1961.

[12] Raytheon. We were created to create. *Electrical Engineering*, page 68A, November 1959.

[13] Mainland CCTT. On the left, a photograph of william c. brown hold the helicopter prototype and, on the right, of the helicopter in-fligh. http://mainland.cctt.org/istf2008/brown.asp.

[14] Nuno Miguel Coluna Bonifácio. Transmissão de energia sem fios. Master's thesis, University of Aveiro, 2009.

[15] Constantine A. Balanis. *Antenna Theory: Analysis and Design*. John Wiley & Sons, Inc., 2005.

[16] Tesla Innovations. Typical arrangement of an inductive coupled power transfer system. `http://ramrods.sdsu.edu/research.html`, 2009.

[17] Andé Kurs, Aristeidis Karalis, Robert Moffatt, J. D. Joannopoulos, Peter Fisher, and Marin Soljači. Wireless power transfer via strongly coupled magnetic resonances. *Science*, 317(5834):83–86, July 2007.

[18] M. Kiani, Uei-Ming Jow, and M. Ghovanloo. Design and optimization of a 3-coil inductive link for efficient wireless power transmission. *IEEE Transactions on Biomedical Circuits and Systems*, 5(6):579–591, July 2011.

[19] encryptechno.com — Inside technology. Wireless electricity. http://encryptechno.com/wp-content/uploads/2014/01/witricity.jpg, August 2013.

[20] Ying Yi, U. Buttner, Yiqiang Fan, and I.G. Foulds. 3-coil resonance-based wireless power transfer system for implantable electronic. In *2013 IEEE Wireless Power Transfer (WPT)*, pages 230–233. IEEE, May 2013.

[21] Margaret Rouse. Definition: Dielectric material. `http://whatis.techtarget.com/definition/dielectric-material`, November 2010.

[22] Nikola Tesla. Experiments with alternate currents of very high frequency and their application to methods of artificial illumination,. AIEE, May 1891.

[23] Chao Liu, A.P. Hu, and N.C. Nair. Coupling study of a rotary capacitive power transfer system. In *IEEE International Conference on Industrial Technology*, pages 1 – 6. IEEE, February 2009.

[24] Ricardo Dias Fernandes, Jo ao Nuno Matos, and Nuno Borges Carvalho. Behavior of resonant electrical in terms of range and relative orientation. In *IEEE Wireless Power Transfer Conference (WPTC)*, pages 118 – 121. IEEE, May 2014.

[25] Fraunhofer ISE. World record solar cell with 44.7% efficiency, September 2013.

[26] NASA. `http://www.nasa.gov/offices/oct/early_stage_innovation/centennial_challenges/cc_pb_feature_11_10_09.html`, November 2009.

[27] LaserMotive. Welcome to lasermotive... `http://lasermotive.com/`, July 2014.

[28] William C. Brown and E.E. Eves. Beamed microwave power transmission and its application to space. *IEEE Transactions on Microwave Theory and Techniques*, 40(6):1239–1250, June 1992.

[29] S Kawasaki. The green energy harvesting winds by the rf/microwave power transmission. In *Wireless Power Transfer (WPT), 2013 IEEE*, pages 111–114, May 2013.

[30] Wireless Power Consortium. System description wireless power transfer, volume 1: Low power. part 1: Interface definition, June 2013.

[31] Statista The Statistics Portal for Market Data. Average number of rechargeable electronic devices in u.s. households* in 2009 (housing units in millions). http://www.statista.com/statistics/187657/average-number-of-rechargeable-electronic-devices-in-us-households/.

[32] Powermat. http://www.powermat.com/announcements/national-rollout-wireless-charging-duracell-powermat-begins-starbucks/, June 2014.

[33] Duracell Powermat. Powermat for three devices. http://www.duracellpowermat.com/powermat/three-devices.html, 2014.

[34] WiTricity Corporation — Wireless Power Over Distance. http://www.witricity.com/technology/intellectual-property/, 2014.

[35] Murata. Wireless power transmission module. http://www.murata.com/products/wireless_power/, November 2011.

[36] Integrated Device Technology. Wireless Charging ICs, Wireless Power ICs. http://www.idt.com/products/power-management/wireless-charging-ics-wireless-power-ics#/?tfm_cck_field__input_voltage_range_v=[4%20TO%2021], 2014.

[37] Linear Technology. Wireless Power Transfer (WPT) & LTC4120. http://www.linear.com/solutions/4444, October 2014.

[38] PRIMOVE. The technology behind primove. http://primove.bombardier.com/about/technical-principle/, 2014.

[39] Georgia Tech. UAV Research Facility. http://controls.ae.gatech.edu/wiki/UAV_Research_Facility, October 2014.

[40] G.C.H.E. de Croon, M.A. Groen, C. De Wagter, B.D.W. Remes, R. Ruijsink, and B.W. van Oudheusden. Design, aerodynamics, and autonomy of the delfly. *Bioinspiration and Biomimetics*, 7(2), 2012.

[41] B. Griffin and C. Detweiler. Resonant wireless power transfer to ground sensors from a uav. *Proceedings of IEEE International Conference on Robotics and Automation (ICRA)*, 2012.

[42] Tiago Miguel Valente Varum. Antena para comunicações dsrc. Master's thesis, University of Aveiro, 2010.

[43] A. A. Abdelaziz. Bandwidth enhancement of microstrip antenna. *Progress in Electromagnetics Research*, pages 311–317, 2006.

[44] Emtalk.com. Microstrip patch antenna: From simulation to realization. http://www.emtalk.com/mwt_mpa.htm, 2014.

[45] Thomas A. Milligan. *Modern Antenna Design.* John Wiley & Sons, Inc., 2nd edition, 2005.

[46] J. F. Rocha Pereira. Apontamentos, chapter 4 - agregados. Universidade de Aveiro.

[47] Donald A. Neamen. *Semiconductor Physics and Devices: Basic Principles*. McGraw-Hill, 3rd edition, 2003.

[48] Adel S. Sedra and Kenneth C. Smith. *Microelectronic circuits*. Oxford University Press, 2011.

[49] David M. Pozar. *Microwave engineering*. John Wiley & Sons, Inc., 2012.

[50] R. Ludwig and P. Bretchko. *RF Circuit Design: Theory and Applications*. Prentice-Hall, Upper Saddle-River, N.J., 2000.

[51] Christopher R. Valenta and Gregory D. Durgin. Harvesting wireless power. *IEEE Microwave Magazine*, 15(4):108–120, June 2014.

[52] James O. McSpadden, Lu Fan, and Kai Chang. Design and experiments of a high-conversion-efficiency 5.8-ghz rectenna. *IEEE Transactions on Microwave Theory and Techniques*, 46(12):2053–2060, December 1998.

[53] Erez Faleknstein Michael Roberg and Zoya Popovic. High-efficiency harmonically-terminated rectifier for wireless powpower applications. *IEEE MTT-S International Microwave Symposium Digest*, pages 1–3, June 2012.

[54] Diana Lúcia de Jesus Teixeira. Analysis on rf-dc converters for integration in radio receivers. Master's thesis, University of Aveiro, 2011.

[55] Tae-Whan Yoo and Kai Chang. Theoretical and experimental development of 10 and 35 ghz rectennas. *IEEE Transactions on Microwave and Techniques*, 40(6):1259 – 1266, June 1992.

[56] Henrique Morais Saraiva. Desenvolvimento de dispositivos de recolha de energia electromagnética integrados em vestuário e aplicados a redes sem fios de Área corporal. Master's thesis, Universidade da Beira Interior, October 2013.

[57] Avago Technologies. [Datasheet] HSMS-281x, Surface Mount RF Schottky Barrier Diodes.

[58] Avago Technologies. Linear models for diode surface mount packages. Application Note 1124, July 2010.

[59] Naoki Shinohara. Rectennas for microwave power transmission. *IEICE Electronics Express*, 10(21):1–13, November 2013.

[60] J. Huh, S.W. Lee, W.Y. Lee, G.H. Cho, and C.T. Rim. Narrow-width inductive power transfer system for online electrical vehicles. *IEEE Transactions on Power Electronics*, 26(12):3666 – 3679, December 2011.

[61] Y. Zhang, Z. Zhao, and T. Lu. Quantitative analysis of system efficiency and output power of four-coil resonant wireless power transfer. *IEEE Journal of Emerging and Selected Topics in Power Electronics*, PP(99):1, April 2014.

[62] Yiming Zhang and Zhengming Zhao. Frequency splitting analysis of two-coil resonant wireless power transfer. *IEEE Antennas and Wireless Propagation Letters*, 14:400 – 402, February 2014.

[63] K. Inoue, Nagashima, T., Xiuqin Wei, and H. Sekiya. Design of high-efficiency inductive-coupled wireless power transfer system with class-de transmitter and class-e rectifier. In *IECON 2013 - 39th Annual Conference of the IEEE Industrial Electronics Society*, pages 613 – 618. IEEE, November 2013.

[64] S. RamRakhyani, A.K.and Mirabbasi and Mu Chiao. Design and optimization of resonance-based efficient wireless power delivery systems for biomedical implants. *IEEE Transactions on Biomedical Circuits and Systems*, 5(1):48 – 63, February 2011.

[65] Young-Sik Seo, Minh Quoc Nguyen, Zachariah Hughes, and S. Rao. Wireless power transfer by inductive coupling for implantable batteryless stimulators. In *2012 IEEE MTT-S International Microwave Symposium Digest (MTT)*, pages 1 – 3. IEEE, June 2012.

[66] M.W. Baker and R. Sarpeshkar. Feedback analysis and design of rf power links for low-power bionic systems. *IEEE Transactions on Biomedical Circuits and Systems,*, 1(1):28 – 38, March 2007.

[67] R.R Harrison. Designing efficient inductive power links for implantable devices. In *IEEE International Symposium on Circuits and Systems*, pages 2080 – 2083. IEEE, May 2007.

[68] G. Yilmaz and C. Dehollaini. An efficient wireless power link for implanted biomedical devices via resonant inductive coupling. In *2012 IEEE Radio and Wireless Symposium (RWS)*, pages 235 – 238. IEEE, January 2012.

[69] Minfan Fu, Tong Zhang, Xinen Zhu, and Chengbin Ma. A 13.56 mhz wireless power transfer system without impedance matching networks. In *IEEE Wireless Power Transfer (WPT)*, pages 222 – 225. IEEE, May 2013.

[70] Uei-Ming Jow and Maysam Ghovanloo. Design and optimization of printed spiral coils for efficient transcutaneous inductive power transmission. *IEEE Transactions on Biomedical Circuits and Systems*, 1(3):193–202, September 2007.